Aalto University
School of Electrical
Engineering

E4230
Microwave EO Instrumetation
SAR Interferometry

(5 cr)
Jaan Praks, Oleg Antropov
Aalto University

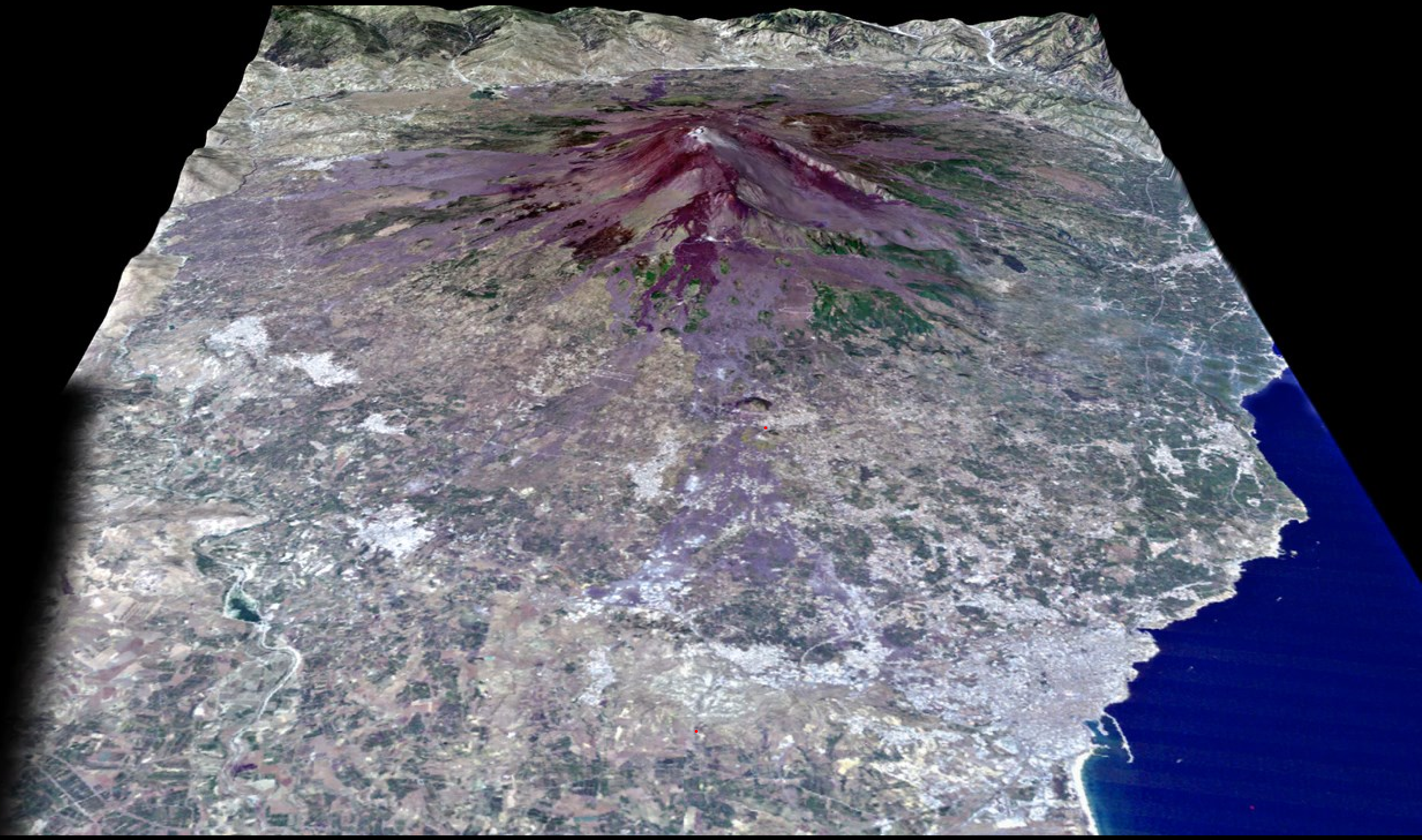

Topography map

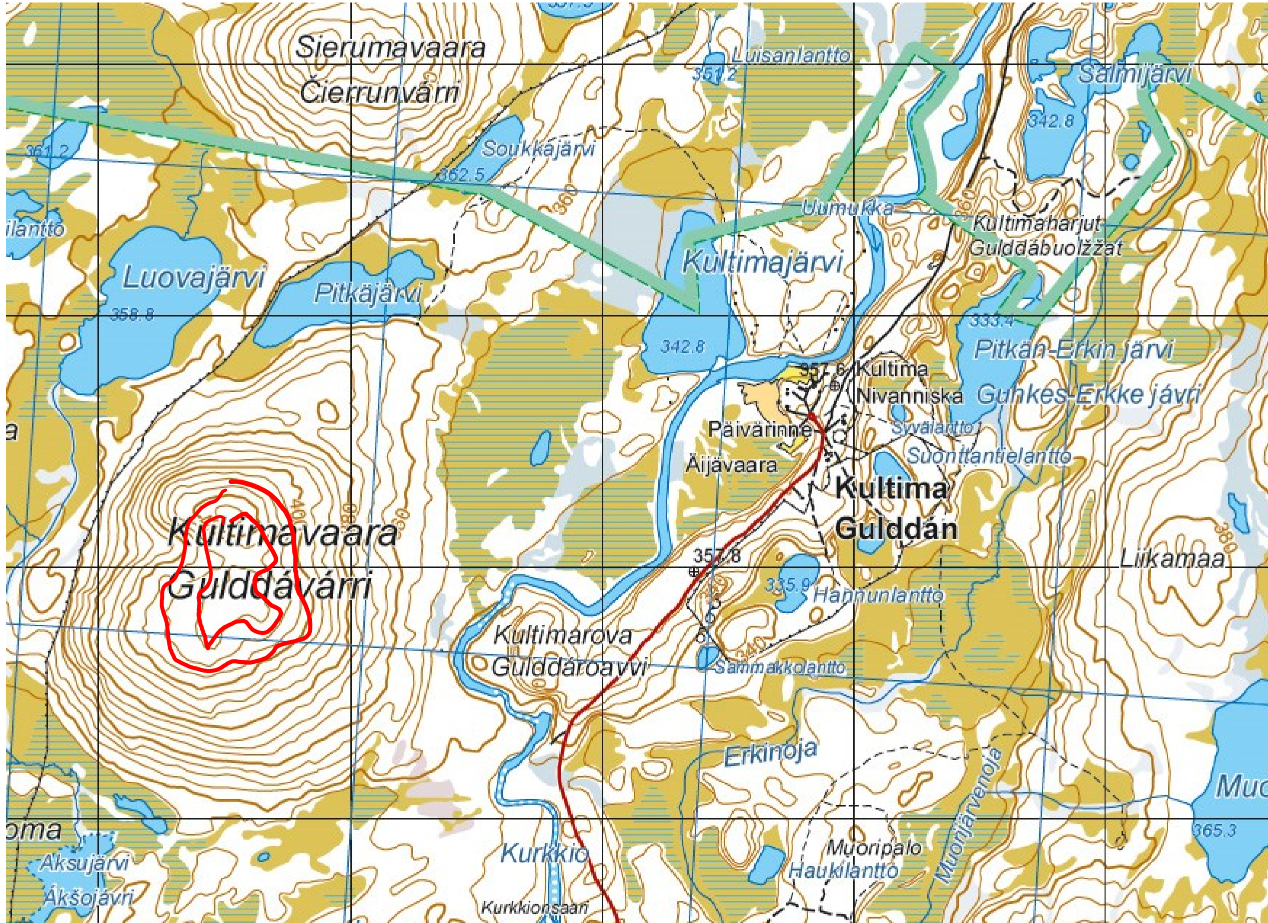

Contour line is easy way to describe topography

Isoheight, isodepth, isoline

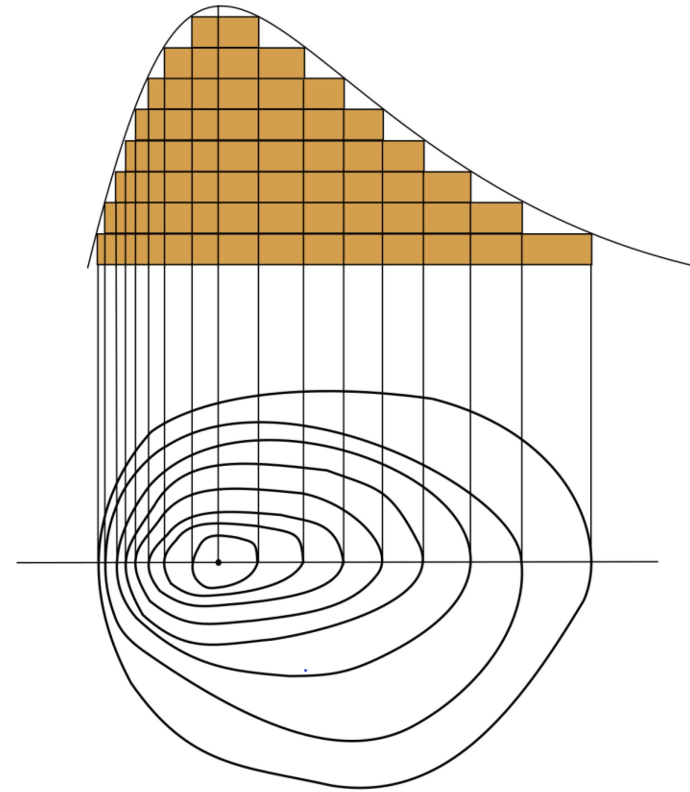

How to measure topography from distance

For example structured light fotogrammetry

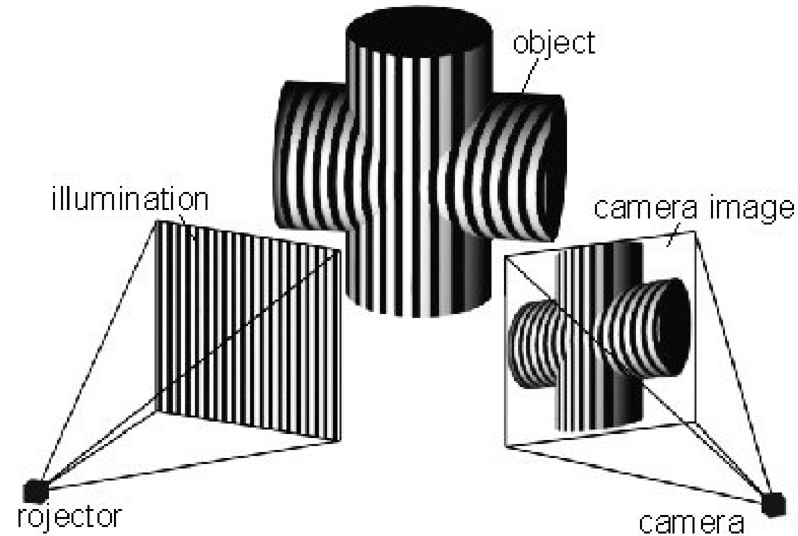

Aalto University
School of Electrical Engineering

Projecting a grid to the topography

Allows to compute the elevation!

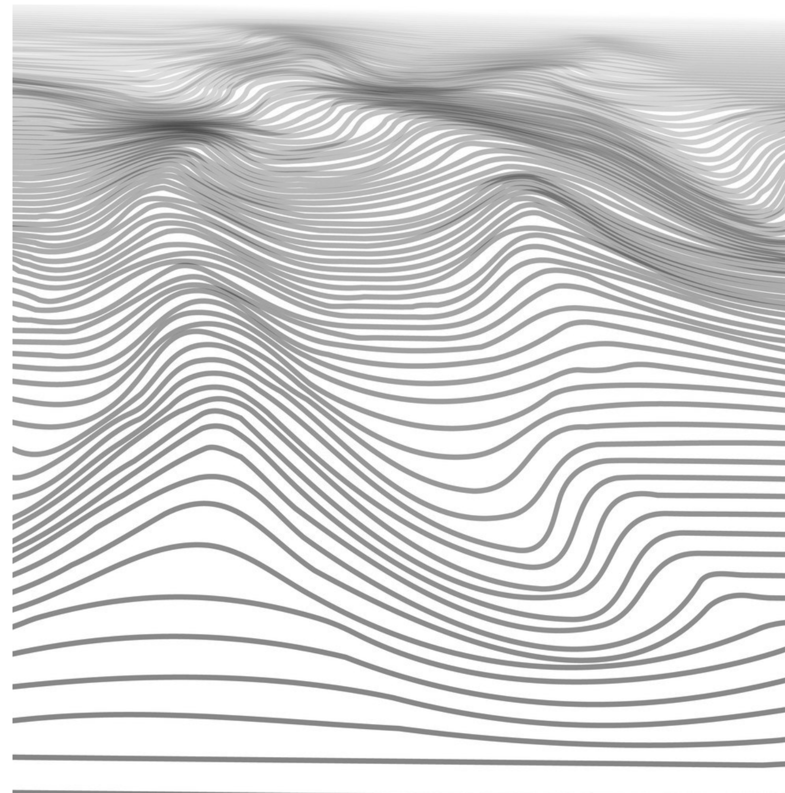

Aalto University
School of Electrical
Engineering

SAR Interferometry

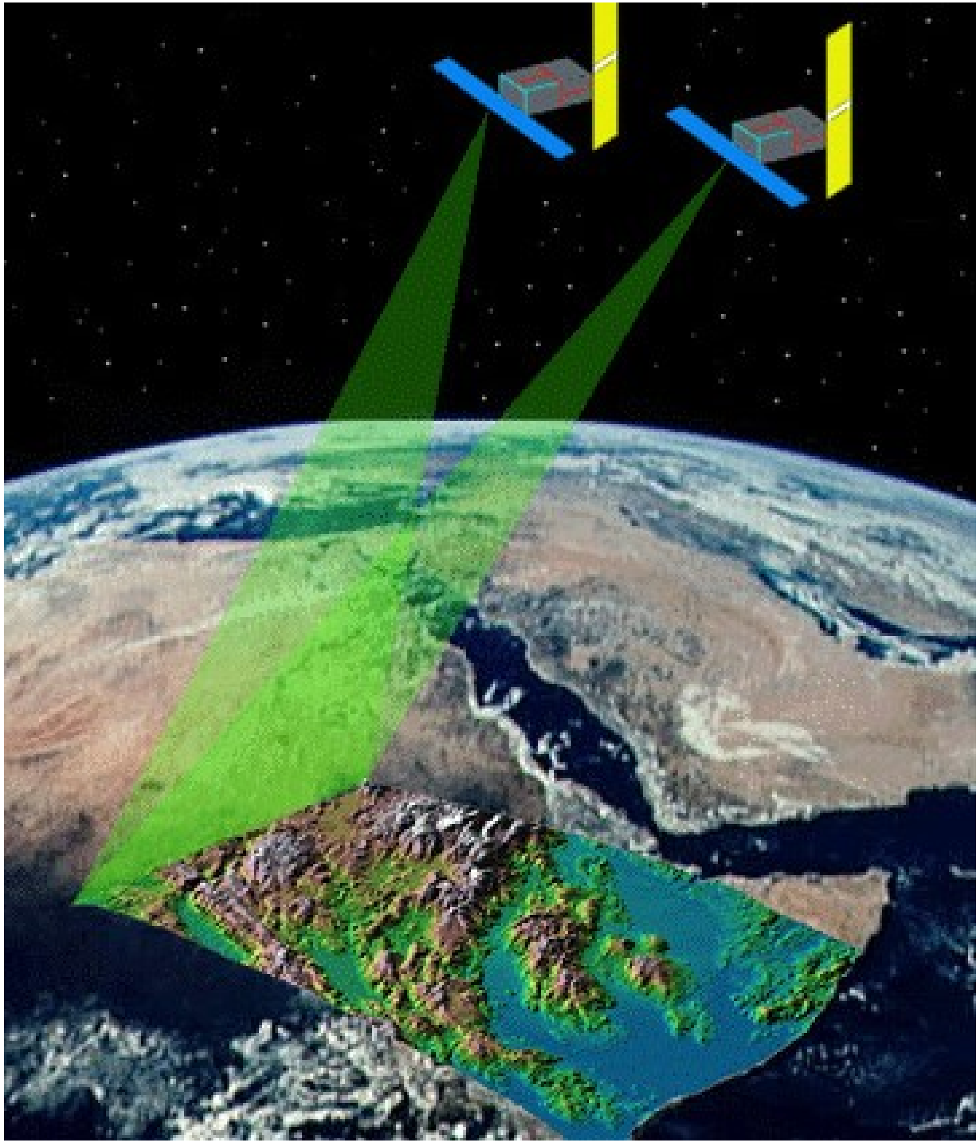

DEM formation

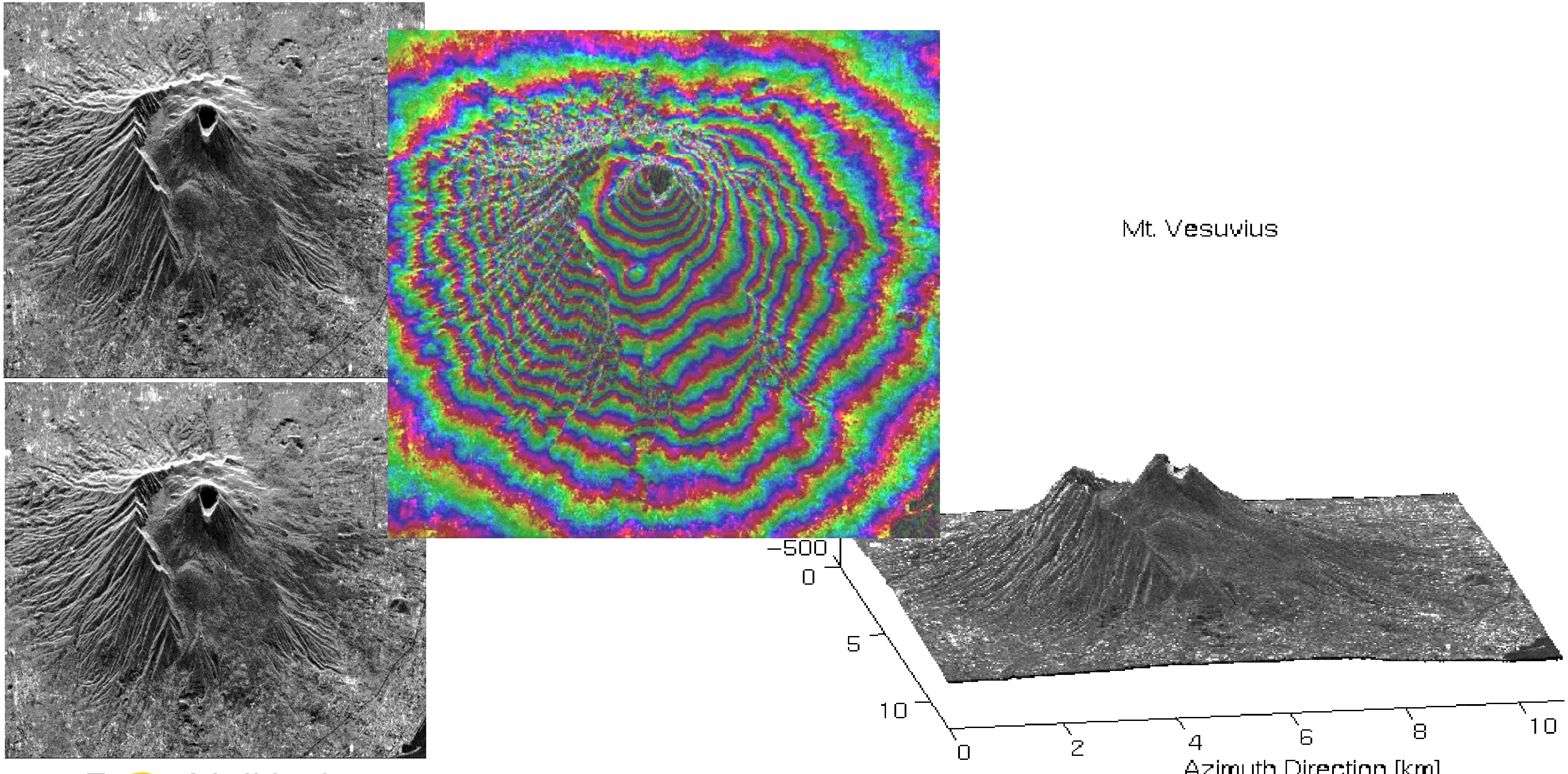

How to get regular grid projected to the ground with SAR?

Two problems:

Phase pattern is too dense!

Phase appears to be random?

Measurement phase creates regular line pattern on the ground!

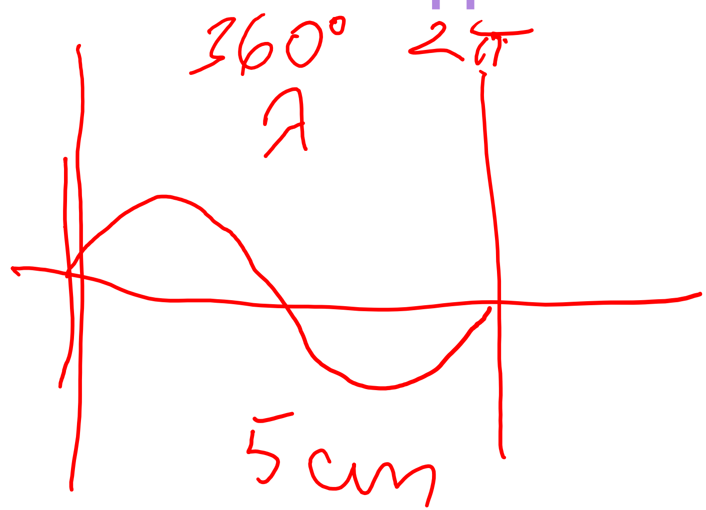

Aalto University
School of Electrical Engineering

SAR

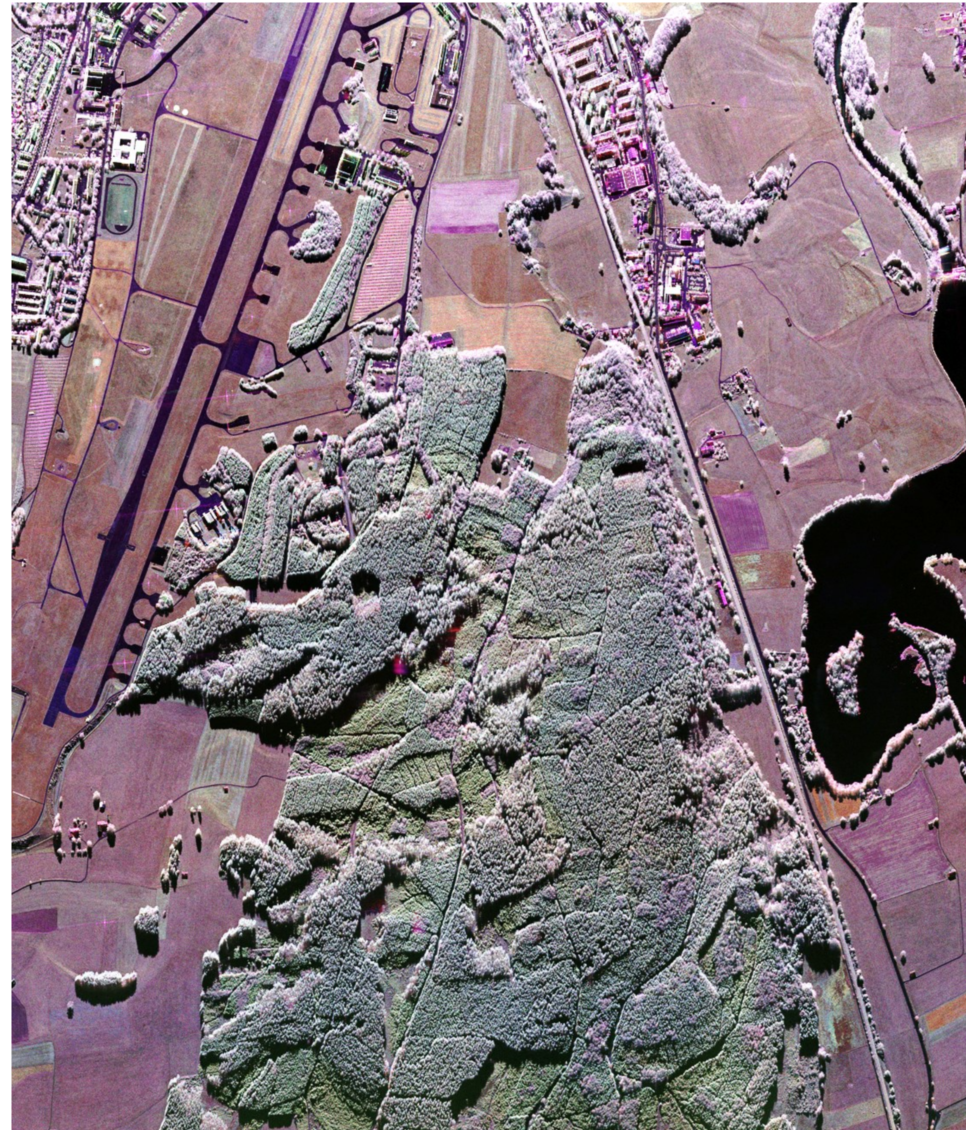

SAR

$$\rho = \frac{E_r}{E_i} = a + jb = Ae^{j\phi}$$

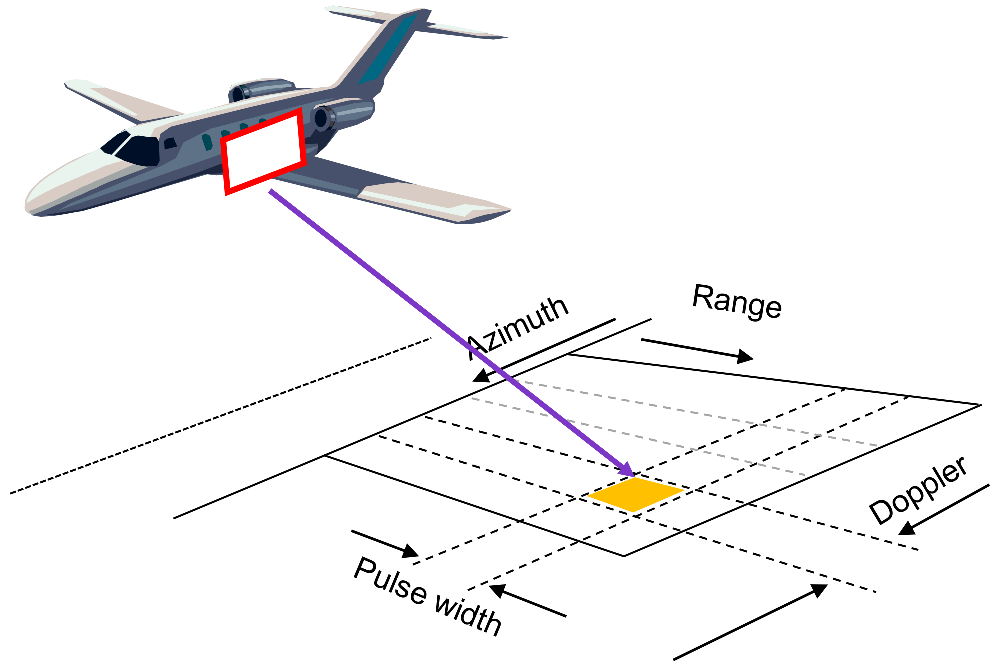

Phase after traveling a distance R

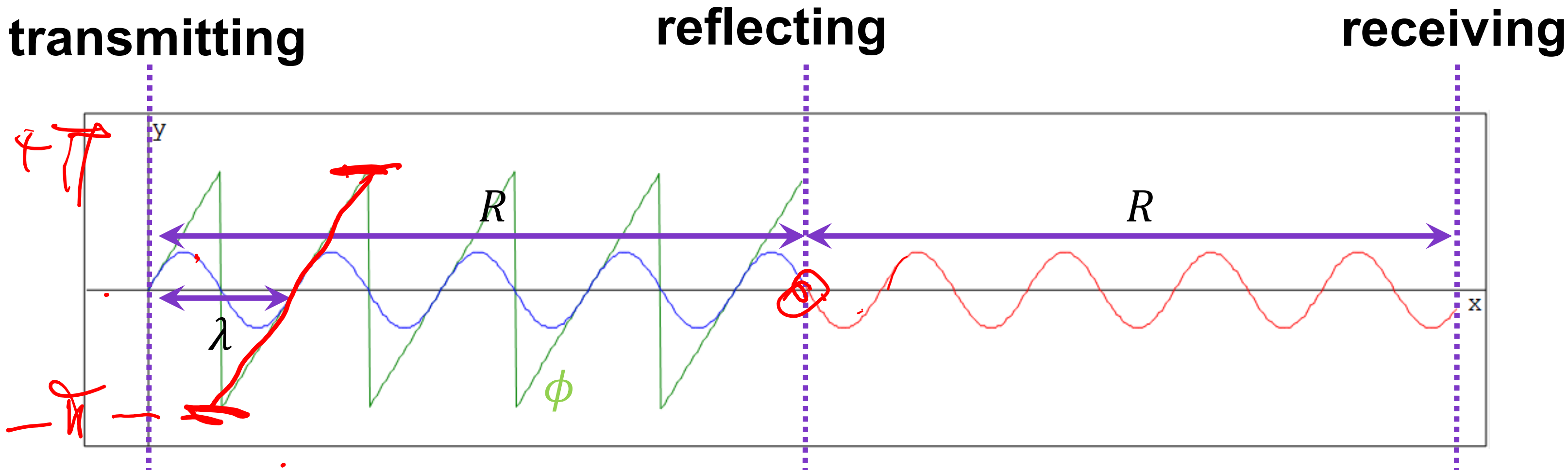

$$A = e^{j\phi r}$$

$$\rho = \frac{E_r}{E_i} = a + jb = Ae^{j\phi}$$

$$\phi = 2\pi \frac{R}{\lambda} = 2\pi \frac{f}{c} R$$

Distance and phase

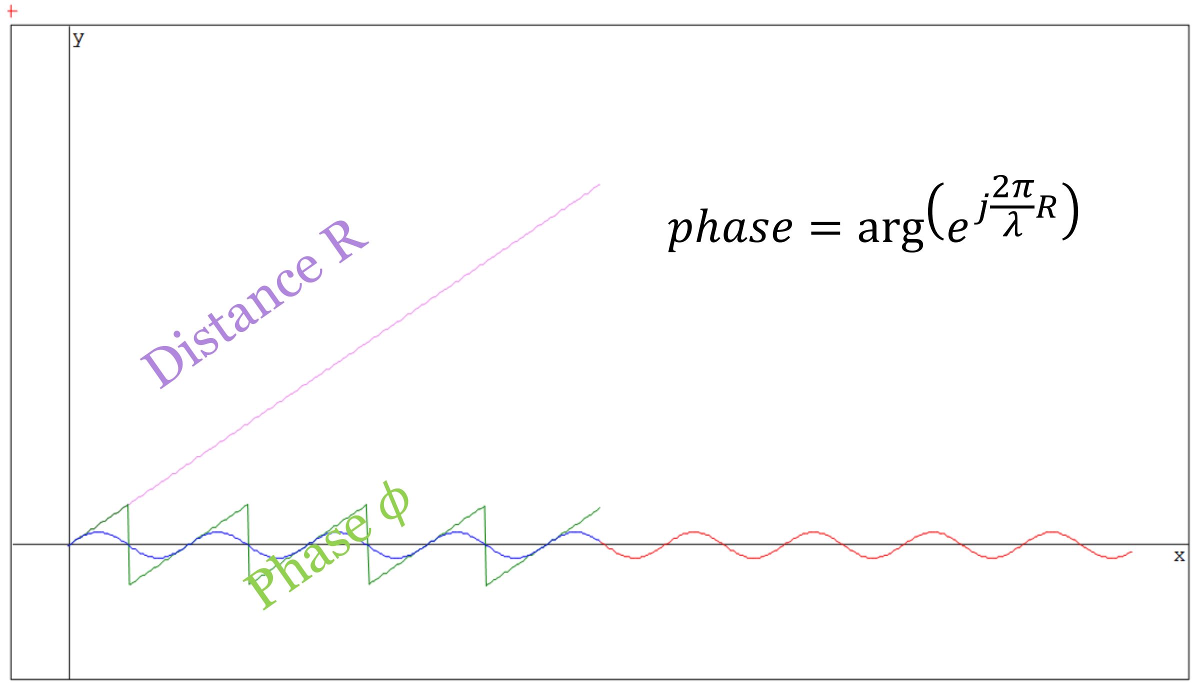

$$phase = \arg\left(e^{j\frac{2\pi}{\lambda}R}\right)$$

Phase creates the grid to the ground!

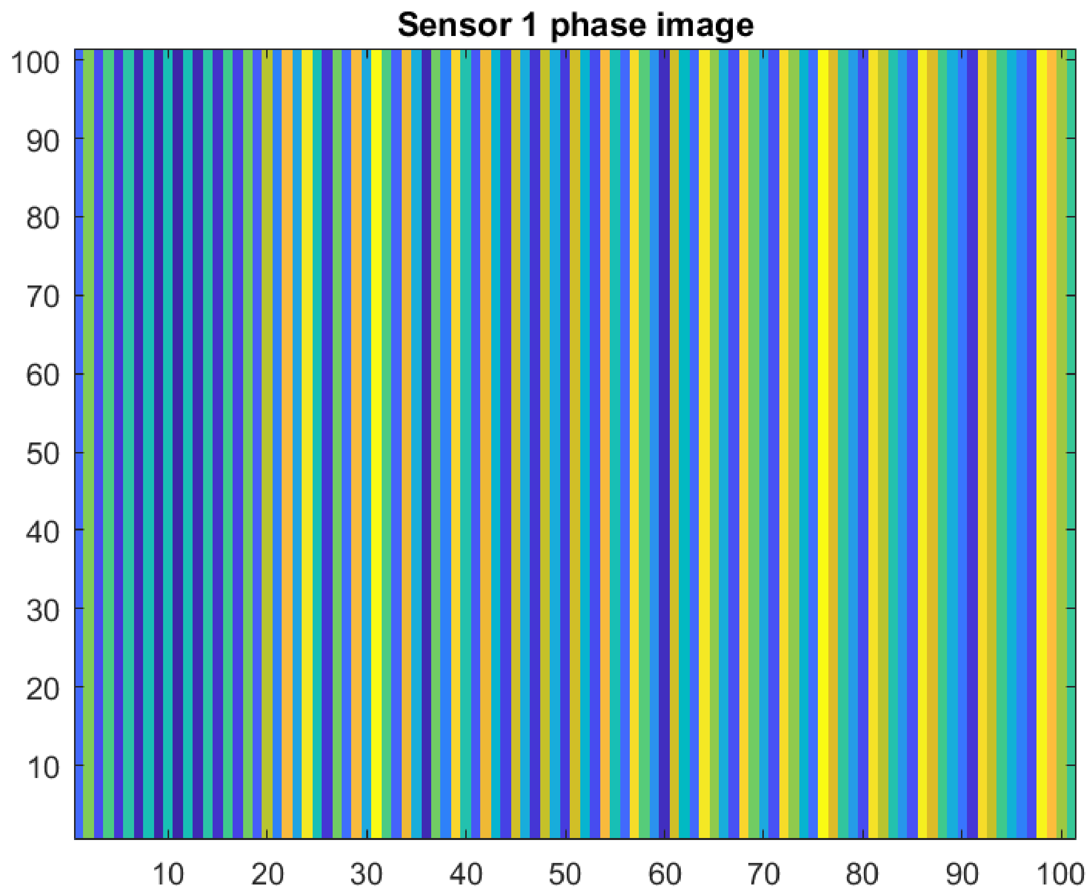
Sensor 1 phase image
100
90
80
70
60
50
40
30
20
10
10
20
30
40
50
60
70
80
90
100

Making the phase pattern less dense

Merging two images

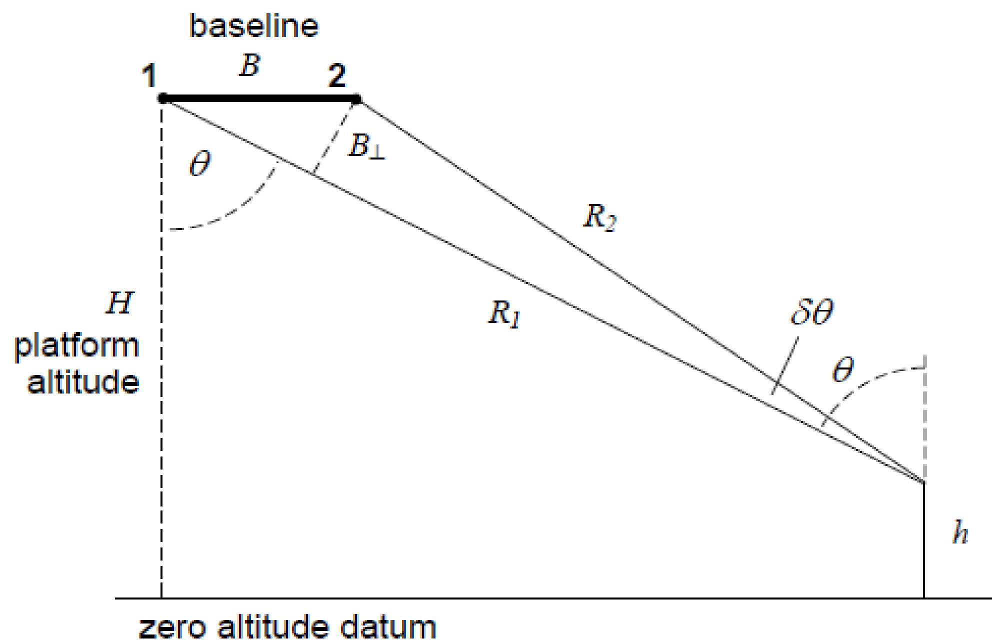

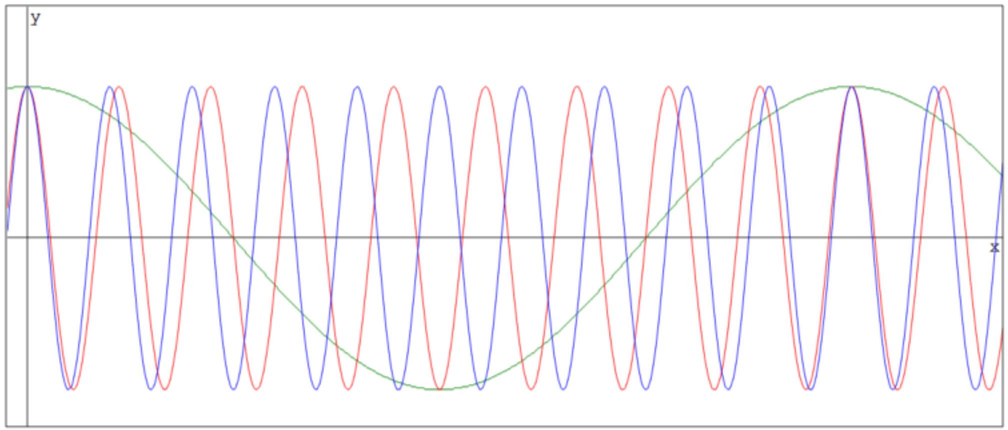

$$\begin{cases} \mathrm{Re}\left(e^{(i)\cdot x}\right) \\ \mathrm{Re}\left(e^{(i)\cdot x\cdot 0.9}\right) \\ \mathrm{Re}\left(e^{(i)\cdot x}\cdot e^{-((i)\cdot x\cdot 0.9)}\right) \end{cases}$$

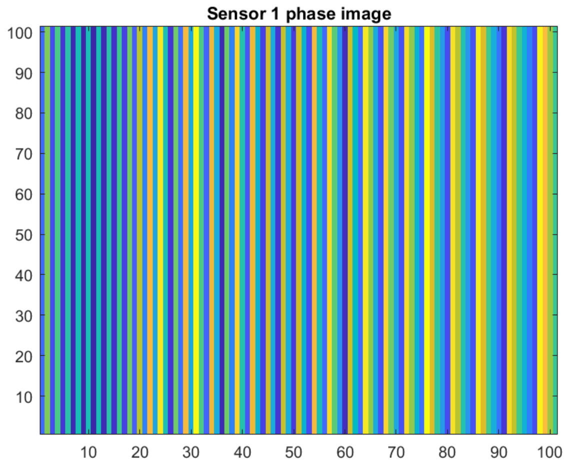

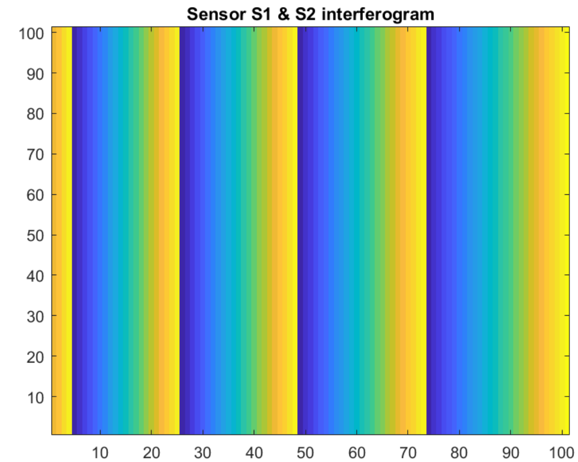

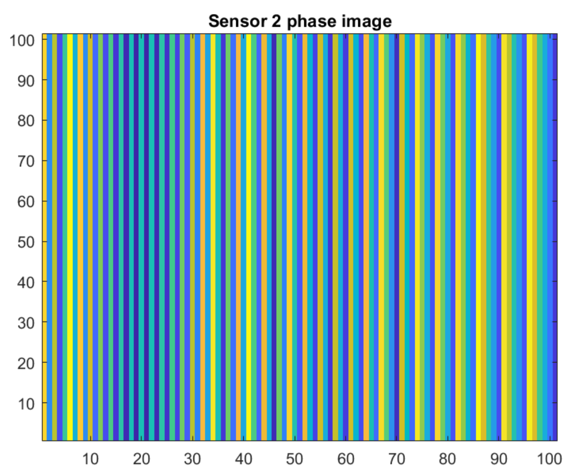

Aalto University
School of Electrical
Engineering

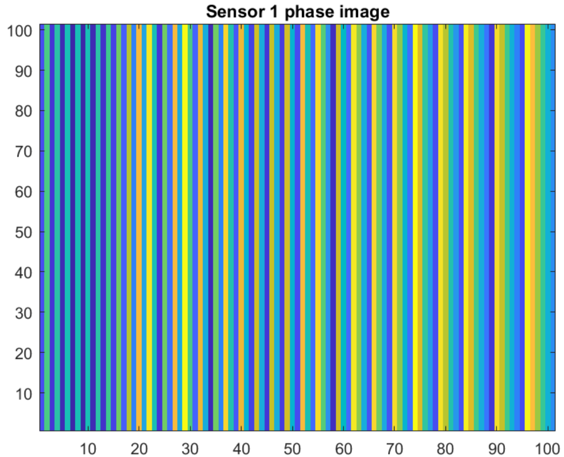
Sensor 1 phase image
100
90
80
70
60
50
40
30
20
10
10 20 30 40 50 60 70 80 90 100

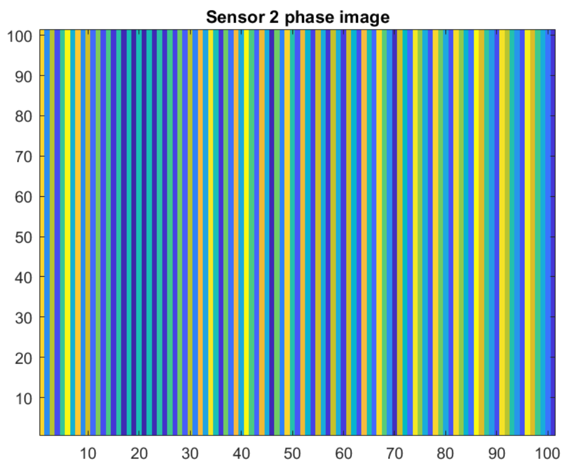
Sensor 2 phase image
100
90
80
70
60
50
40
30
20
10
10 20 30 40 50 60 70 80 90 100

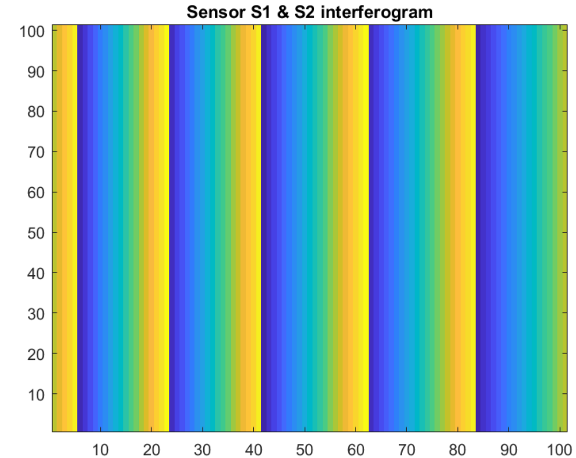
Sensor S1 & S2 interferogram
100
90
80
70
60
50
40
30
20
10
10 20 30 40 50 60 70 80 90 100

Two similar noise terms on two images

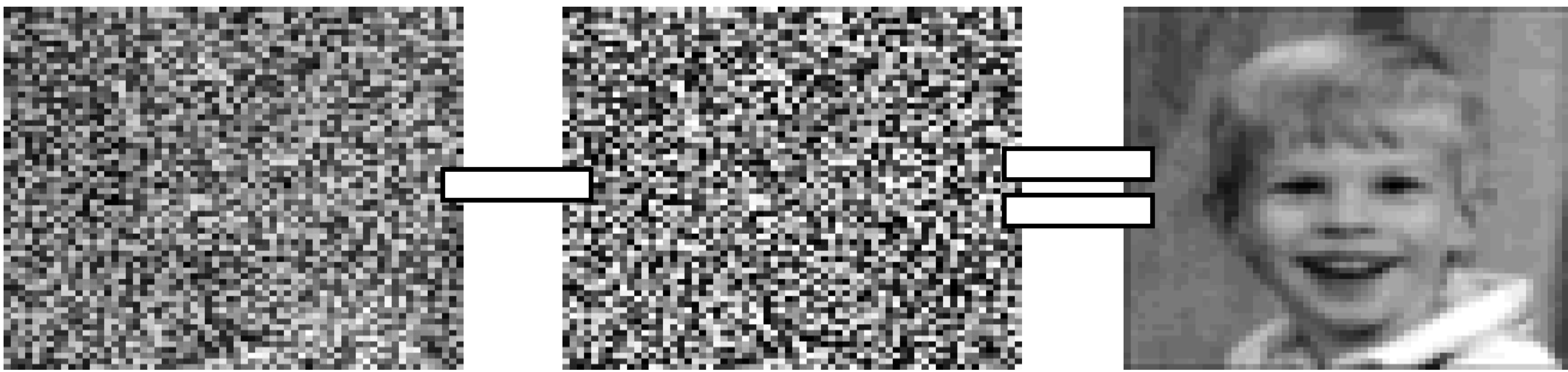

Aalto University
School of Electrical Engineering

Interferometric SAR

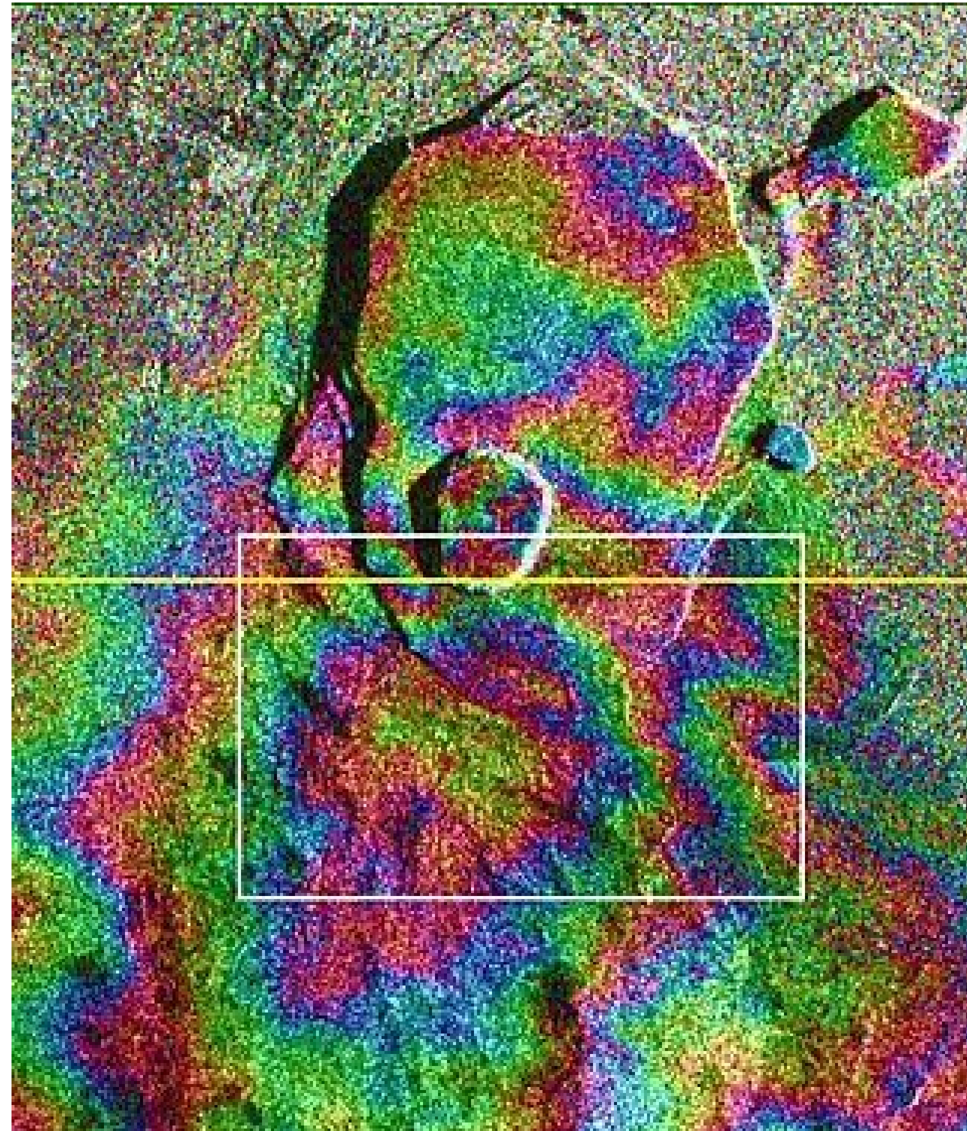


esa
[Tue Jun 12 12:10:00 2012] 7892771.710 from anchor; AO: 0 Shadow dist: 0.00 FPS: 56.09 Lat: 19.47275465 Lon: 69.69388570 Height: 727.90 m l 2388.13 ft

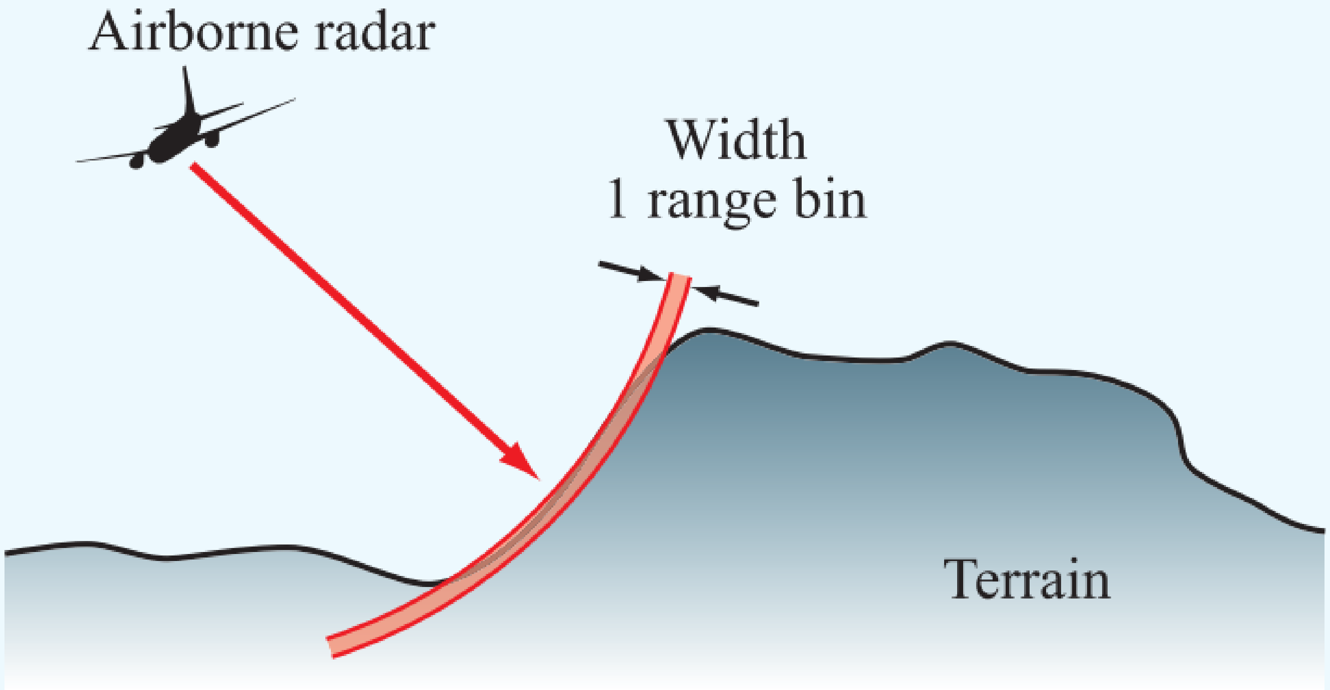

Figure 15-1: Radar returns from all points within any range bin are received at once. Thus conventional radar images cannot properly depict topographic information.

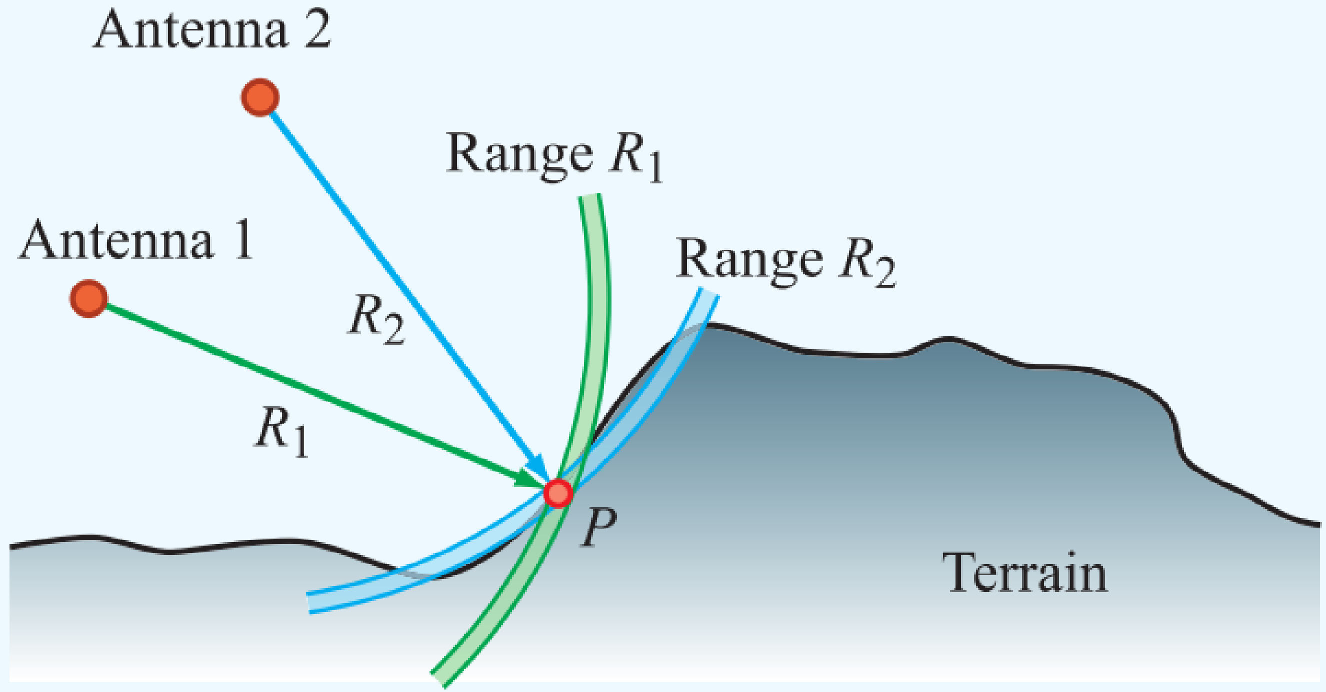

Figure 15-2: Distances to a point P from Antenna 1 and Antenna 2 are R_1 and R_2, respectively. The two arcs of these radii cross at the true position of the point in three-dimensional space.

SAR Interferometry

Phase difference between two SAR images

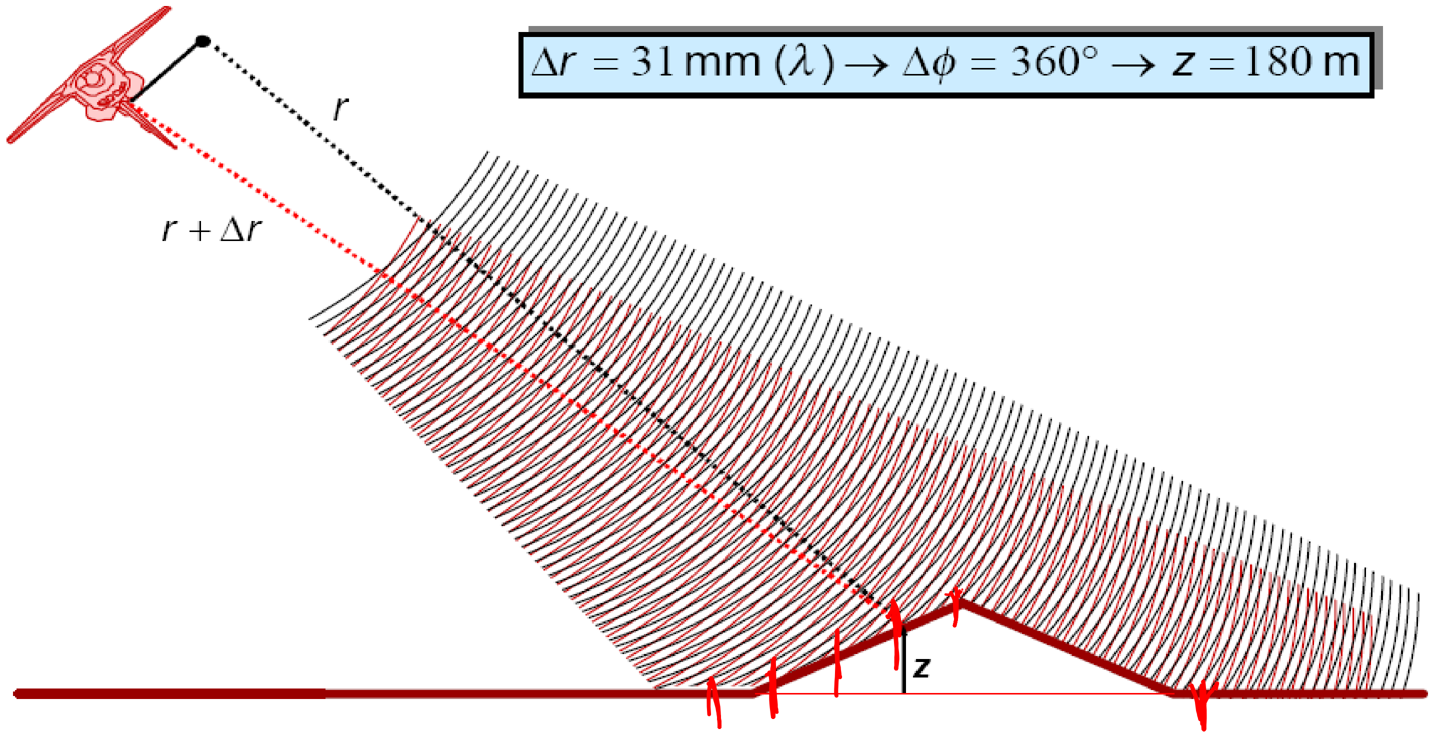

Interferometric measurement principle

Radar phase dif for common transmitter

$$\phi_1 = 2\pi\frac{2R}{\lambda} \qquad \phi_2 = 2\pi\frac{1}{\lambda}(2R + \Delta R)$$

$$\Delta\phi = \phi_1 - \phi_2 = \frac{2\pi}{\lambda}\Delta R$$

For spaceborne SAR $B<<R$

$$(R + \Delta R)^2 = R^2 + B^2 - 2RBcos\left(\frac{\pi}{2} - \Theta + \alpha\right)$$

$$\Delta R \approx -Bsin(\Theta - \alpha)$$

Phase diffrence

$$\Delta\phi = -\frac{2\pi}{\lambda}Bsin(\Theta - \alpha)$$

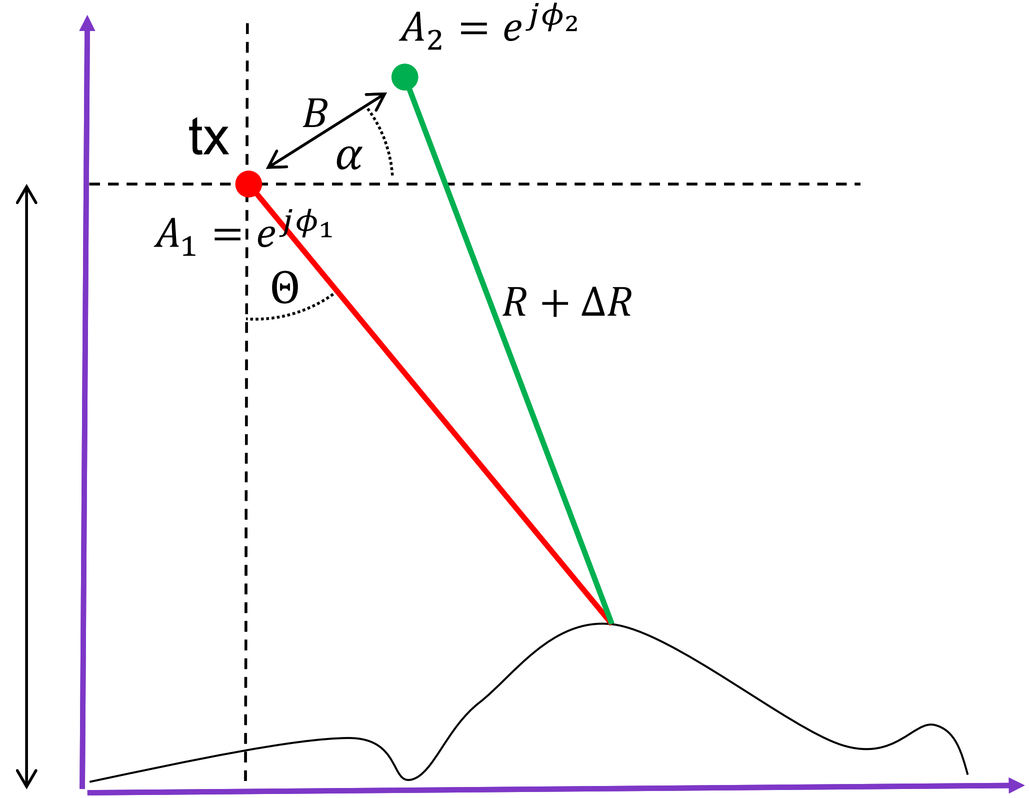

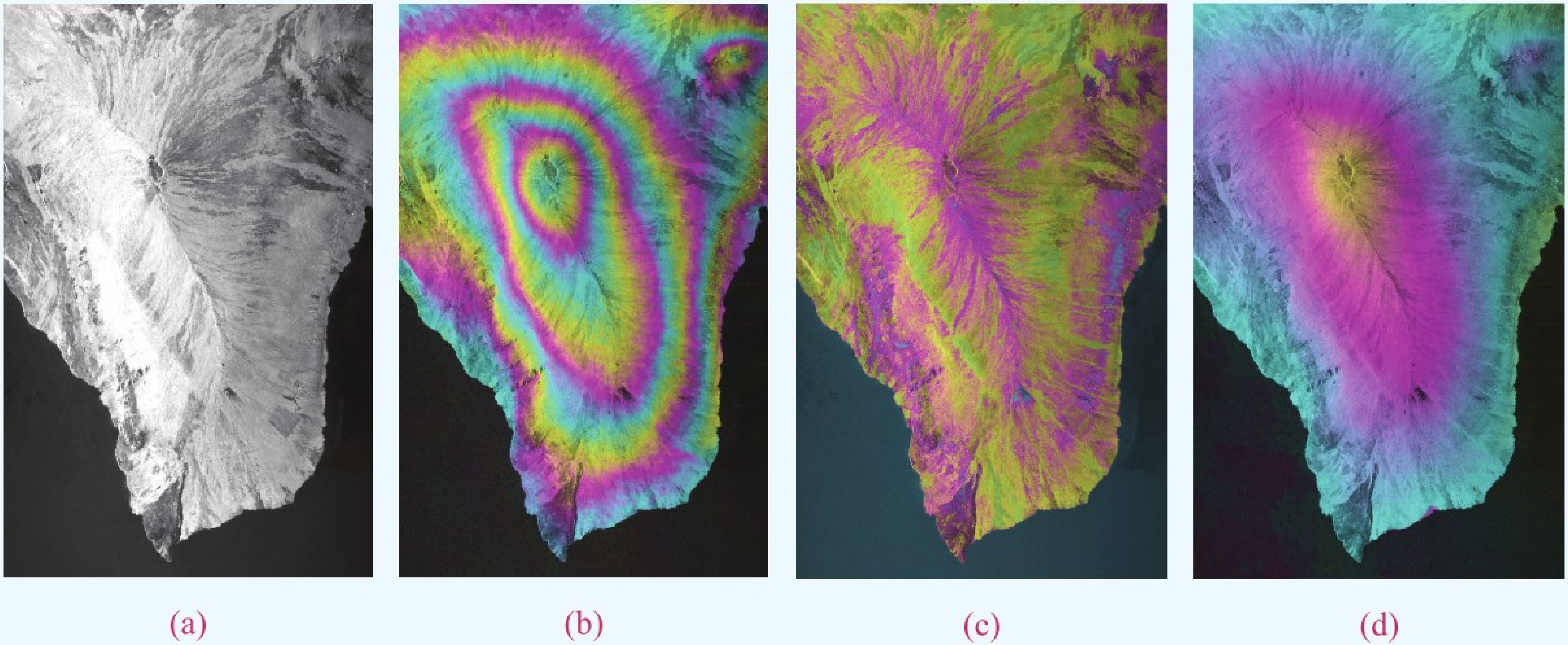

Figure 15-5: Example of interferometric SAR processing: (a) SAR magnitude image, (b) phase difference (interferogram) between two images with flat-Earth phase removed, (c) correlation map between interferogram component scenes, and (d) inferred surface topography.

From: Microwave Radar and Radiometric Remote Sensing, by Ulaby and Long, 2014, with permission.

Aalto University
School of Electrical Engineering

Revisiting SAR image phase

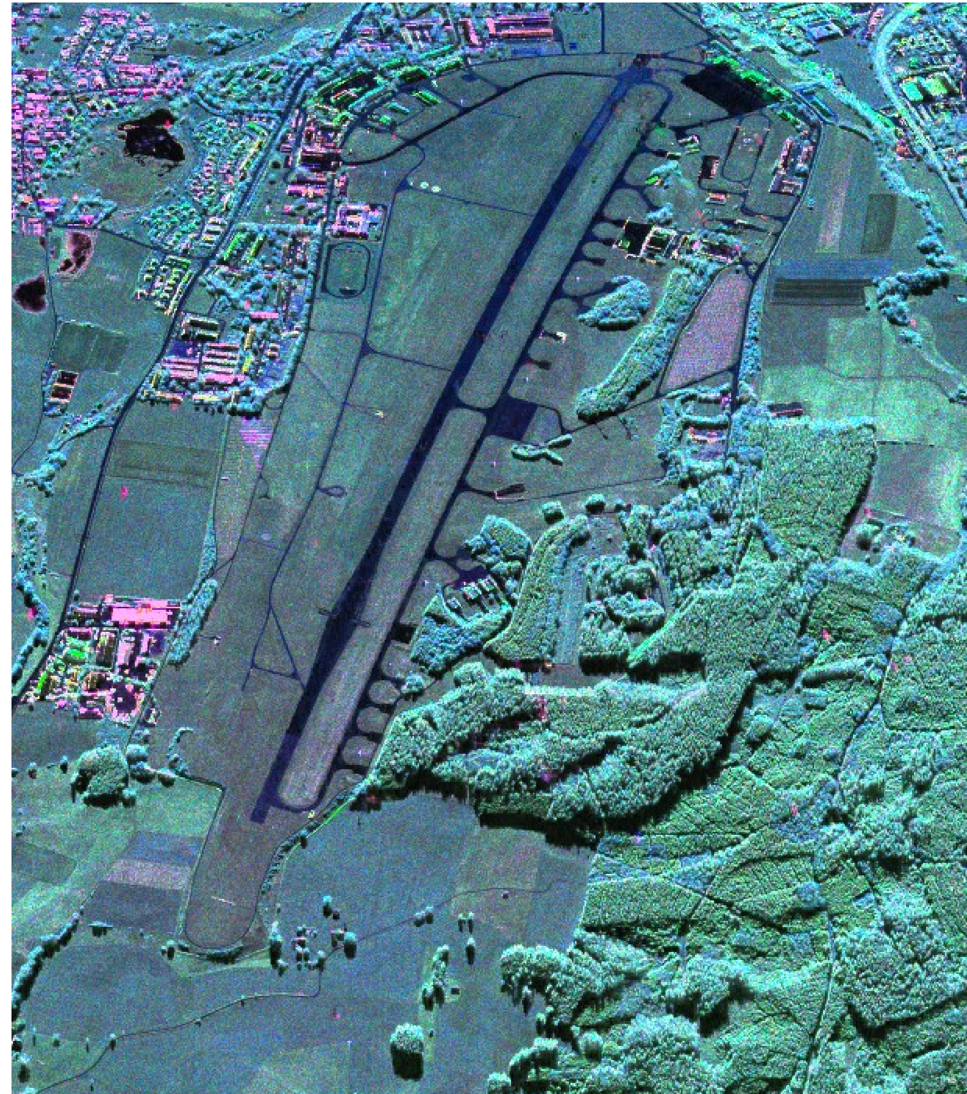

SAR image pixel amplitude

Amplitude tells the amount of signal returned to the radar

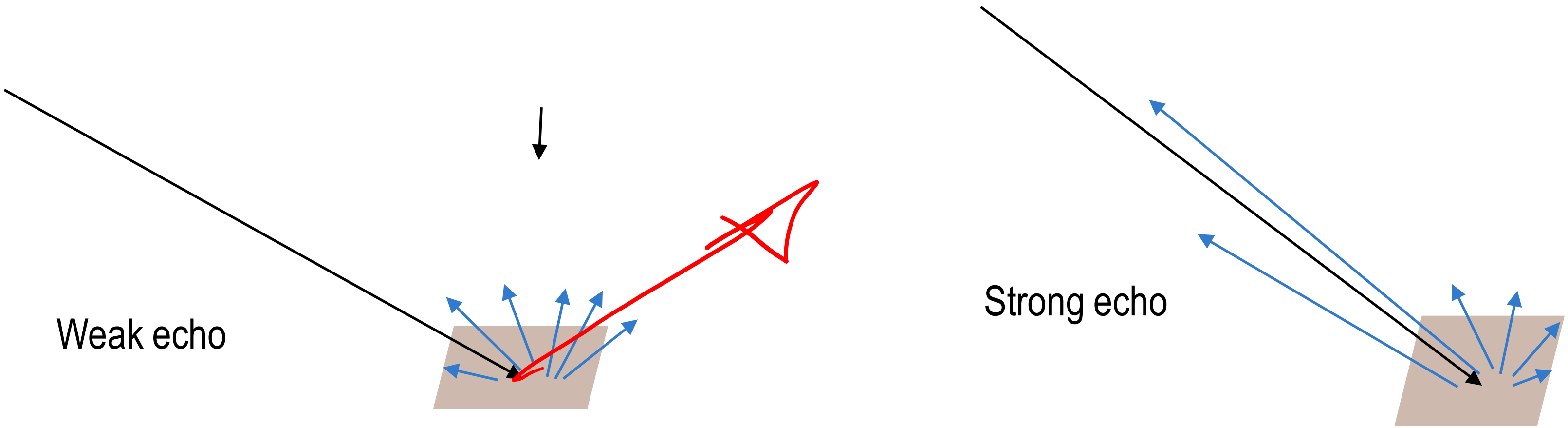

SAR image pixel phase

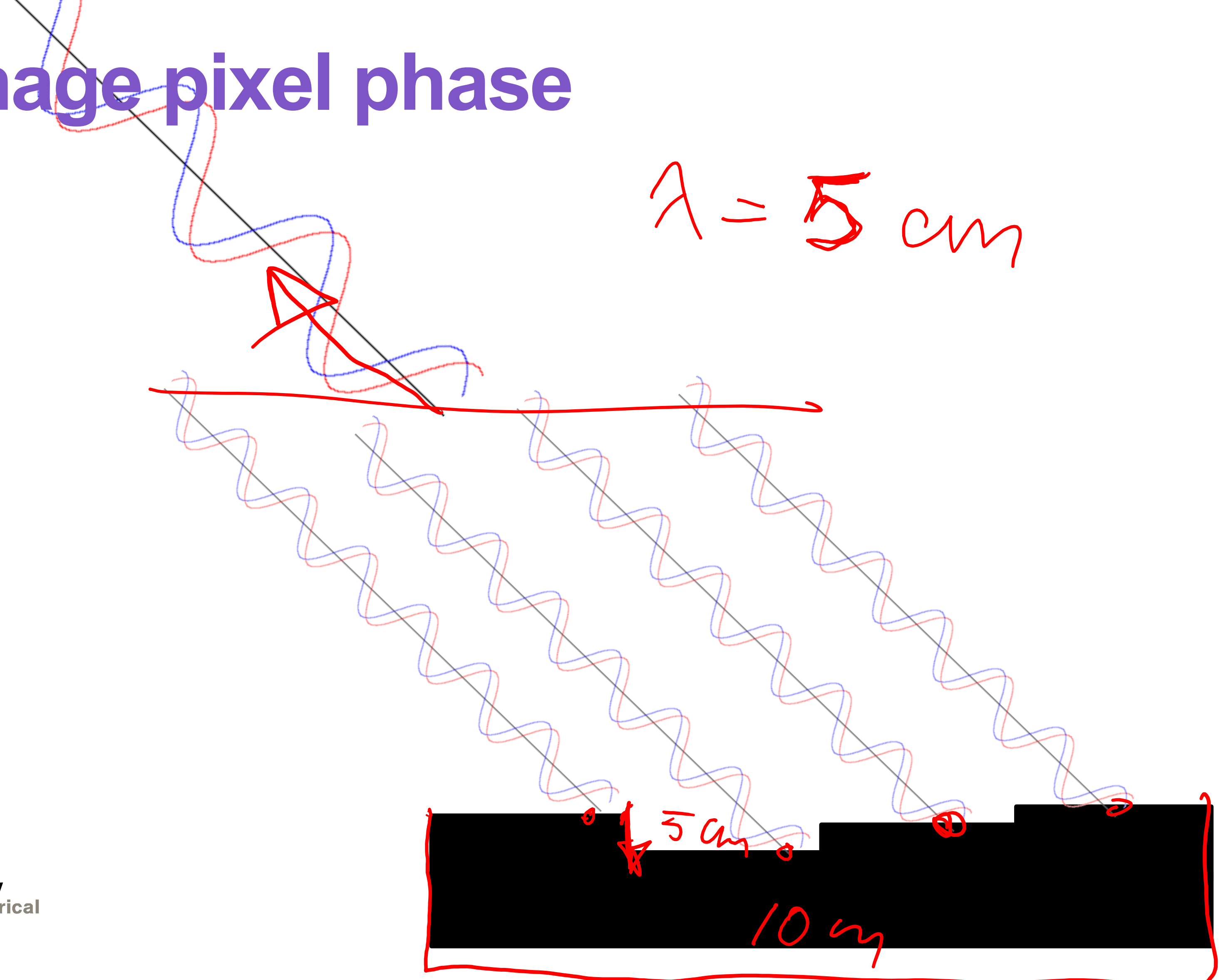

SAR image pixel phase

Phase depends on **distance** from radar to scatterer

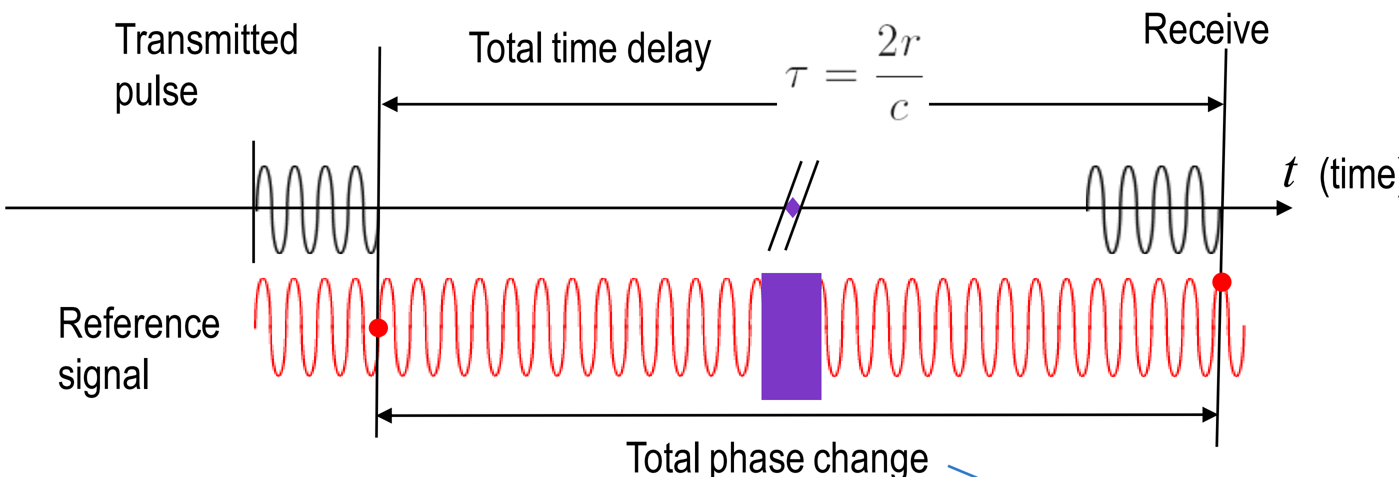

$$\phi = -\frac{4\pi r}{\lambda} + \phi_{scatt}$$

Aalto University
School of Electrical Engineering

Scattering centre phase

- Each pixel of the image (or resolution cell) is usually much larger than the wavelength and contains many scattering elements (scatterers)
- The received signal (pixel value) is the result of the coherent combination (sum) of all individual echoes

Typical types of pixels:

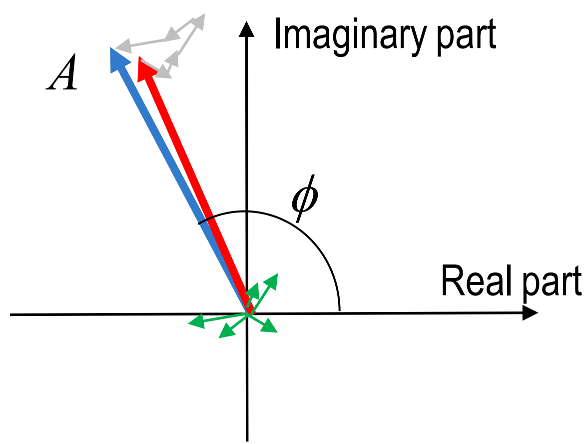

Dominated by a single scatterer

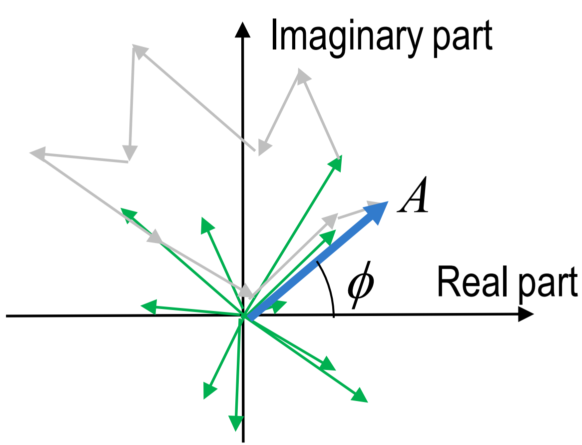

Distributed targets

Phase utility

- So far we have not used the phase of the pixels in the image:
  - Superposition of two terms: path length and scene properties

Millions of phase cycles

$$\phi = -\frac{4\pi r}{\lambda} + \phi_{scatt}$$

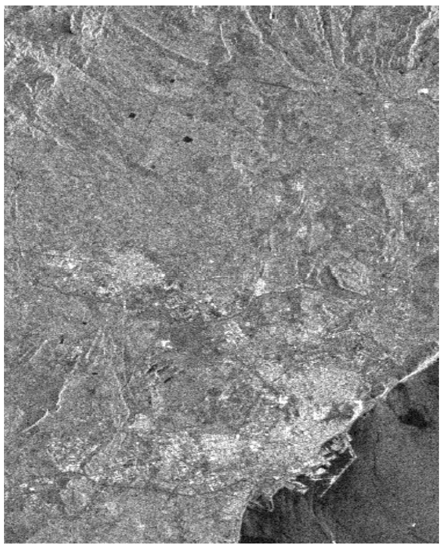

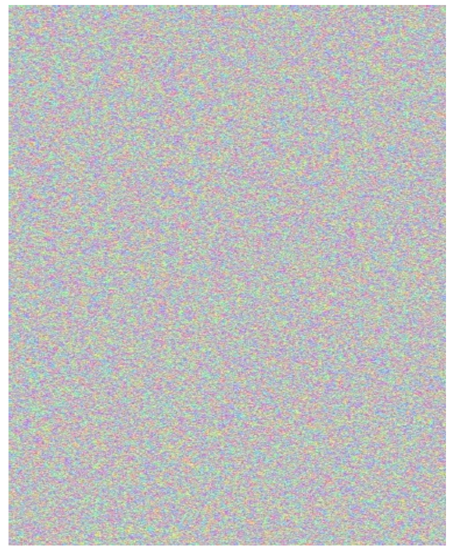

For a single SAR image it may be considered as random (useless)

Phase noise for two images

Phase is random because scatterer placement is random

For two SAR images from almost the same place, the scatterer placement is almost the same:

The scatterer placement noise term is the same for BOTH images!

Two similar noise terms on two images

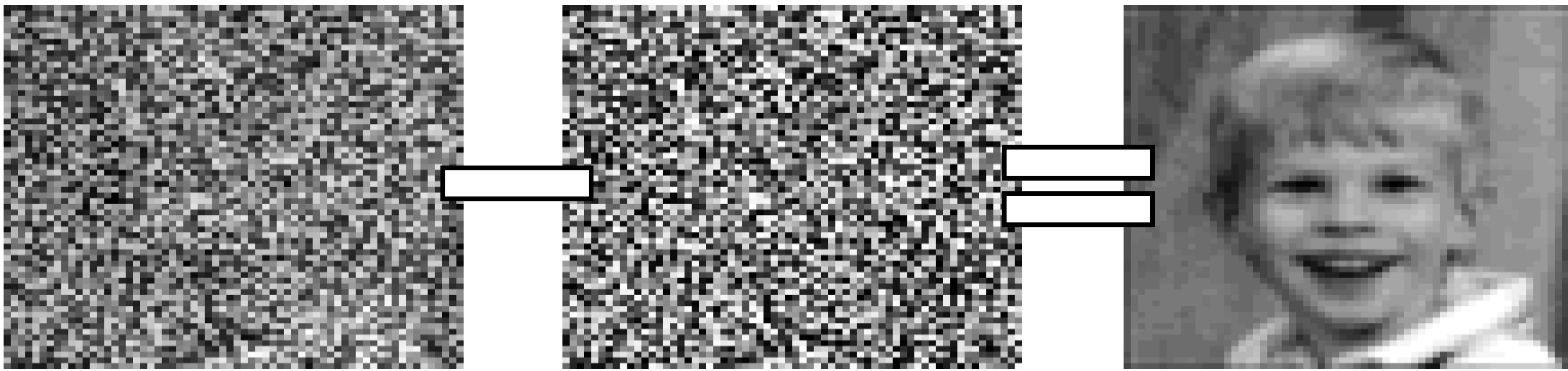

Aalto University
School of Electrical
Engineering

Simple interferometry simulator

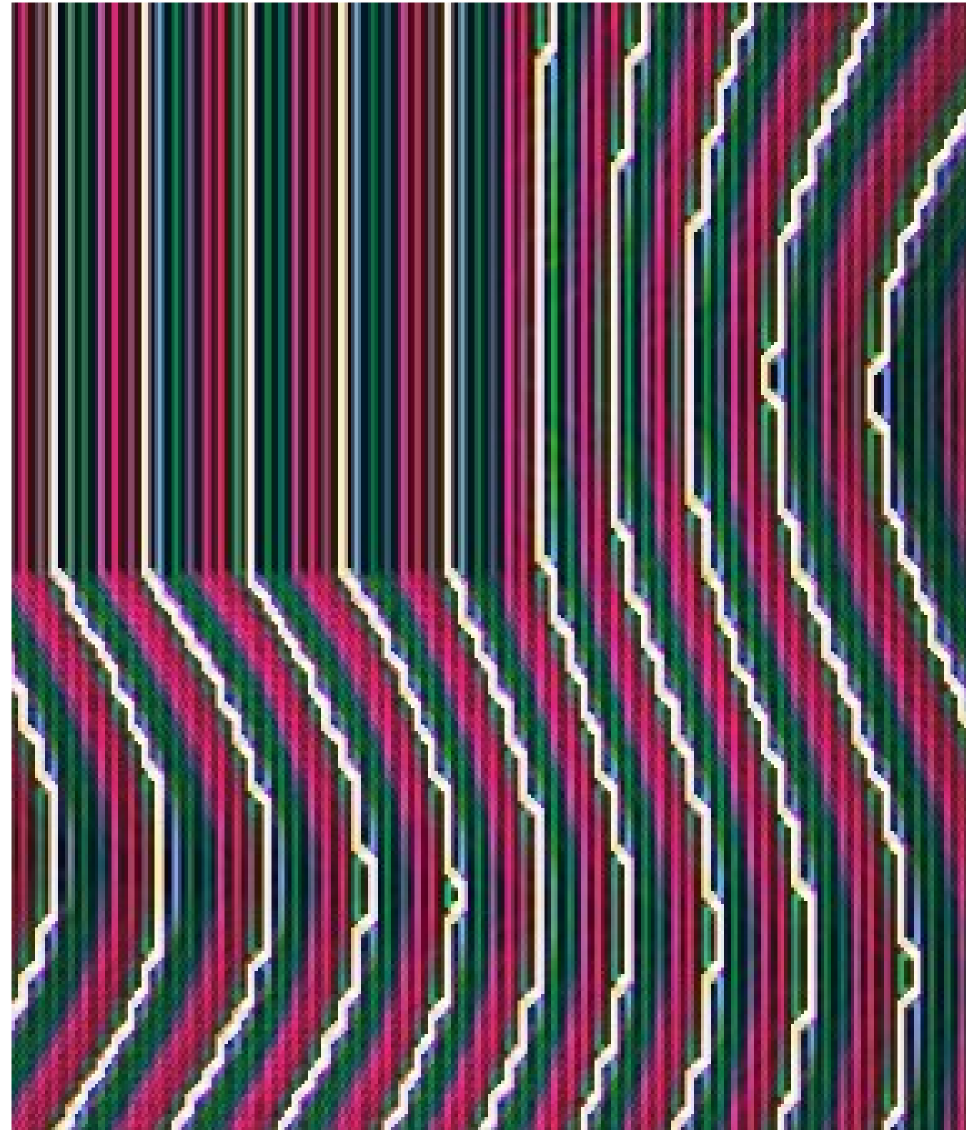

Digital elevation model

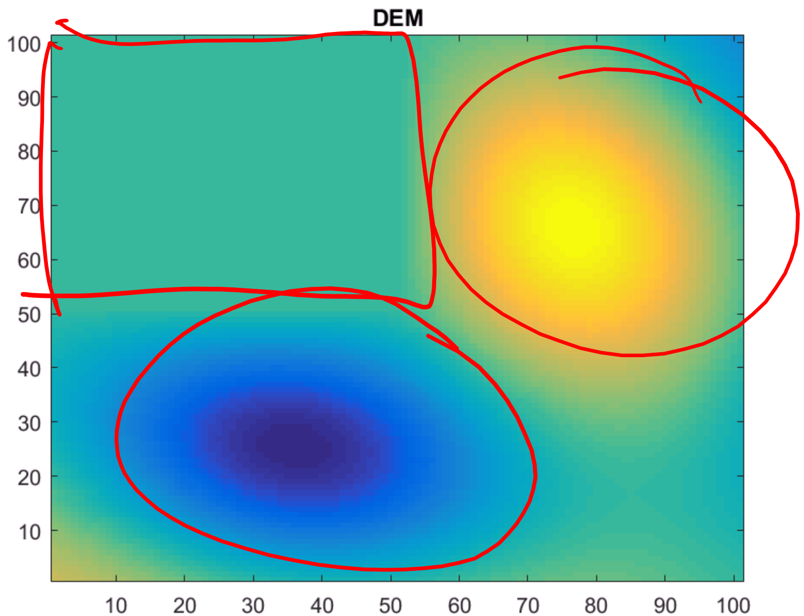

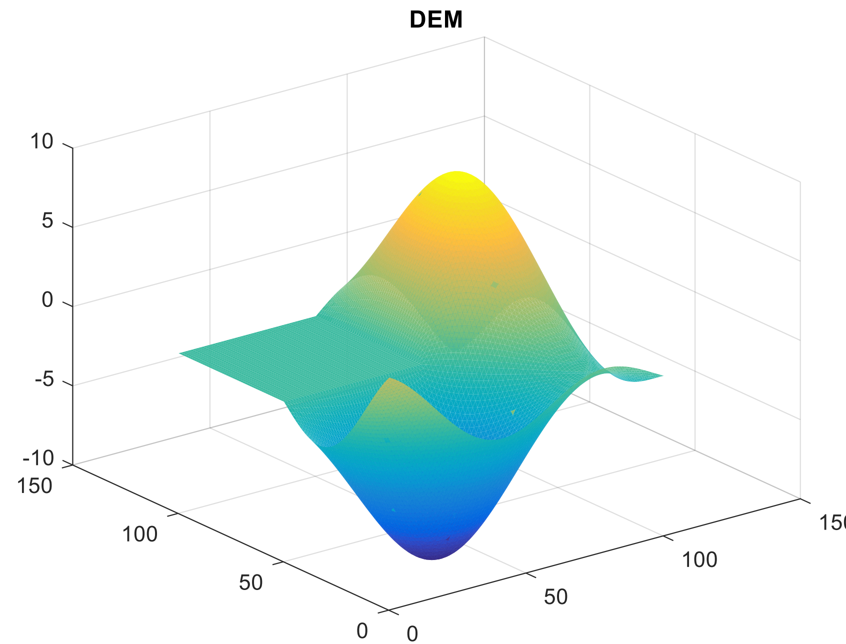

Generic Interferometer Geometry

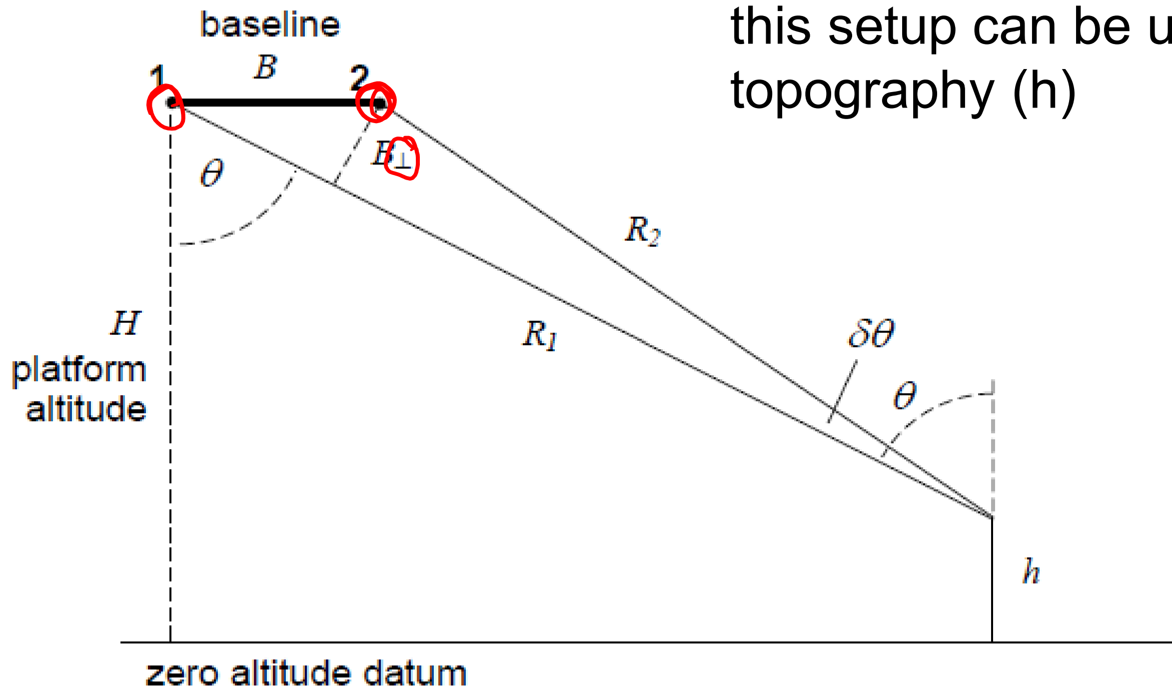

If the acquisition geometry is known, this setup can be used to estimate the topography (h)

Geometry

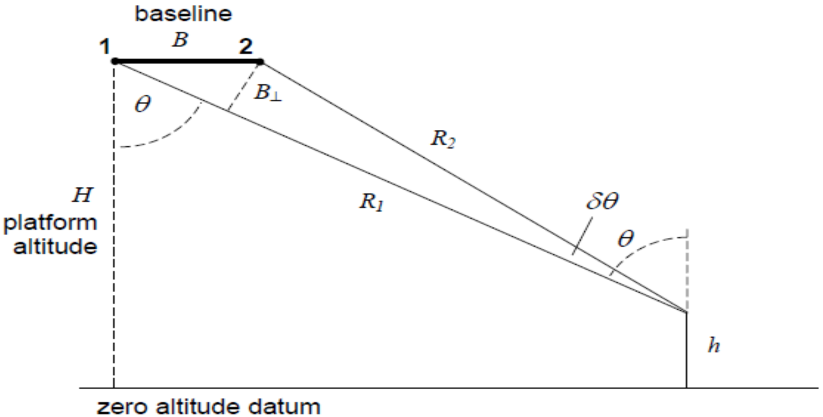

$$E^r(t) = A\rho \exp(j\omega t - \phi_T)$$

$$\phi_T = 2\beta R = \frac{4\pi R}{\lambda}$$

$$R_1 = R_2 \cos\delta\theta + B\sin\theta$$

$$R_1 = R_2 + B\sin\theta$$

$$\Delta R = R_1 - R_2 = B\sin\theta$$

$$\Delta\phi = \frac{4\pi B\sin\theta}{\lambda}$$

interferometric phase angle

$$\frac{d(\Delta\phi)}{dh} = \frac{4\pi B_\perp}{\lambda R_o \sin\theta} = \frac{4\pi B_\perp \cos\theta}{\lambda H \sin\theta}$$

$$\alpha_{IF} = \frac{dh}{d(\Delta\phi)}$$

$$h(x,y) = \alpha_{IF}\Delta\phi(x,y) + \text{constant}$$

Inclined baseline:

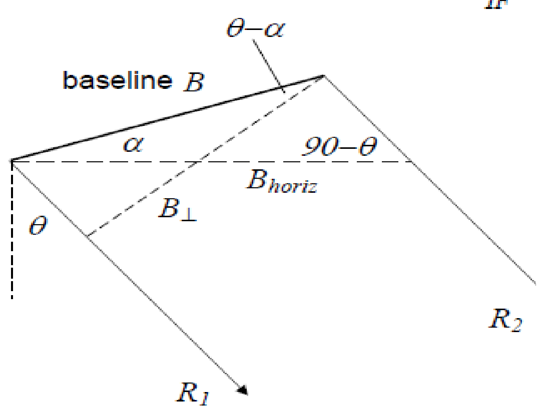

$$\frac{d(\Delta\phi)}{dh} = \frac{4\pi B_\perp}{\lambda R_o \sin\theta} = \frac{4\pi B_\perp \cos(\theta-\alpha)}{\lambda H \sin\theta}$$

Measurement geometry

Let's st up a simple interferometric measurement

H=300

B=25

D=200

λ=0.5

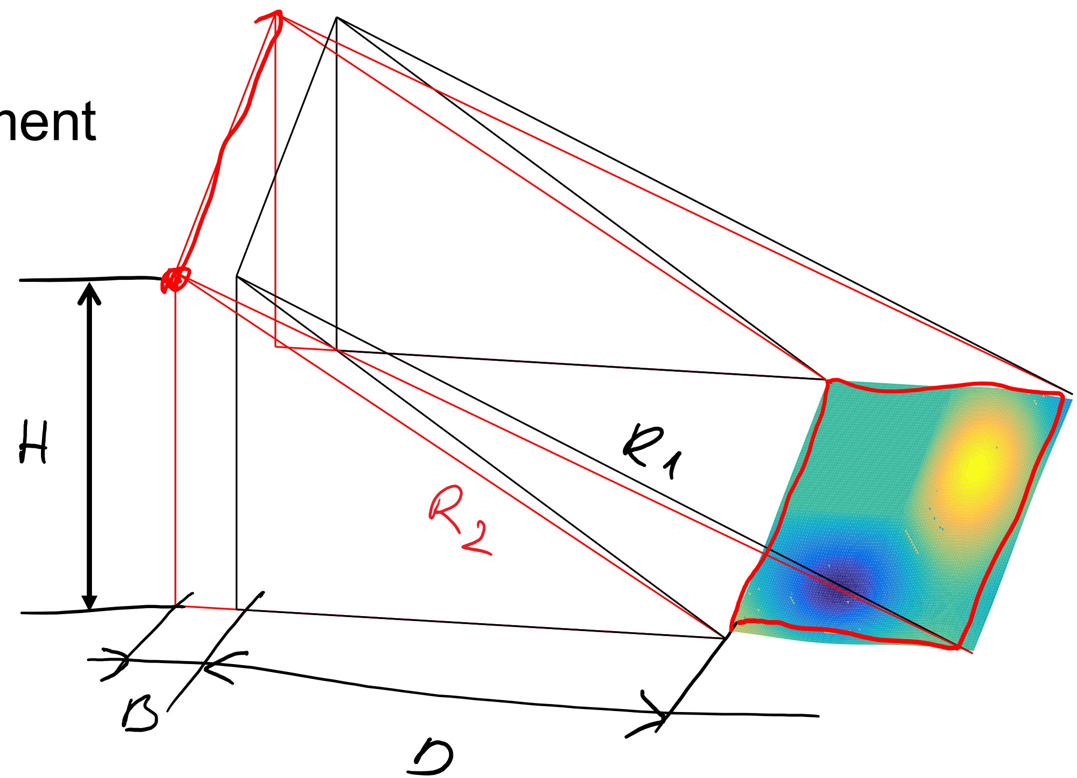

Distance from Sensor 1 to Ground

$$R_1^2 = (H - h)^2 + (D + y)^2$$

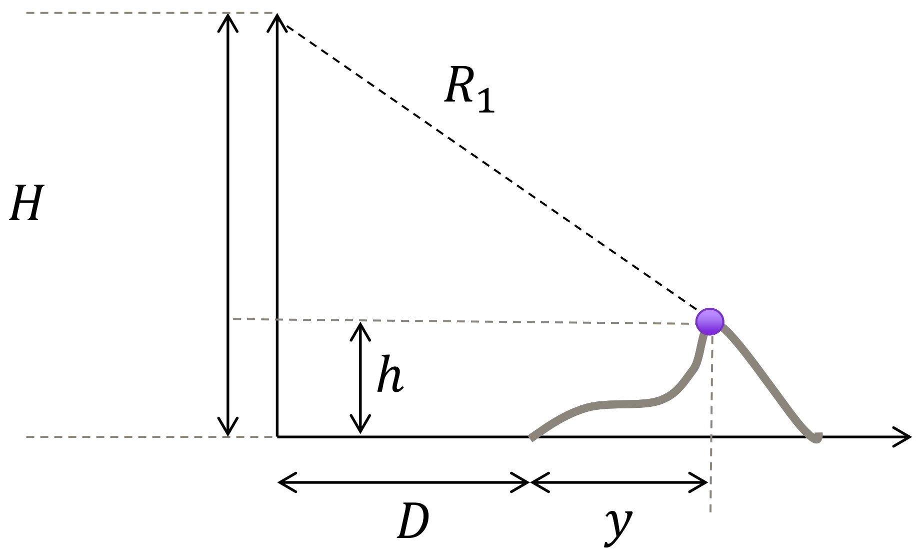

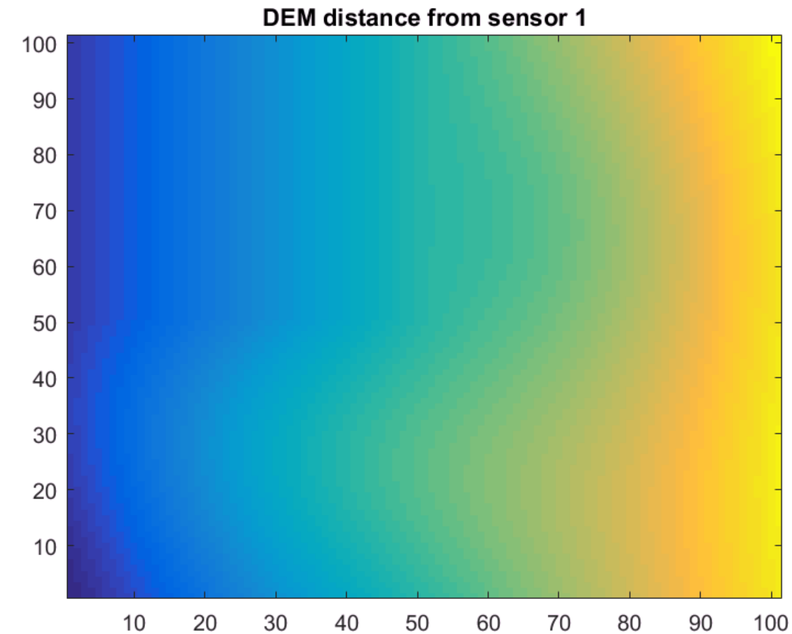

Distance from Sensor 1 to Ground

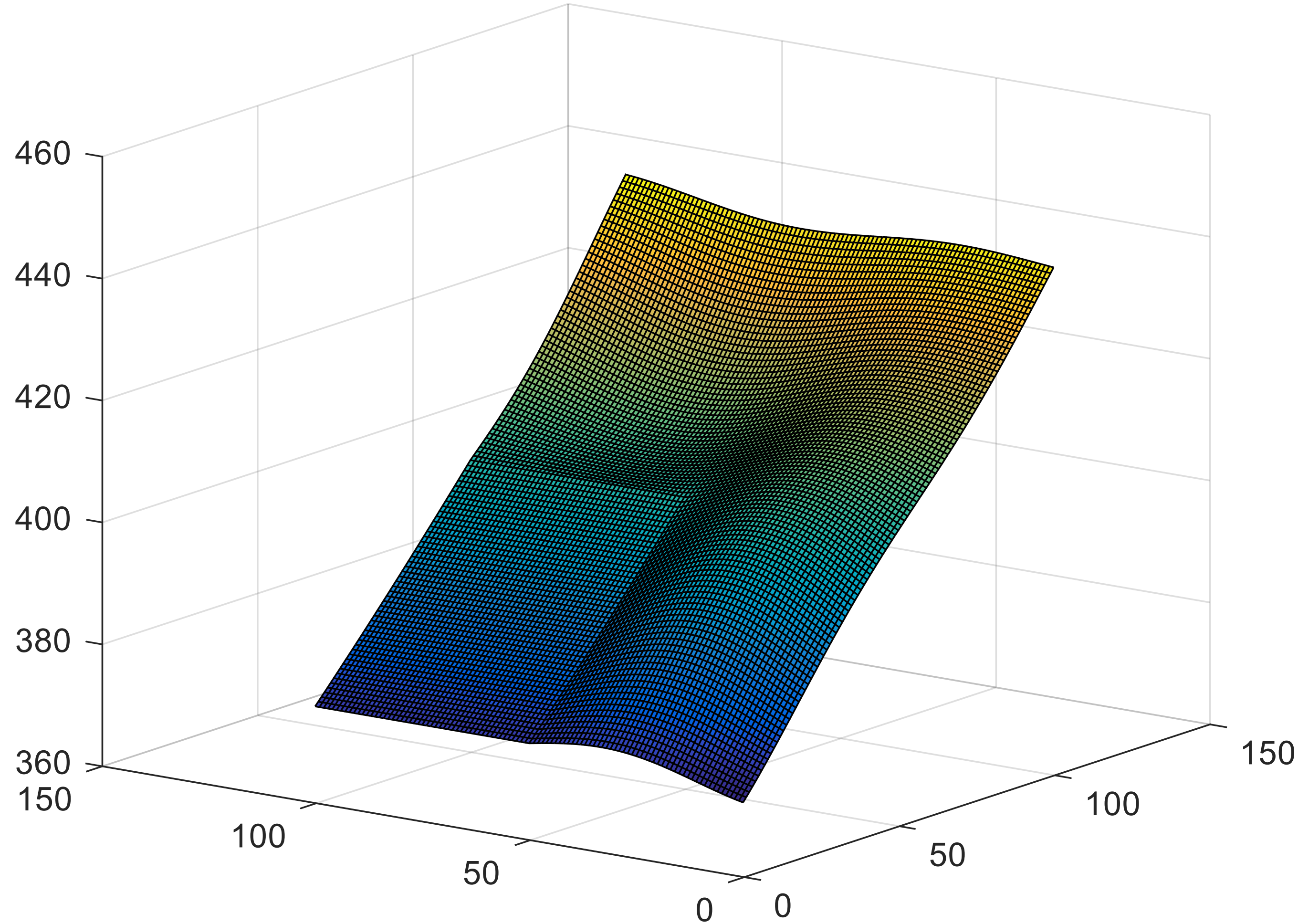

Aalto University
School of Electrical Engineering

Sensor 1 (ideal) phase map

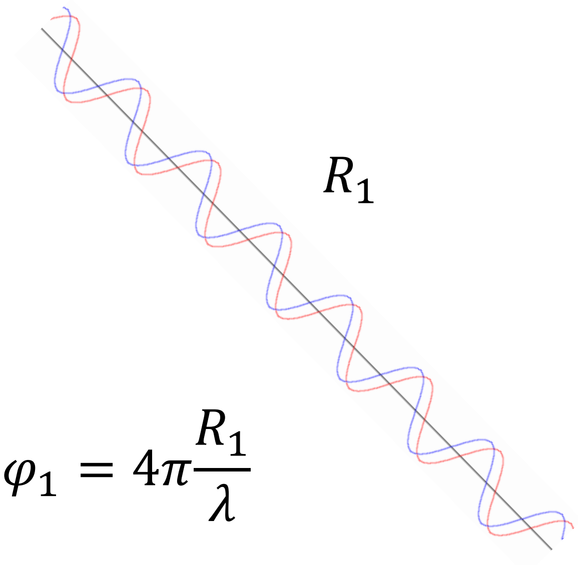

$$\varphi_1 = 4\pi \frac{R_1}{\lambda}$$

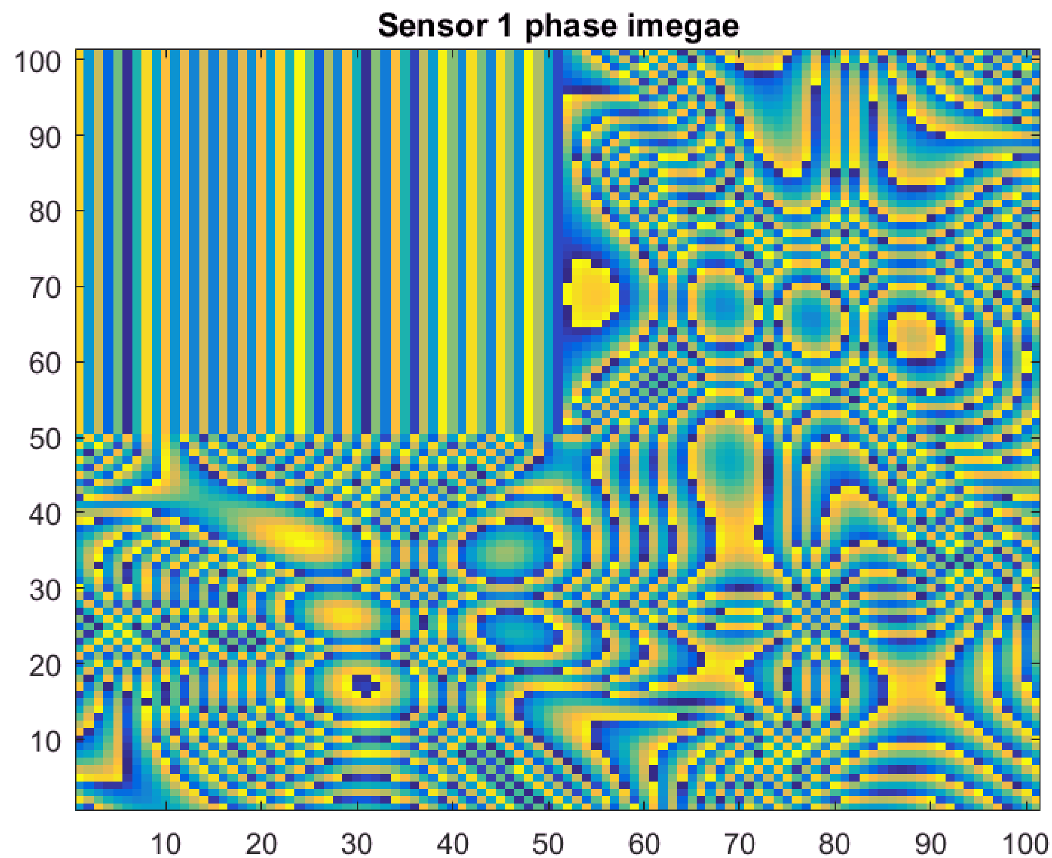

Aalto University
School of Electrical Engineering

Adding random phase component

$$\varphi_1 = 4\pi\frac{R_1}{\lambda} + \varphi_{random}$$

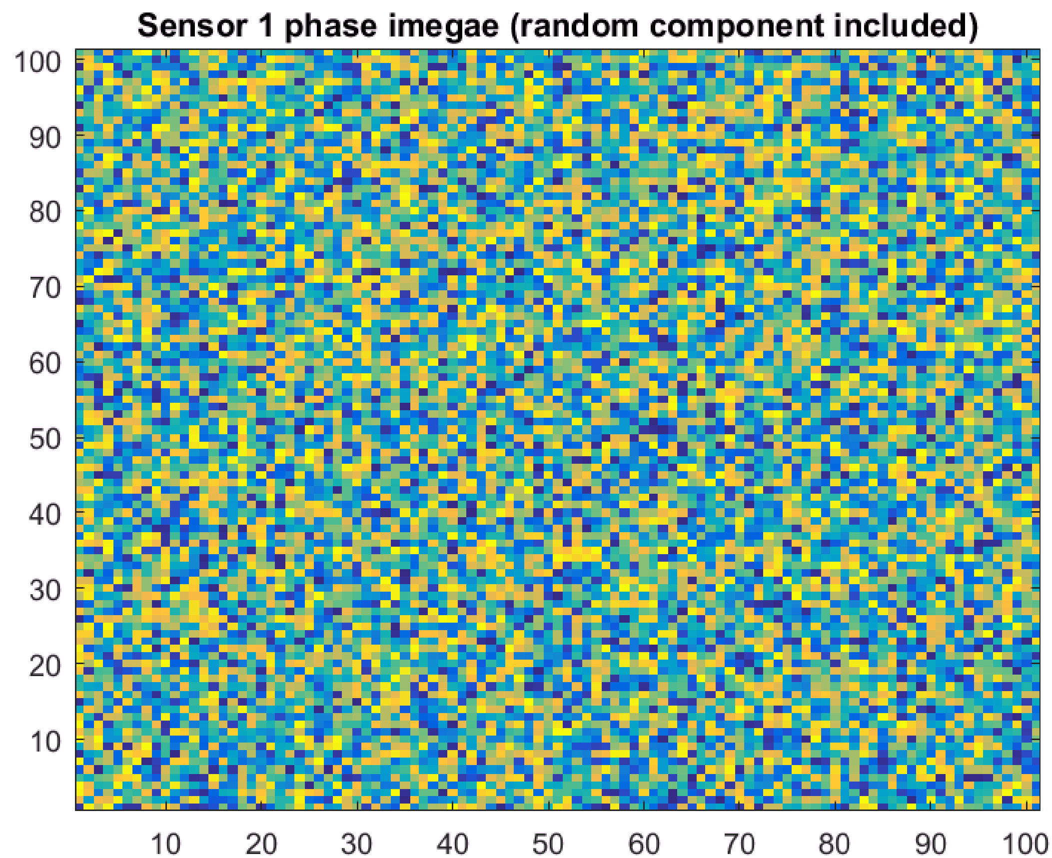

Distance from Sensor 2 to Ground

$$R_1^2 = (H - h)^2 + (D + y)^2$$

$$R_2^2 = (H - h)^2 + (D + B + y)^2$$

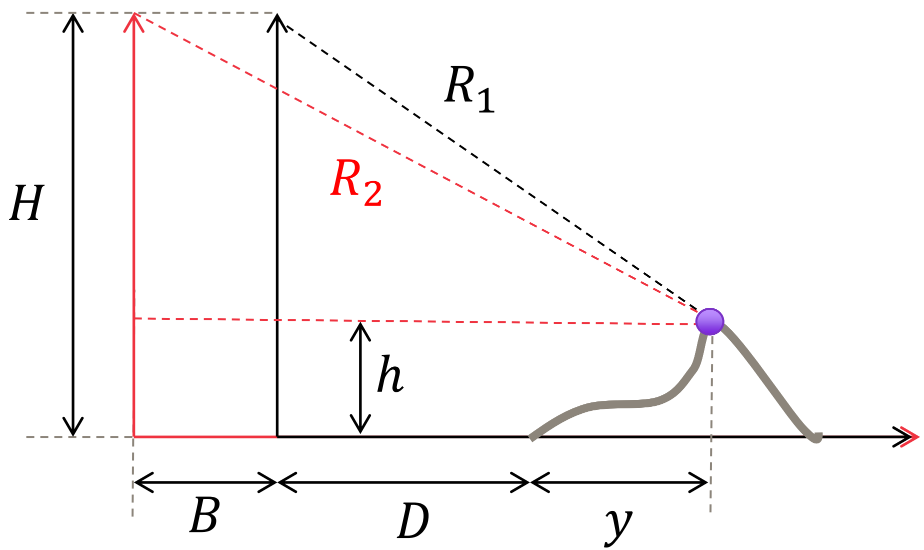

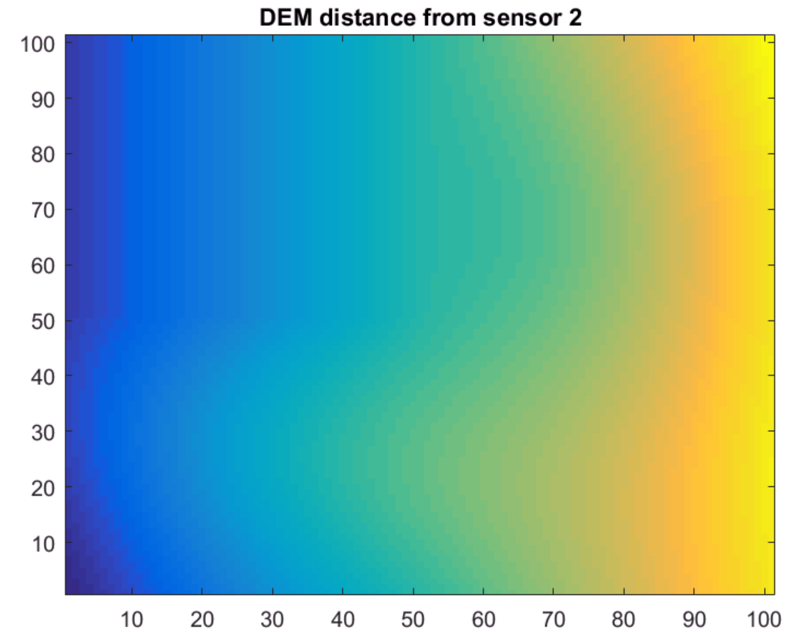

Aalto University
School of Electrical
Engineering

Sensor 2 (ideal) phase map

$$\varphi_2 = 4\pi\frac{R_2}{\lambda}$$

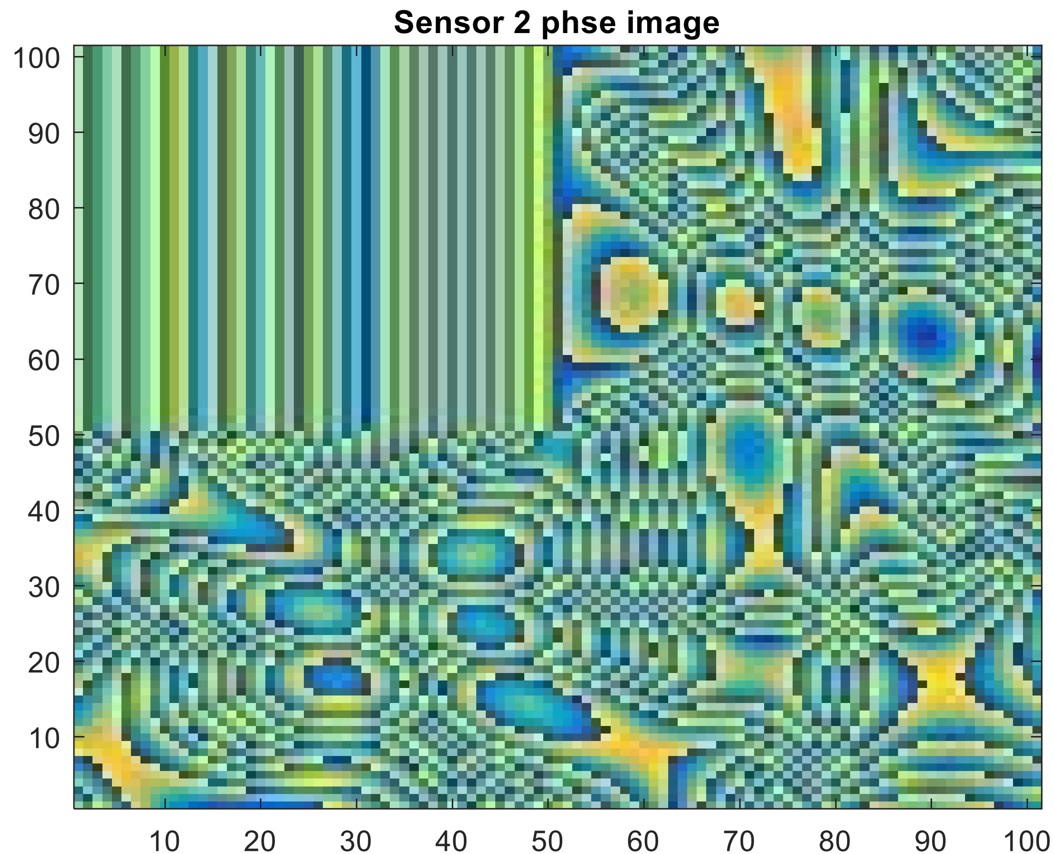

Adding random phase component

$$\varphi_2 = 4\pi\frac{R_2}{\lambda} + \varphi_{random}$$

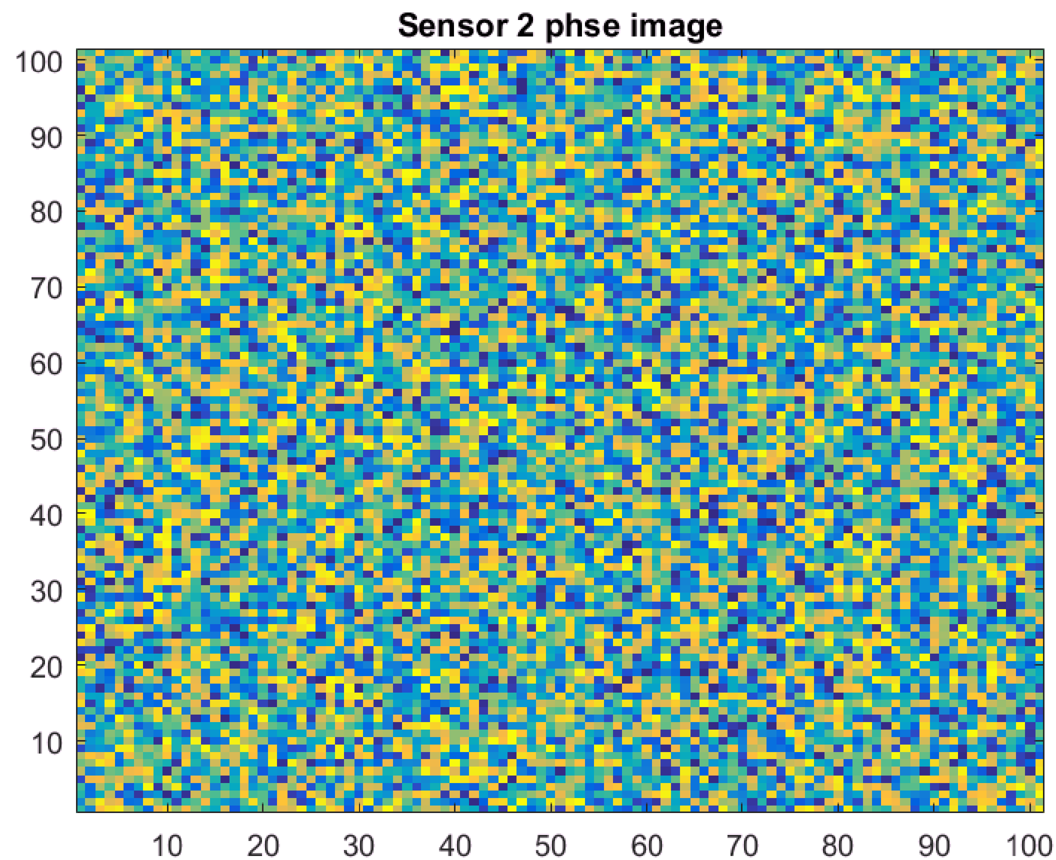

Phase difference of Sensor 1 and 2

Phase difference corresponds to distance difference map

$$\varphi_{int} = \varphi_2 - \varphi_2$$

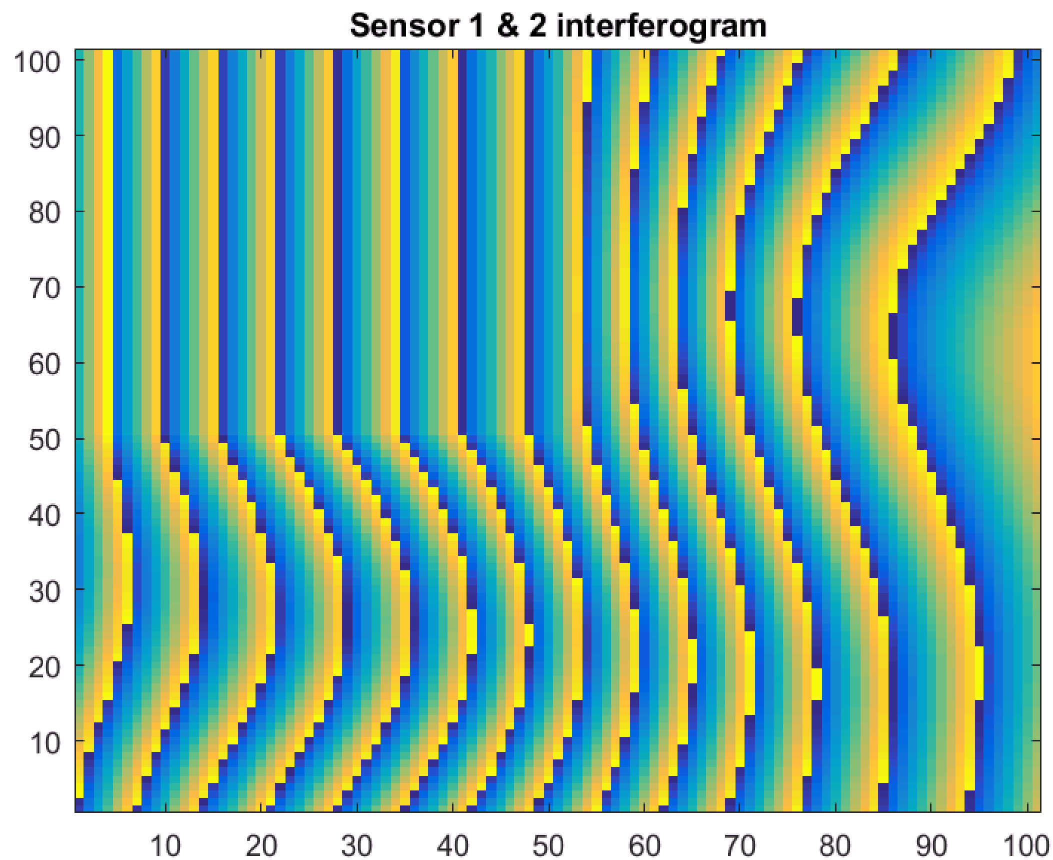

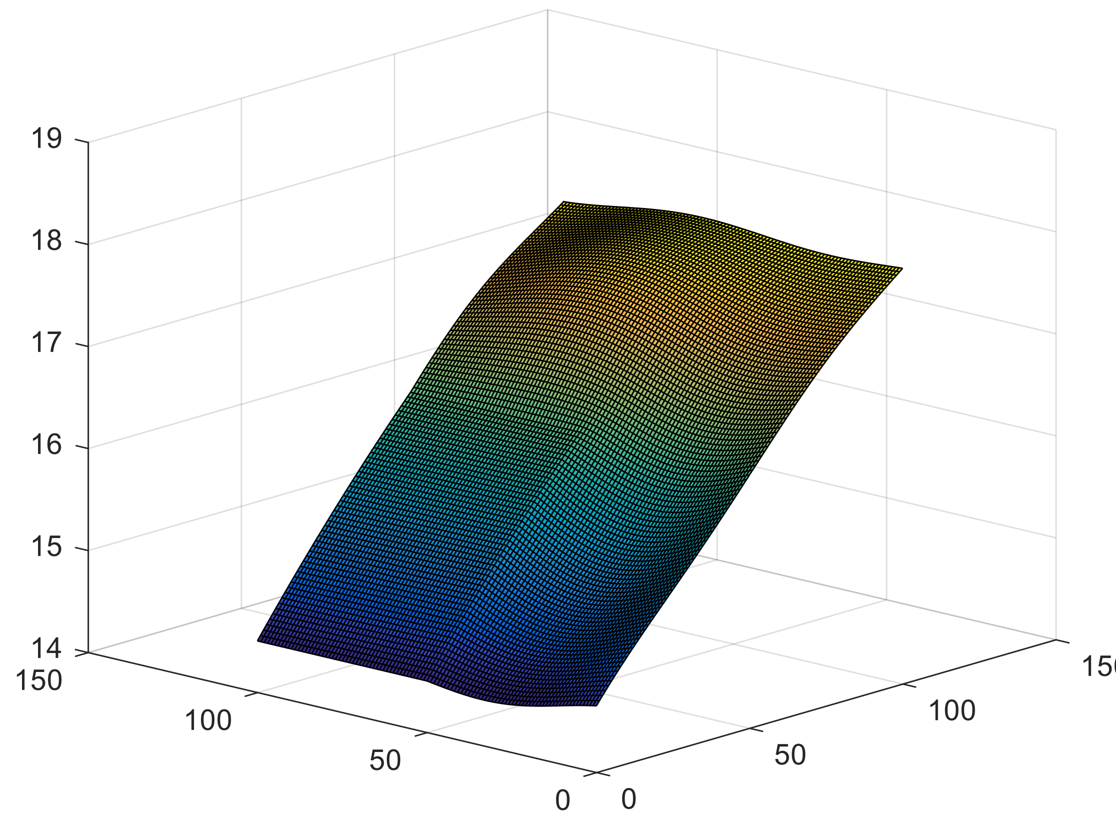
19
18
17
16
15
14
150
100
50
0
0
50
100
150

Flat Earth

$$R_{1Flat} - R_{2Flat}$$

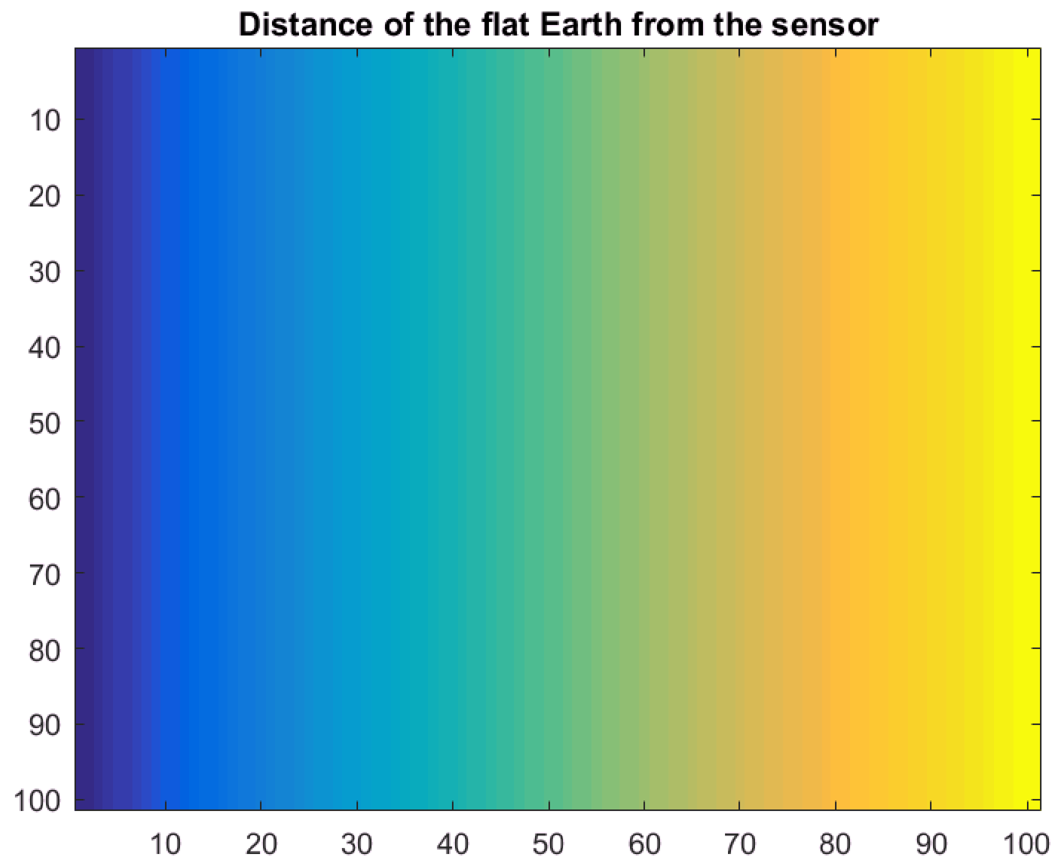

Aalto University
School of Electrical
Engineering

Flat Earth phase

Actually the distance difference to flat Earth

$$\varphi_{Flat} = 4\pi\frac{R_{1Flat} - R_{2Flat}}{\lambda}$$

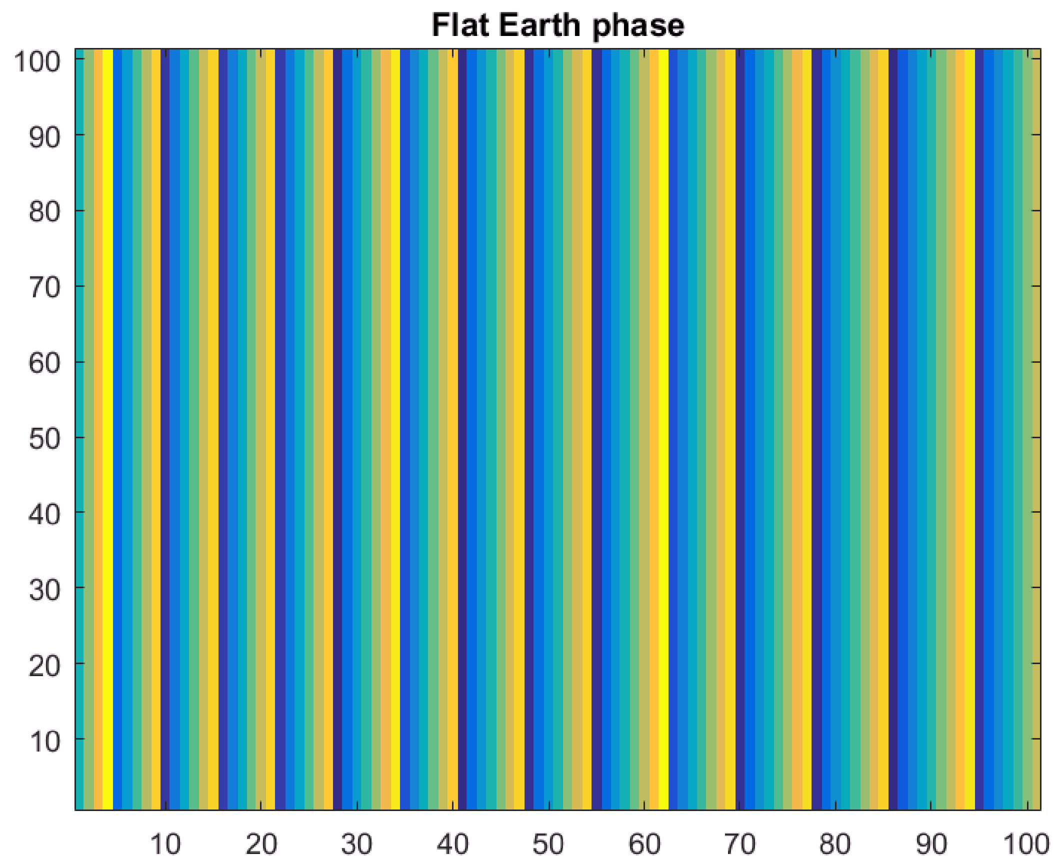

$$\varphi_{int} = \varphi_2 - \varphi_2$$

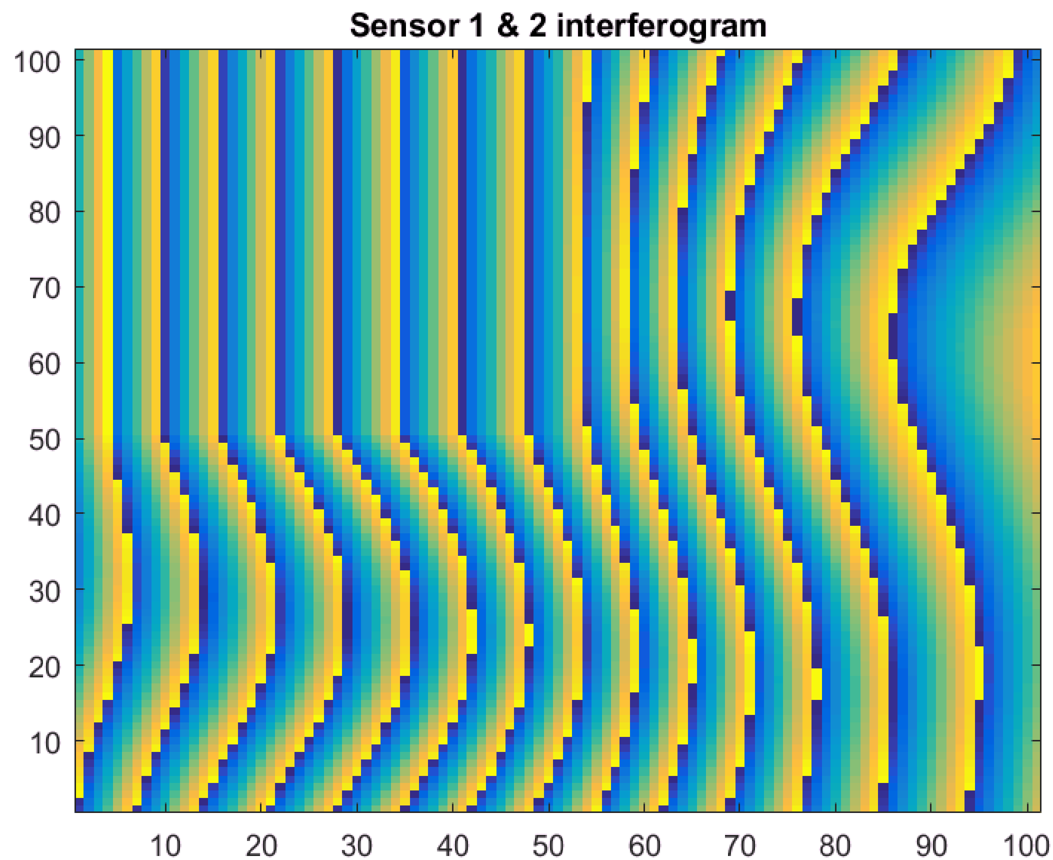

$$\varphi_{int} - \varphi_{Flat}$$

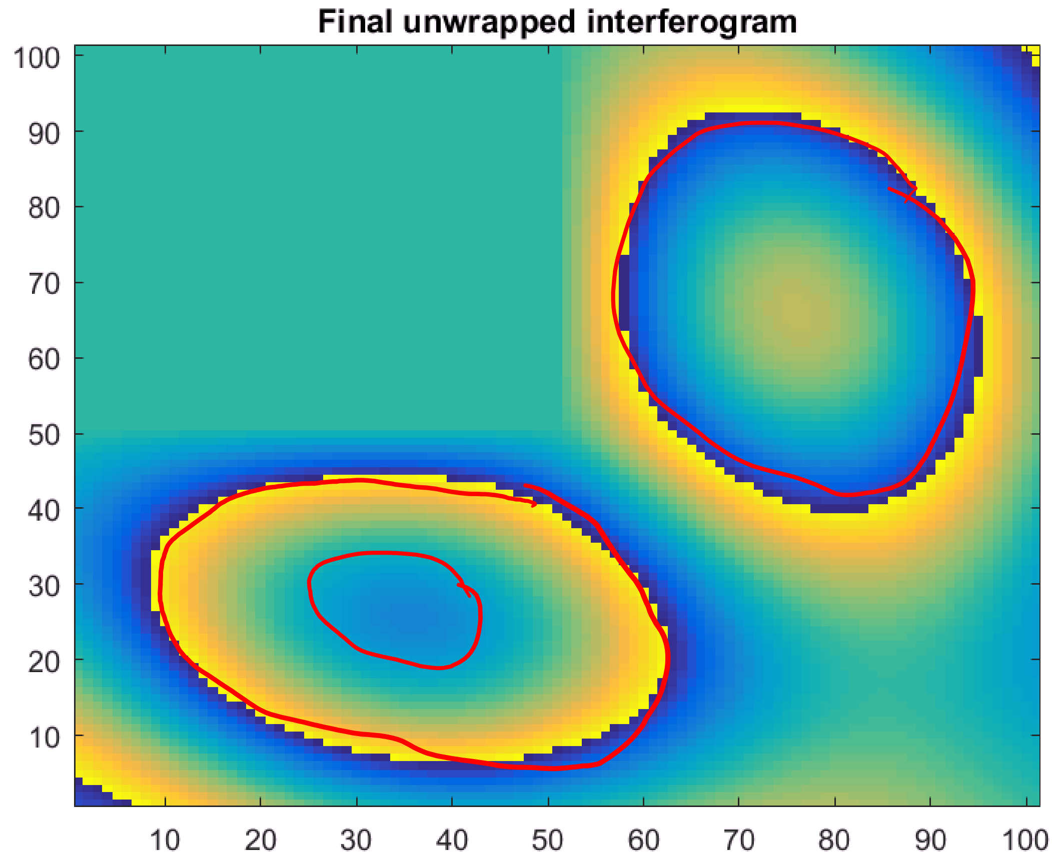

Unwrapped interferogram in 3D plot

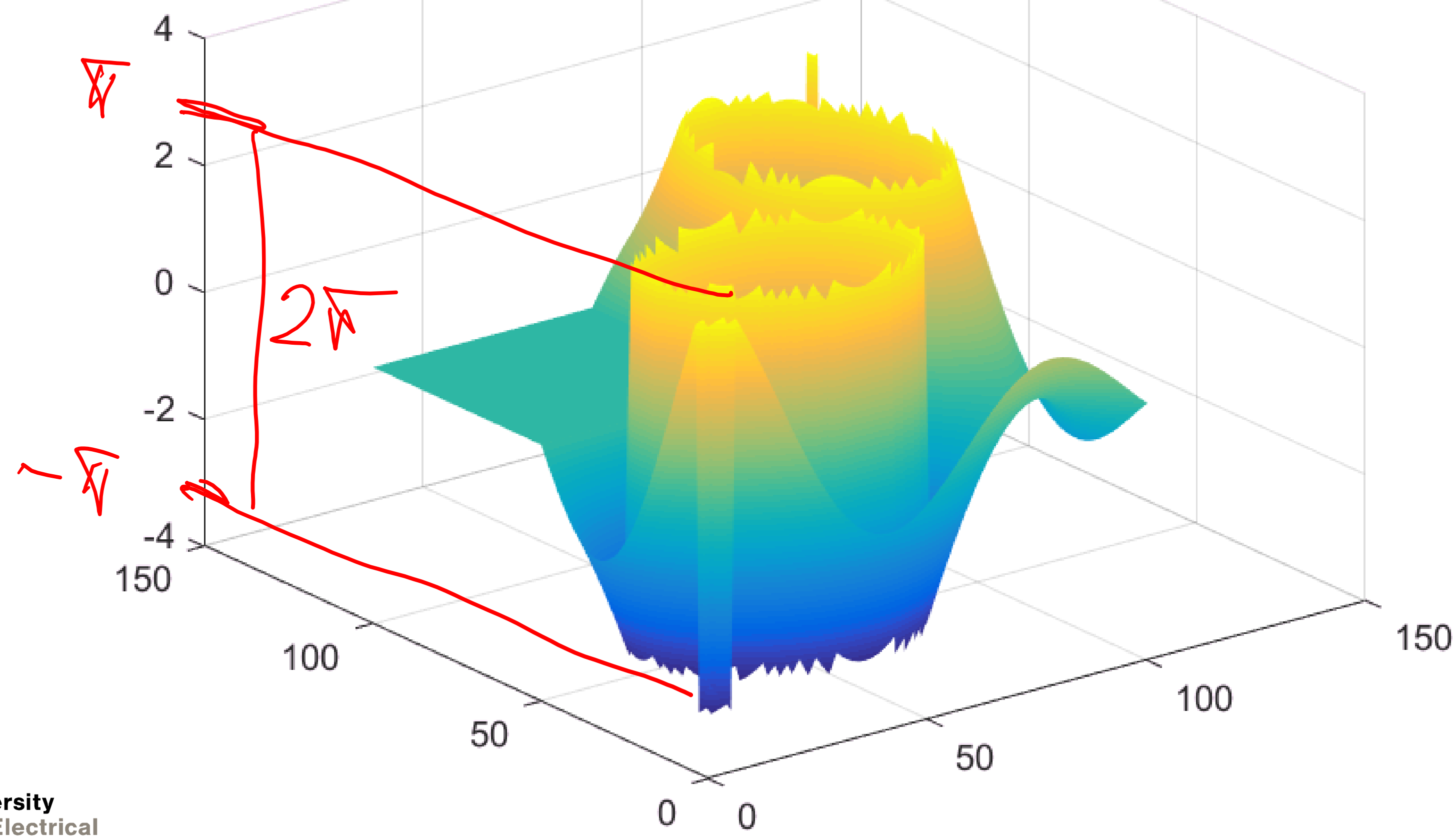

Aalto University
School of Electrical
Engineering

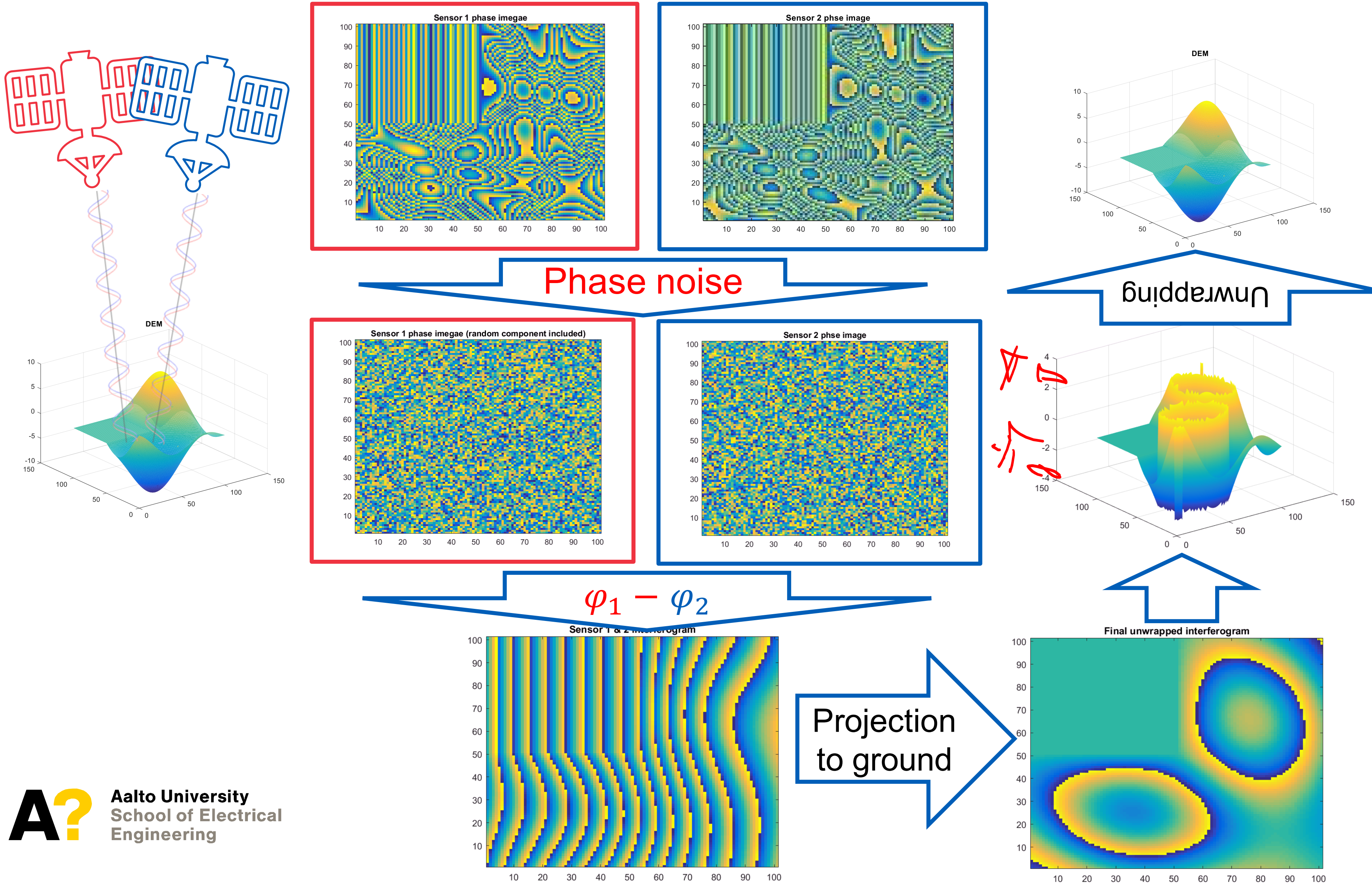

Aalto University
School of Electrical Engineering

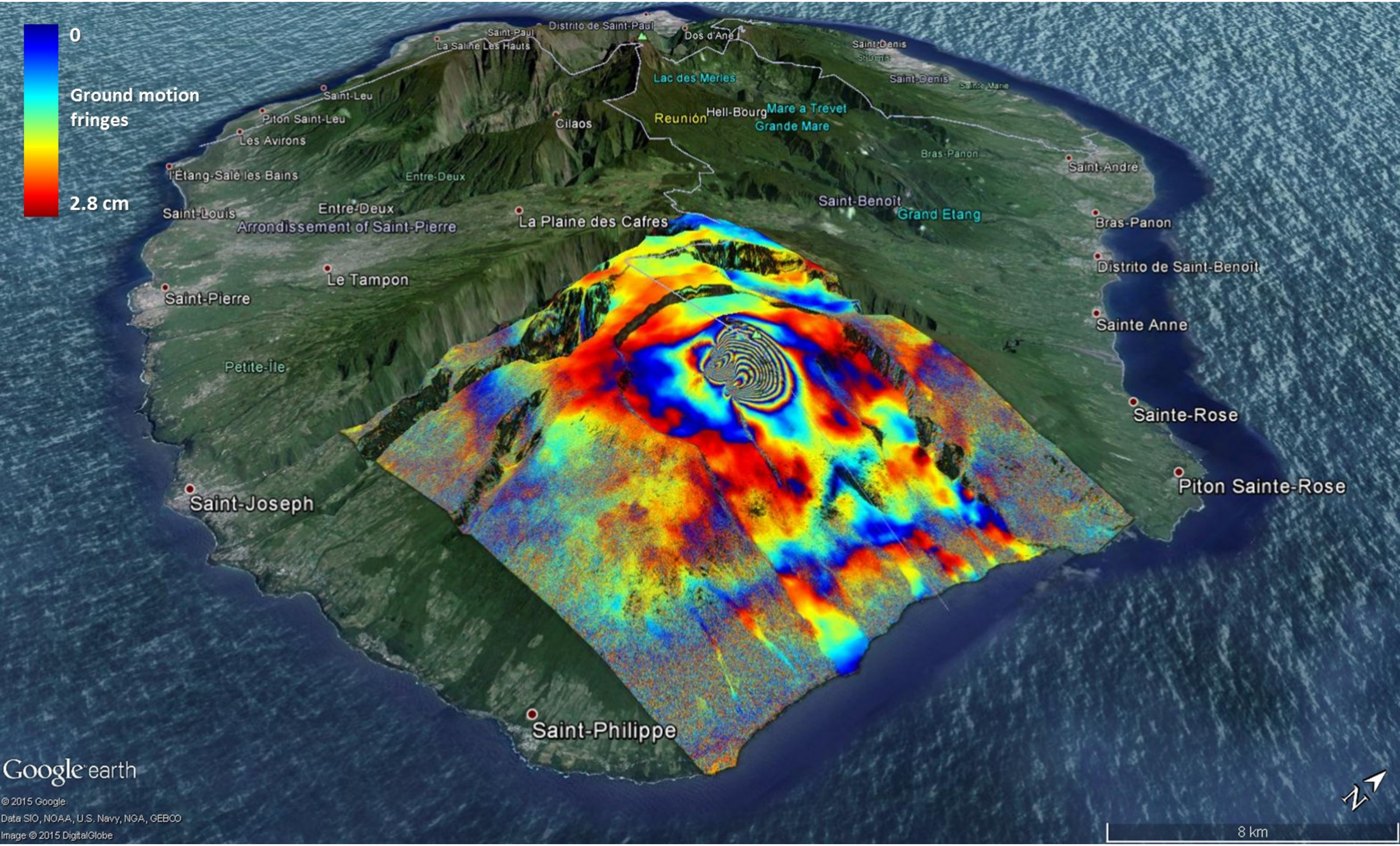
0
Ground motion fringes
2.8 cm
Distrito de Saint-Paul
Saint-Paul
La Saline Les Hauts
Dos d'Ane
Saint-Denis
Lac des Merles
Saint-Denis
Saint-Leu
Piton Saint-Leu
Cilaos
Reunion
Hell-Bourg
Mare a Trevet
Grande Mare
Les Avirons
Bras-Panon
Saint-André
l'Étang-Salé les Bains
Entre-Deux
Saint-Louis
Entre-Deux
Arrondissement of Saint-Pierre
La Plaine des Cafres
Saint-Benoît
Grand Etang
Bras-Panon
Distrito de Saint-Benoît
Le Tampon
Saint-Pierre
Sainte Anne
Petite-Île
Sainte-Rose
Piton Sainte-Rose
Saint-Joseph
Saint-Philippe
Google earth
© 2015 Google
Data SIO, NOAA, U.S. Navy, NGA, GEBCO
Image © 2015 DigitalGlobe
8 km

Aalto University
School of Electrical
Engineering

InSAR

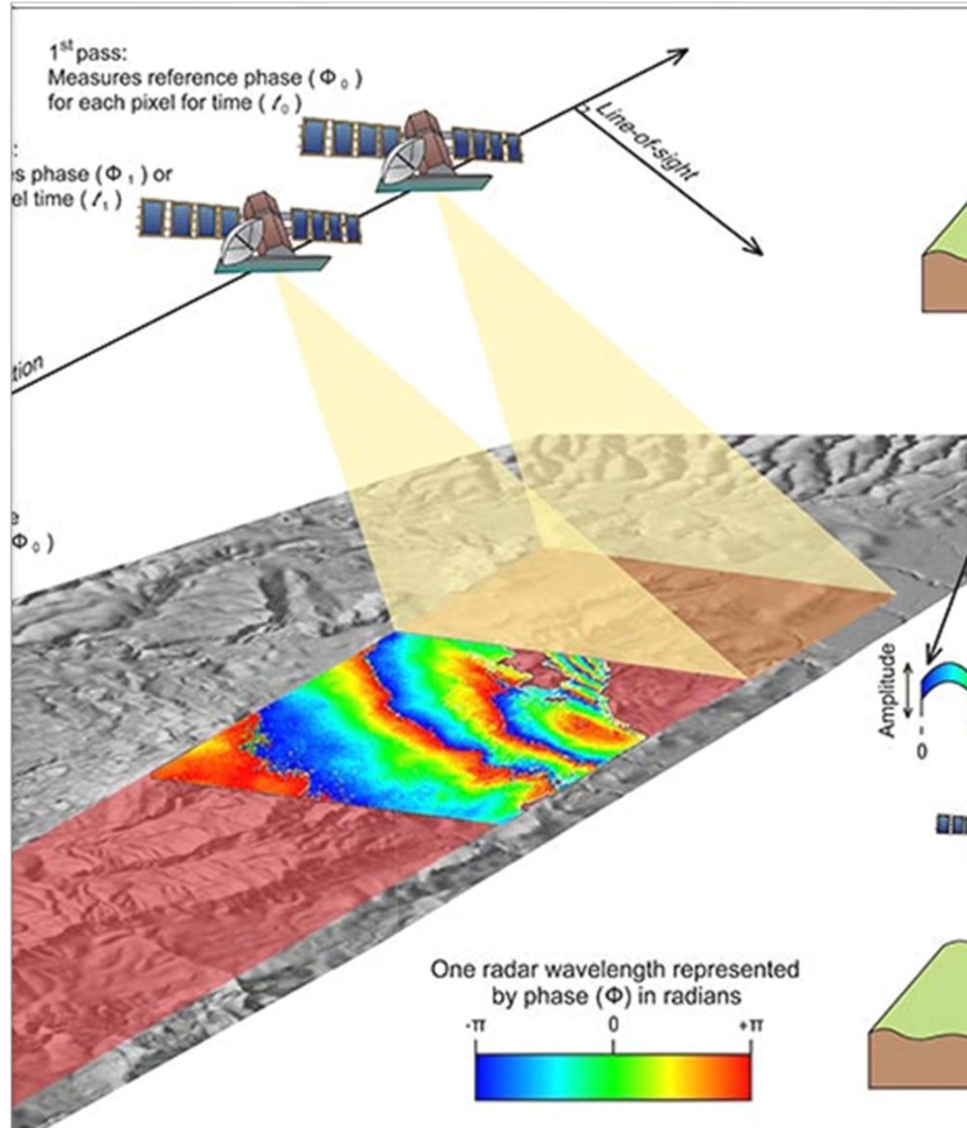

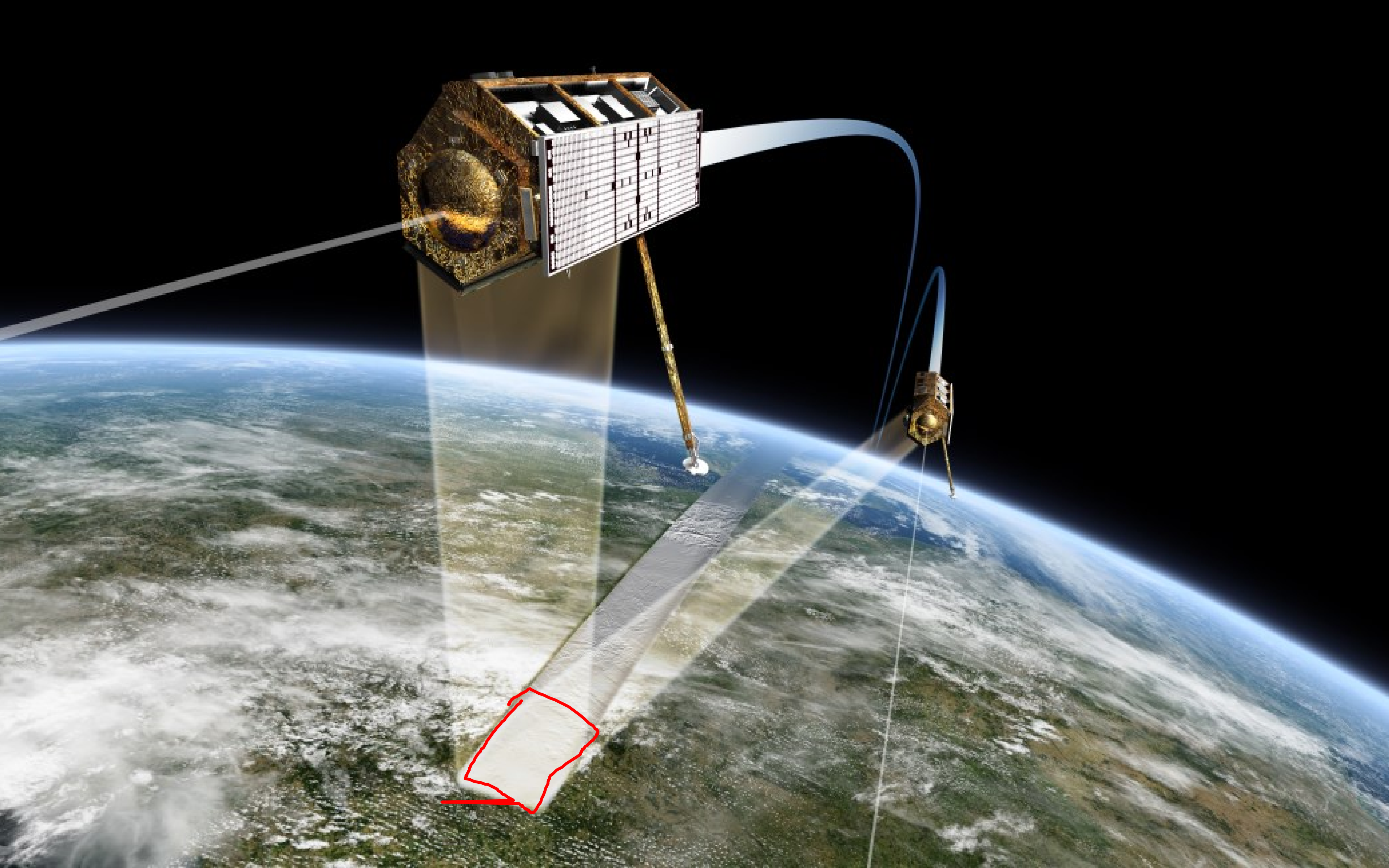

SAR Interferometry

- InSAR methods are based on combining radar returns from two different antennas, displaced from each other in space or time.

$$\phi_1 = -\frac{4\pi r}{\lambda} + \phi_{scatt}$$

$$\phi_2 = -\frac{4\pi (r + \delta r)}{\lambda} + \phi_{scatt}$$

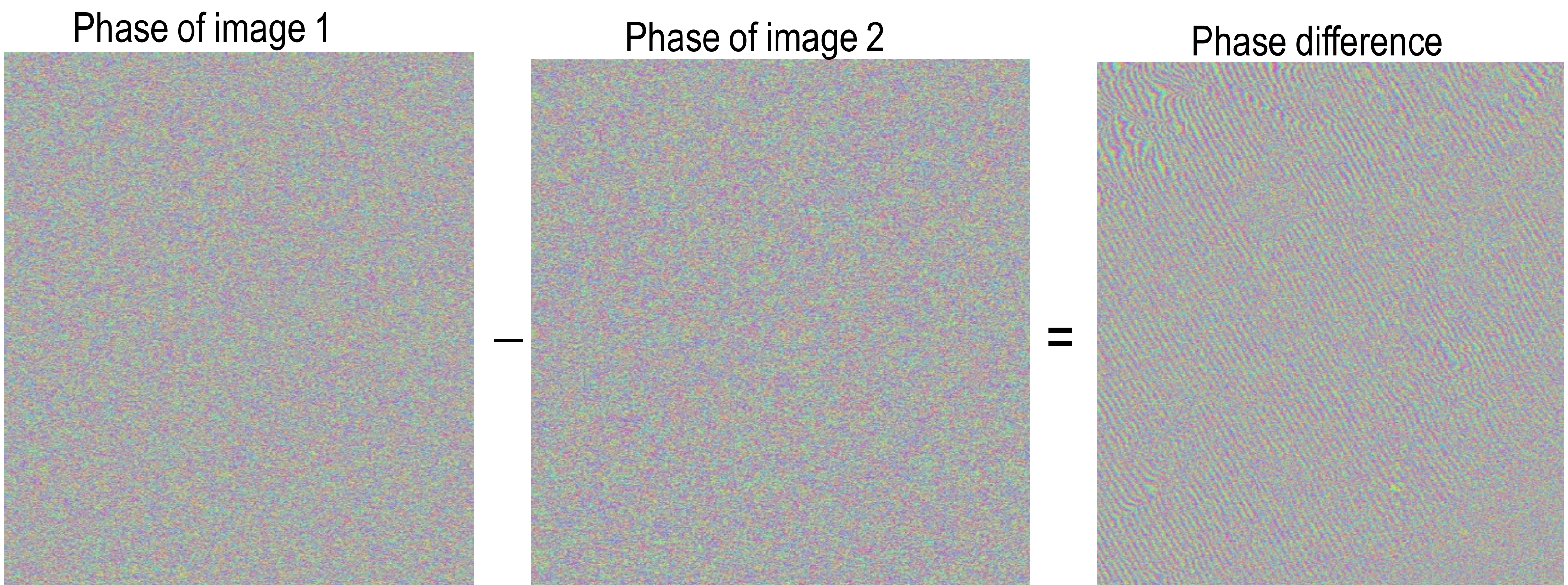

Image matching

It is important that the interferometric image pairs match with high subpixel accuracy.

Otherwise the random nature of the phase destroys the coherence and phase.

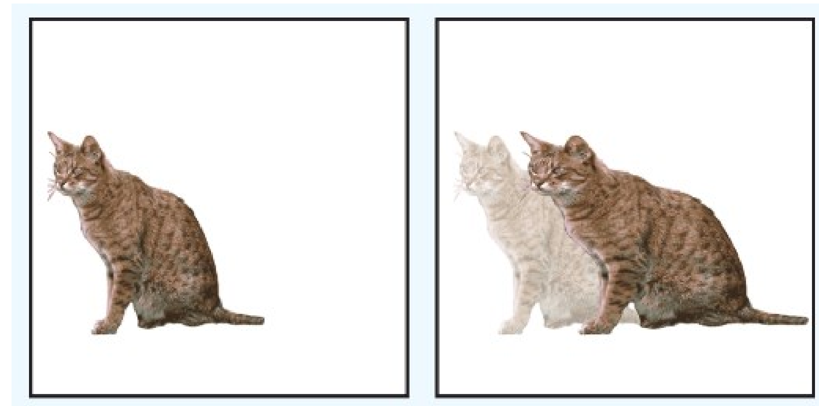

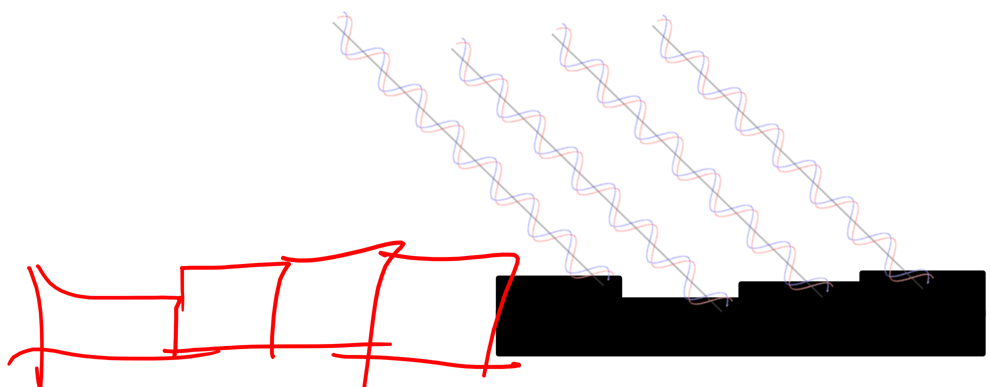

DEM formation

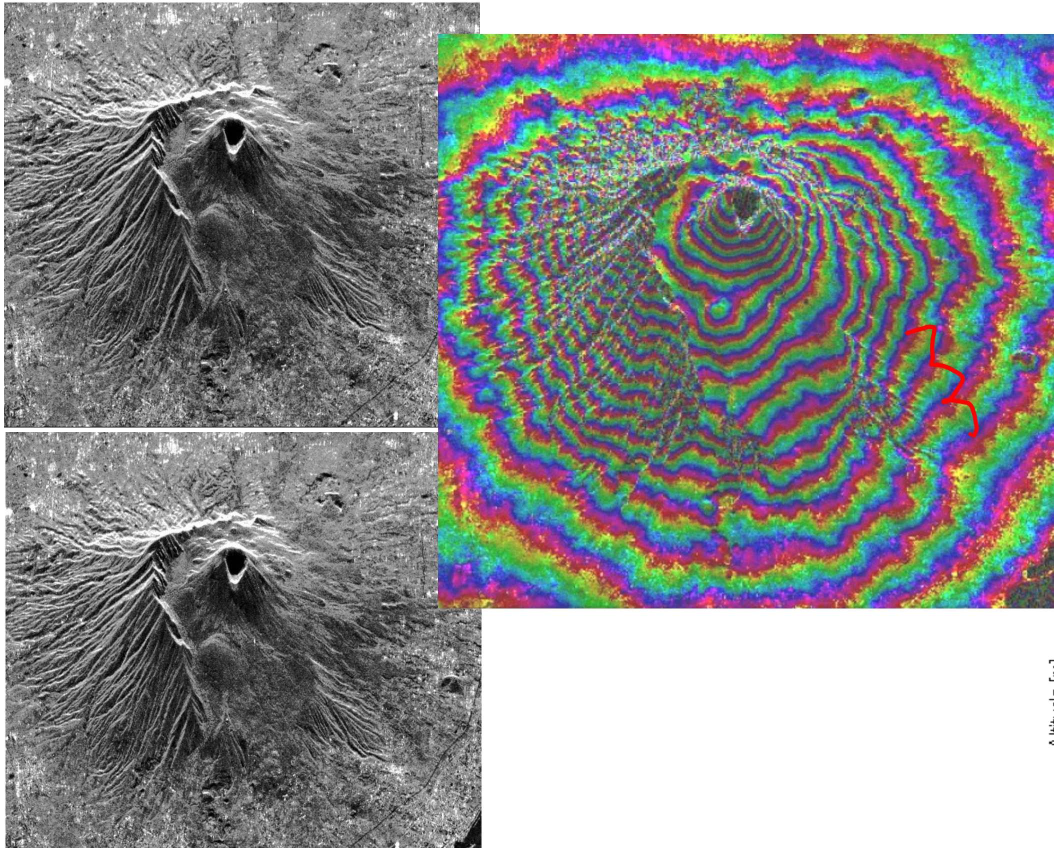

SAR image

SAR image

Interferogram

Flat earth removal

Phase unwrapping

Digital elevation model

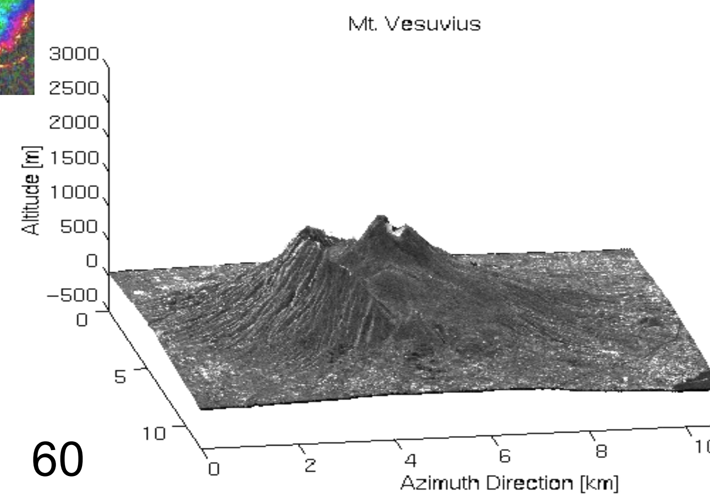

Aalto University
School of Electrical
Engineering

Flat earth removal

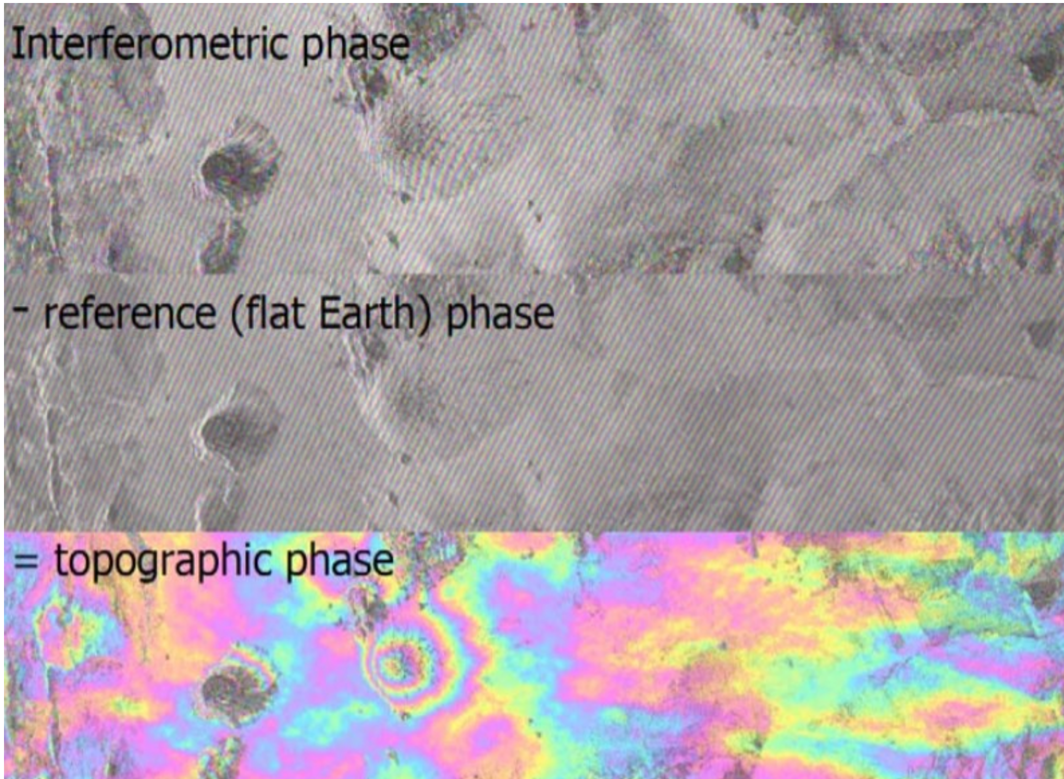

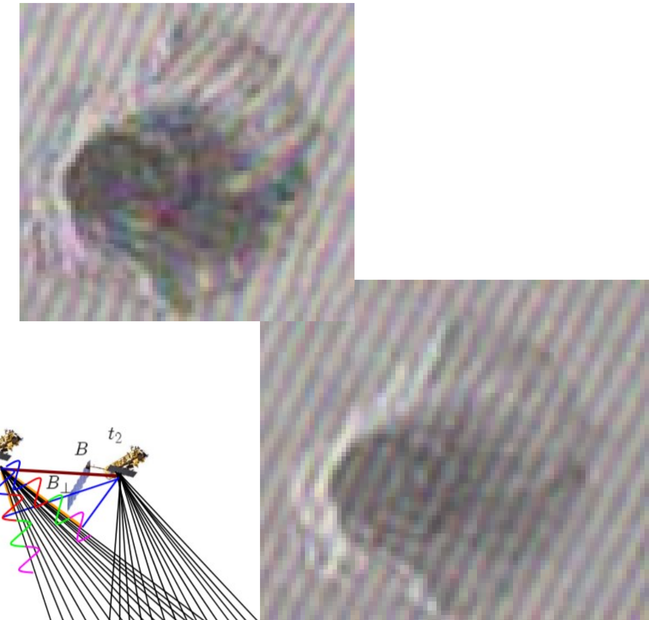

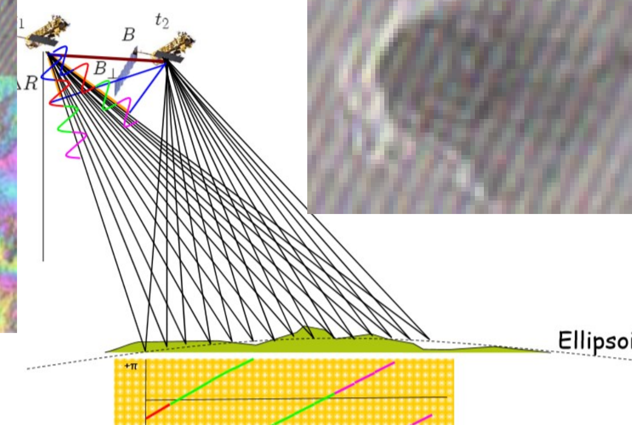

Interferogram formation

phase of a complex SAR image pixel: $\phi_i = -\overbrace{\frac{4\pi}{\lambda} R_i}^{\text{range}} + \overbrace{\phi_{scatt,i}}^{\text{scattering}}$

SAR scene #1: $u_1[i,k] = |u_1[i,k]| \cdot \exp(j\,\phi_1[i,k])$

SAR scene #2: $u_2[i,k] = |u_2[i,k]| \cdot \exp(j\,\phi_2[i,k])$

interferogram: $v[i,k] = u_1[\cdot]\,u_2^*[\cdot] = |u_1[\cdot]|\,|u_2[\cdot]|\,\exp(j\,\phi[\cdot])$

interferometric phase: $\phi[\cdot] = \phi_1[\cdot] - \phi_2[\cdot]$

Aalto University
School of Electrical Engineering

Wavelength sensitivity

$$\Delta\phi = \frac{4\pi B \sin\theta}{\lambda}$$

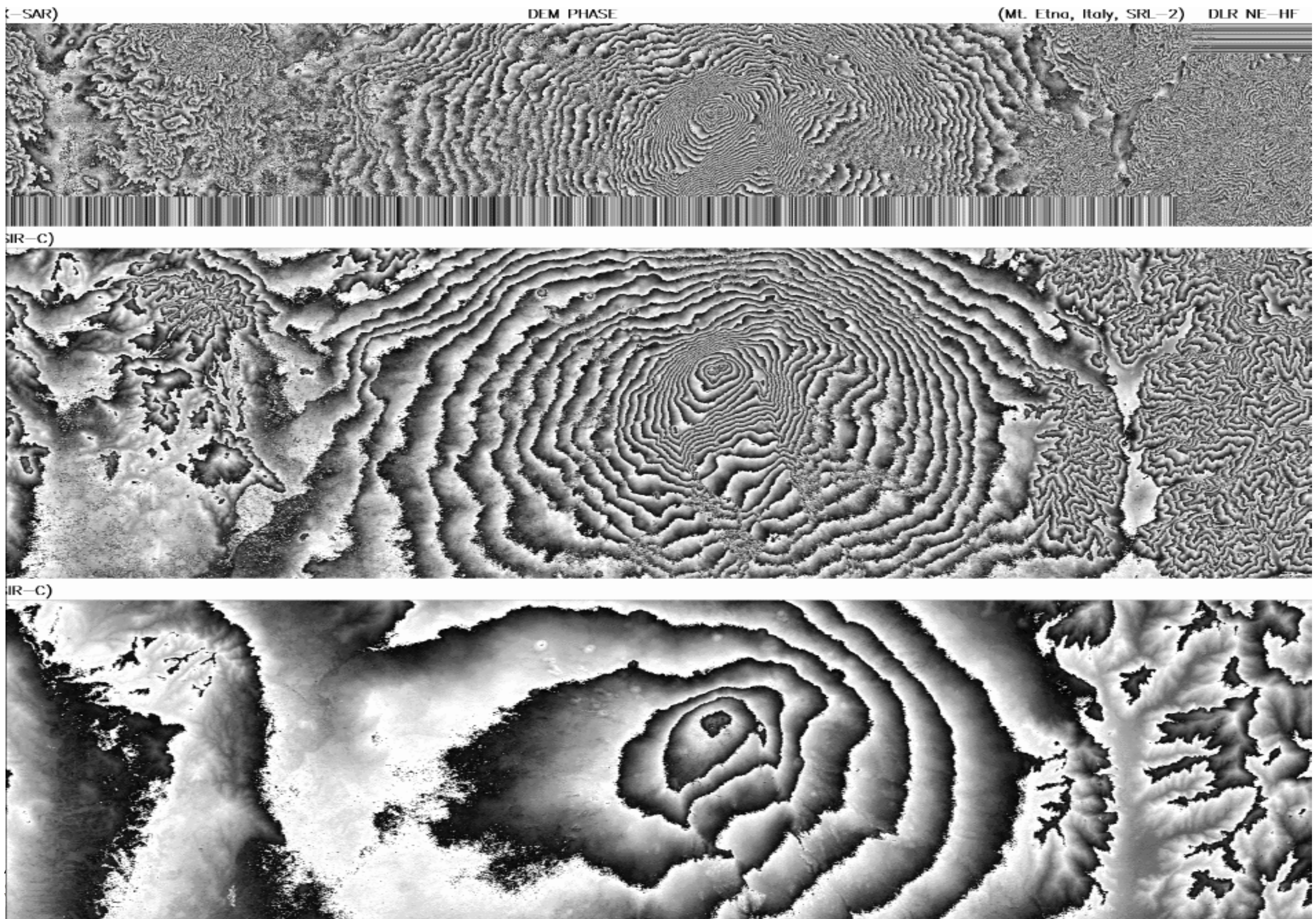

X-band

C-band

L-band

Mt. Etna
data: SRL-2
(© DLR)

Critical baseline

$$\Delta\phi = \frac{4\pi B \sin\theta}{\lambda}$$

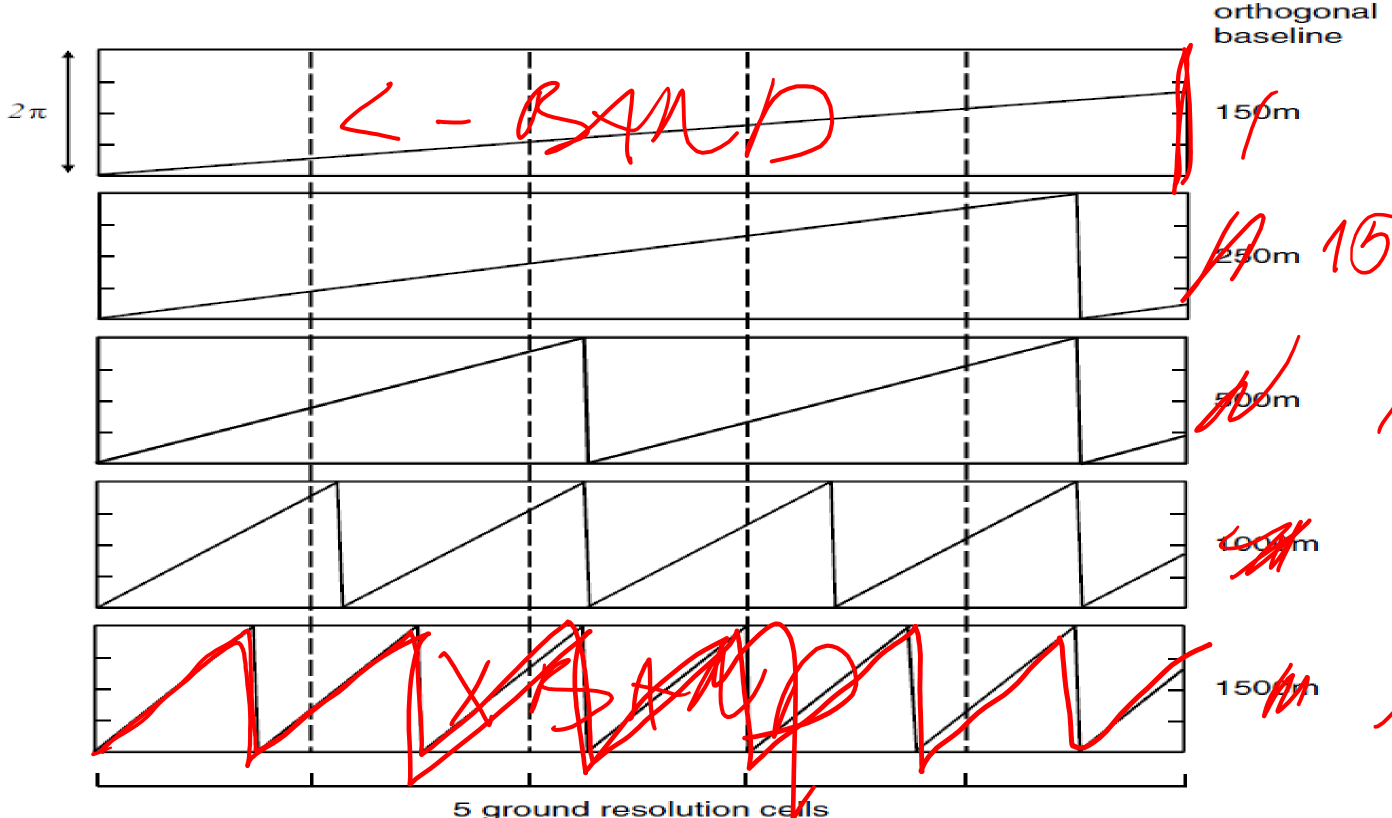

InSAR phase difference for ERS

Aalto University
School of Electrical Engineering

Phase unwrapping

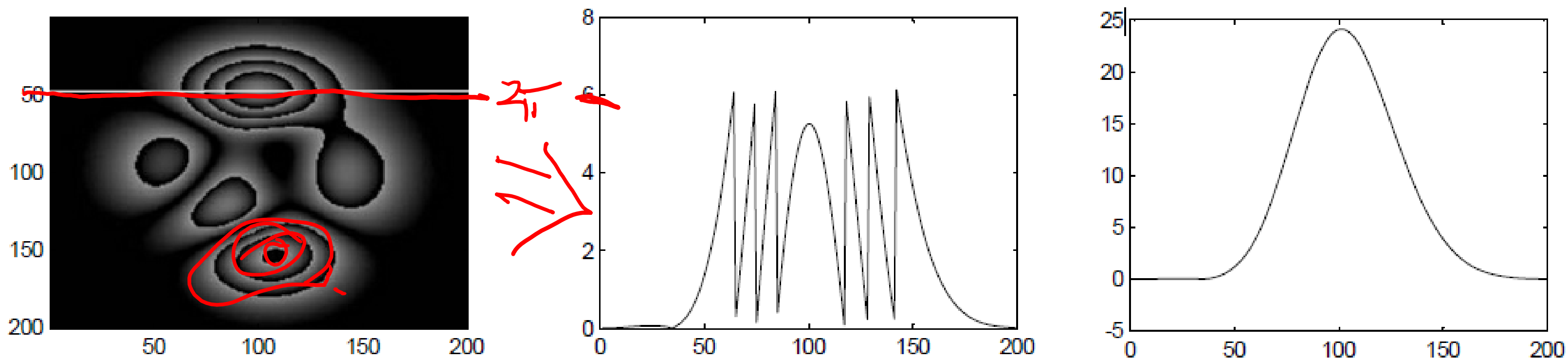

Aalto University
School of Electrical Engineering

Coherence and decorrelation

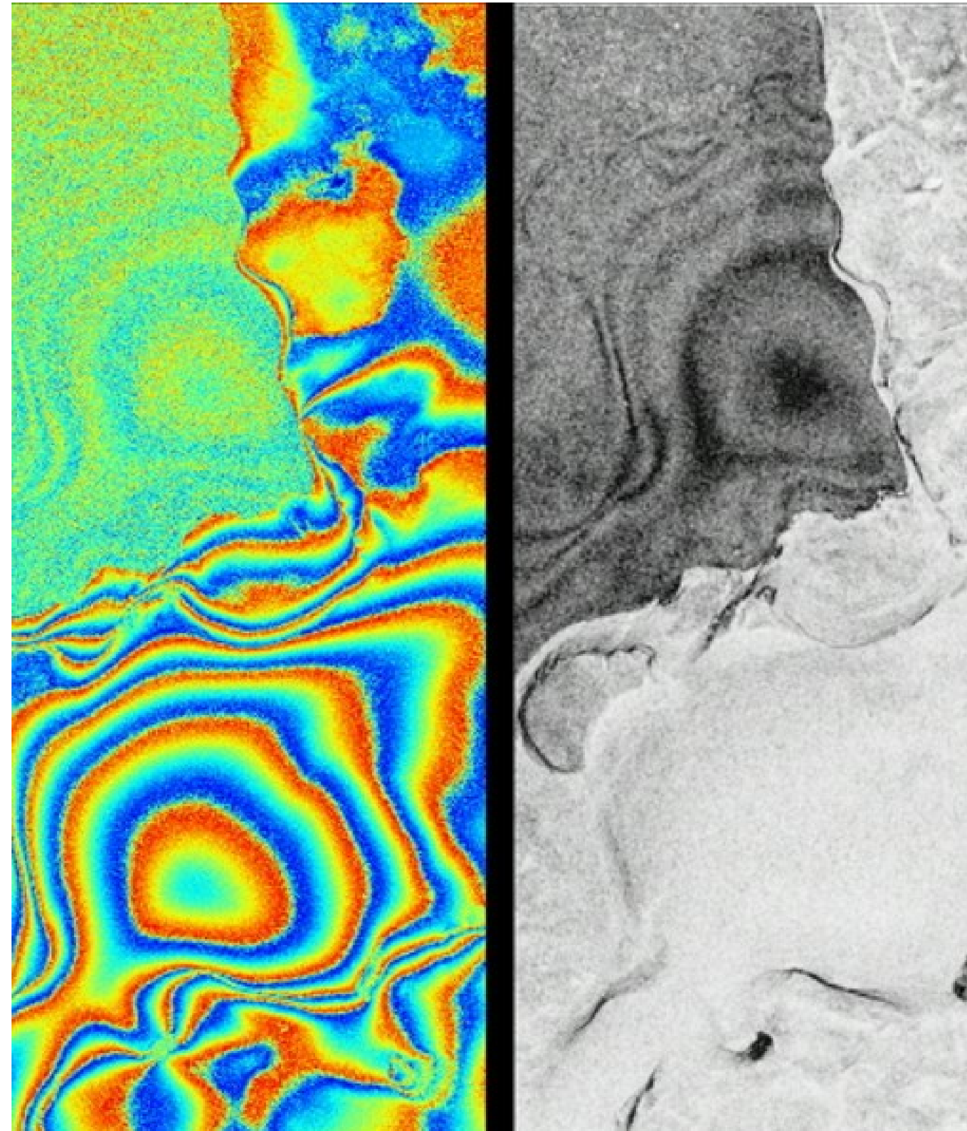

Multiplication with complex conjugate gives phase difference

$$\alpha = A_1 e^{i\varphi_1}$$

$$\beta = A_2 e^{i\varphi_2}$$

$$\alpha \cdot \beta = A_1 \cdot A_2 \cdot e^{i(\varphi_1 + \varphi_2)}$$

$$\alpha \cdot \beta^* = A_1 \cdot A_2 \cdot e^{i(\varphi_1 - \varphi_2)}$$

Complex coherece

- Interferometry uses two SAR images to calculate the complex coherence between the images

$$\gamma_{xy} = \frac{\langle s_1 s_2^* \rangle_{xy}}{\sqrt{\langle s_1^2 \rangle_{xy} \langle s_2^2 \rangle_{xy}}}$$

  - xy denotes pixel and <> spatial average over N pixel window.
- The phase of the coherence is proportional to spatial elevation differences $\Delta\varphi \propto \Delta z$
- The magnitude of the coherence is proportional to scatterer randomness and/or change in placement
- Measurement of coherence allows to calculate the thickness of the random scatterer, for example forest height

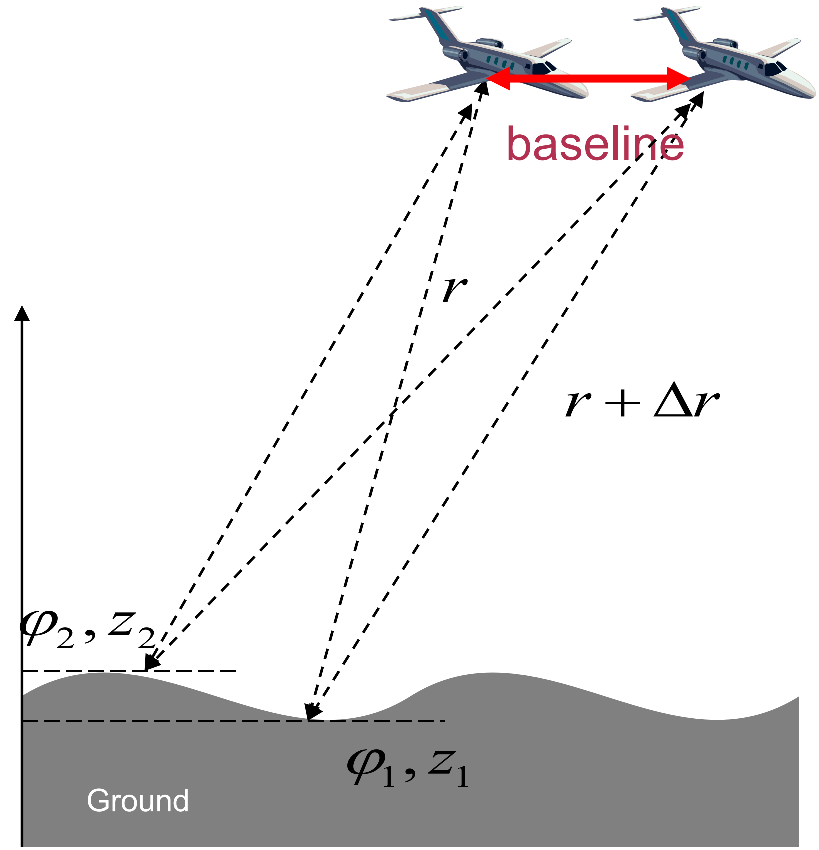

Coherence (degree of correlation)

Measure of interferogram quality is the degree of correlation (coherence) between the two images, or how closely the phase in one image tracks that of the other.

Factors which decrease the correlation is called decorrelation.

$$\rho = \frac{\sum \text{image } 1_i \text{image } 2_i^*}{\sqrt{\sum \text{image } 1_i \text{image } 1_i^*}\sqrt{\sum \text{image } 2_i \text{image } 2_i^*}}, \tag{15.28}$$

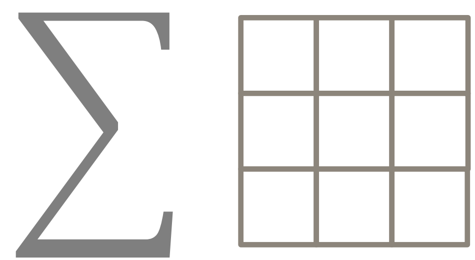

∑ is calculated over a window

$$\rho = \frac{\sum \text{image } 1_i \text{image } 2_i^*}{\sqrt{\sum \text{image } 1_i \text{image } 1_i^*}\sqrt{\sum \text{image } 2_i \text{image } 2_i^*}}, \quad (15.28)$$

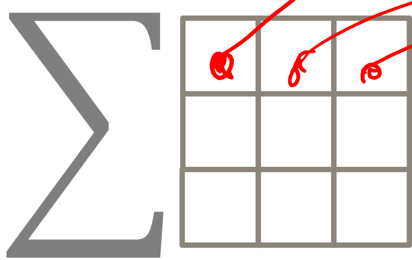

$\sum$ **is calculated over a window**

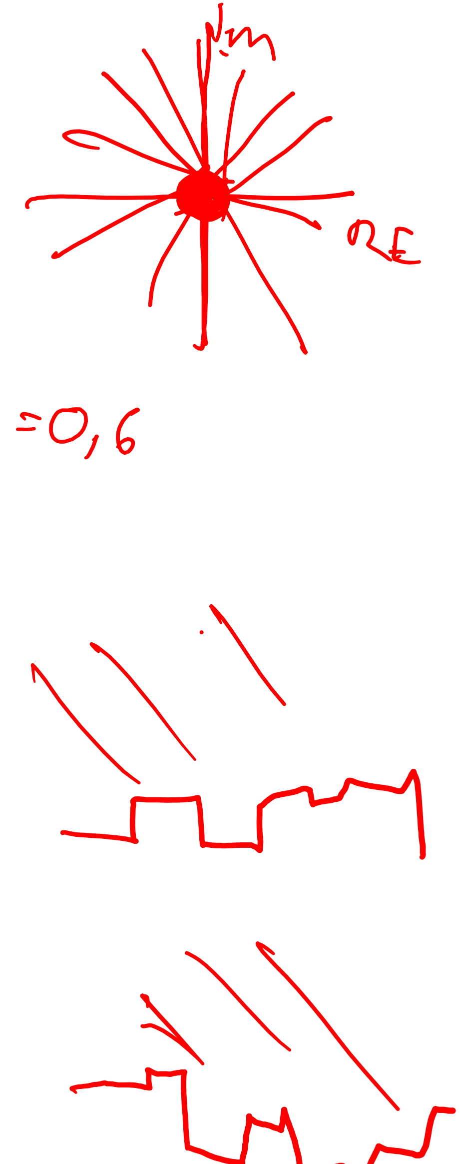

Types on InSAR

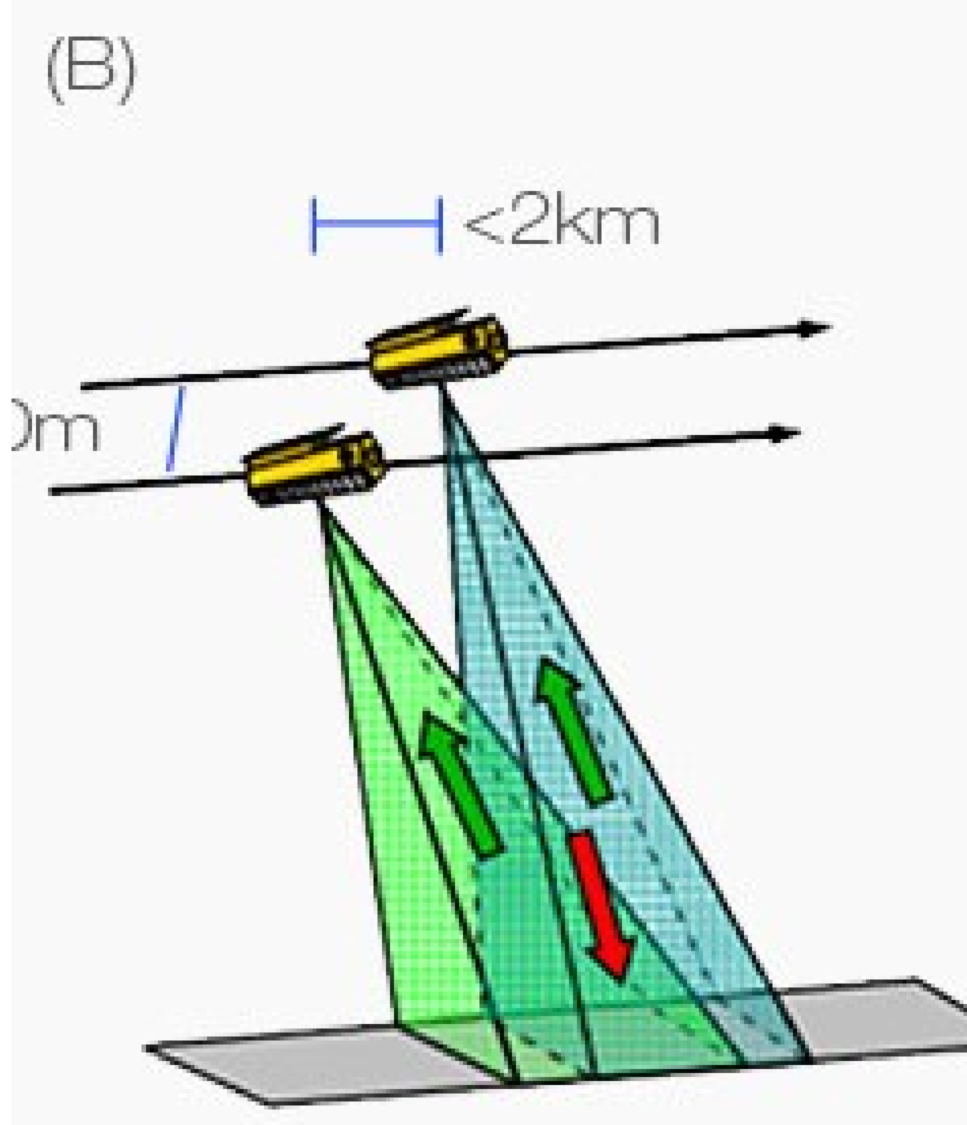

Types of SAR interferometry

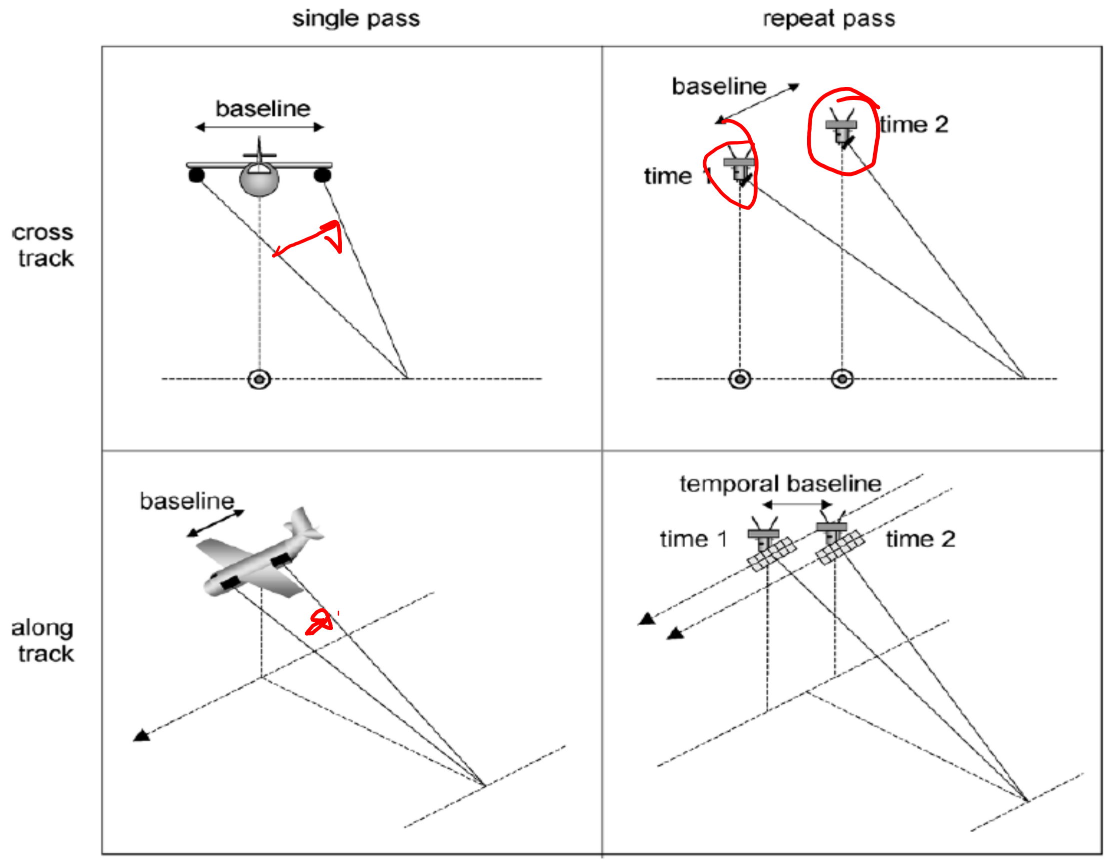

Aalto University
School of Electrical Engineering

Types of SAR interferometry

Single-pass interferometry

- Along-track
  - *Movement measurement (InSAR)*
- Cross-track with common transmit antenna
  - *Elevation models (InSAR)*

Multiple-pass interferometry

- Cross-track with two independent radars
  - *Change detection (InSAR)*
- Cross-track with common transmit antenna
  - *Change detection, differential interferometry (DinSAR, Permanent scatterer interferometry)*

Operation modes

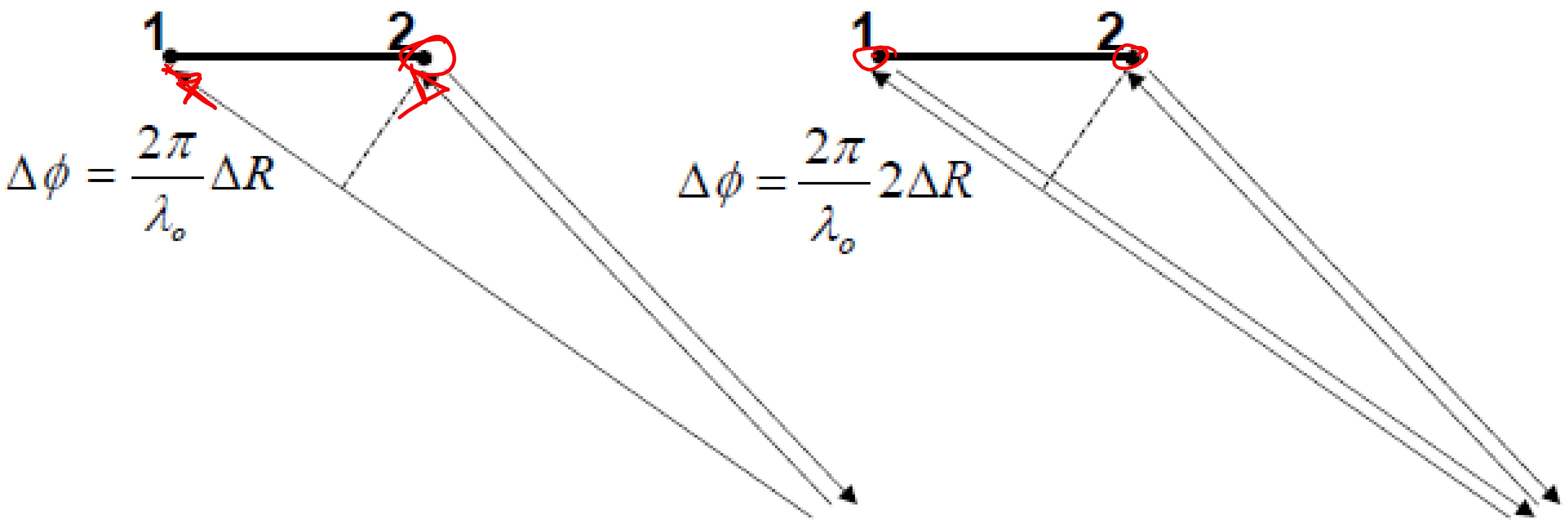

(a) standard mode ***(b) ping pong mode***

Aalto University
School of Electrical Engineering

InSAR applications

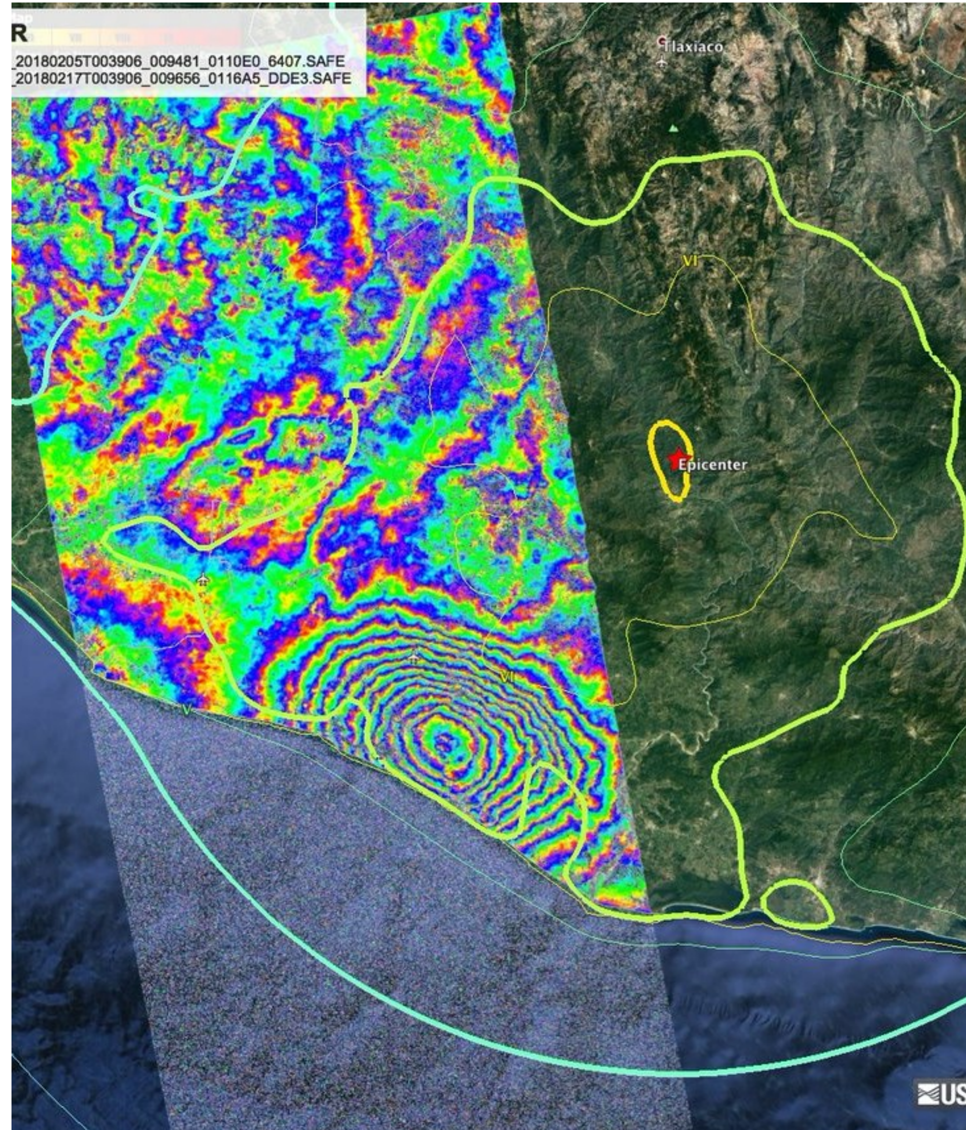

Digital elevation models

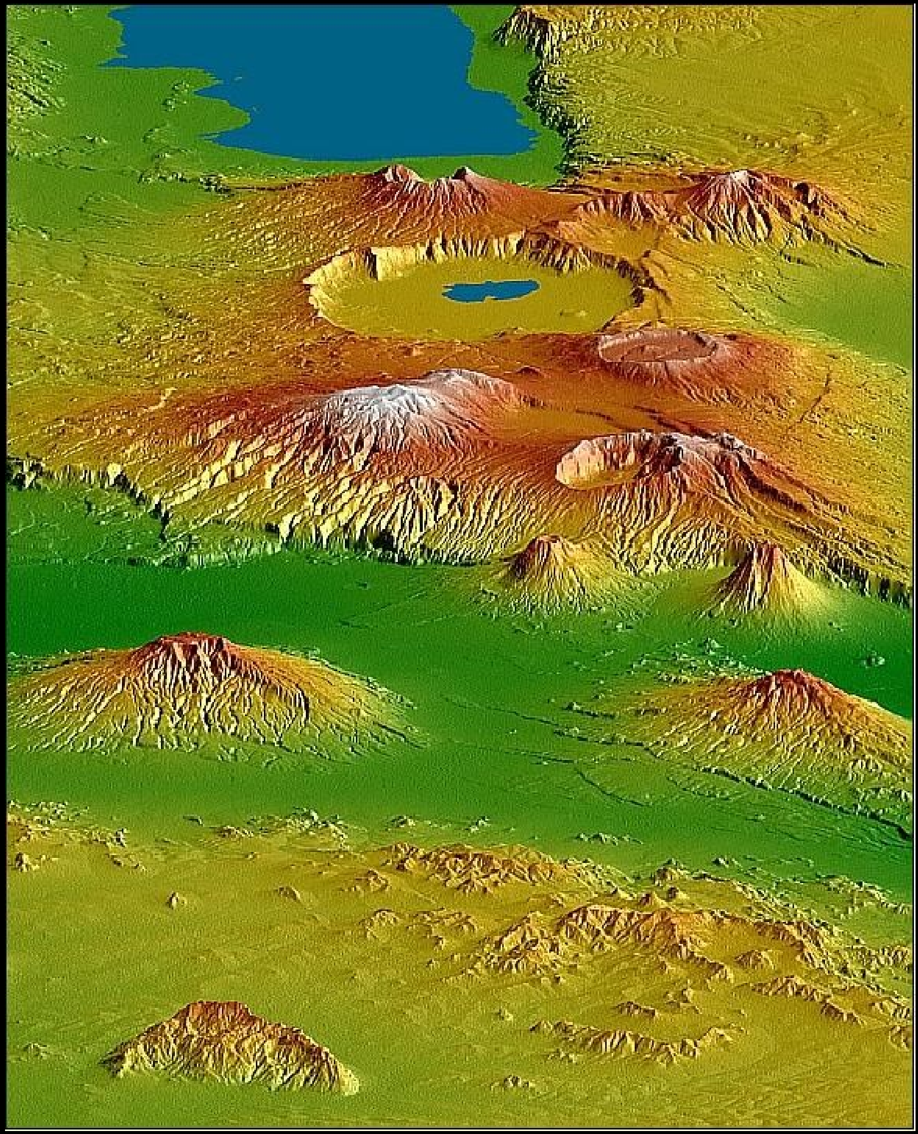

SRTM: Shuttle Radar Topography Mission

- February 2000: 11-day mission of Endeavour
- Topography map of the whole Earth (latitudes < 60º)
- InSAR in C and X-band. Baseline = 60 m

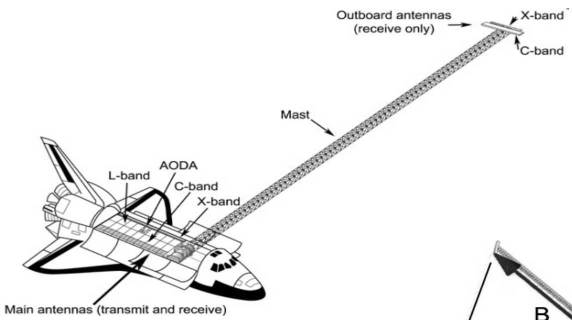

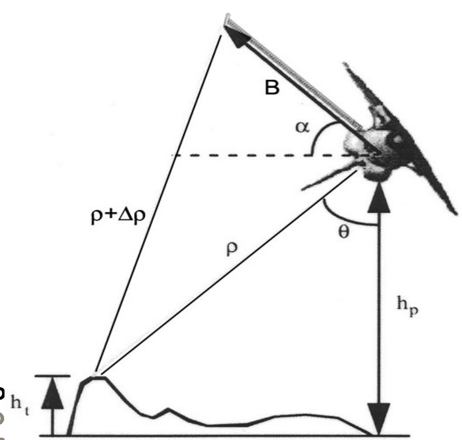

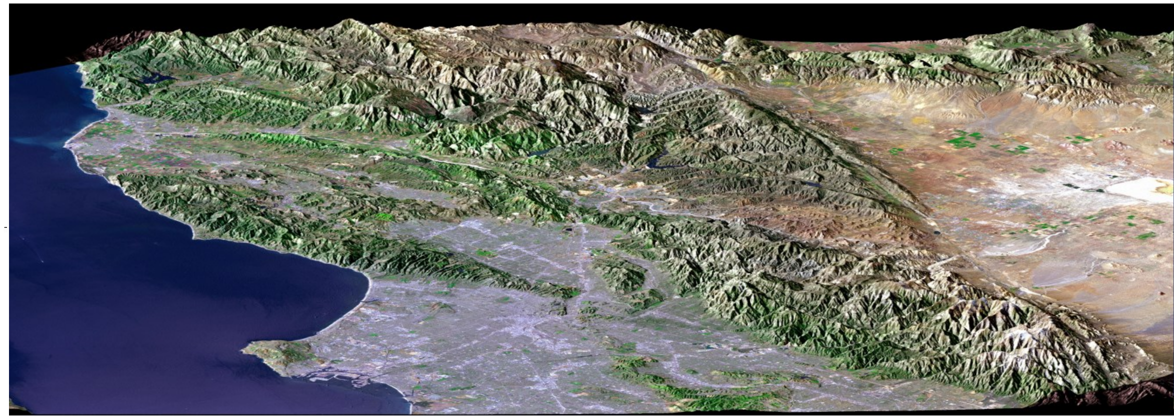

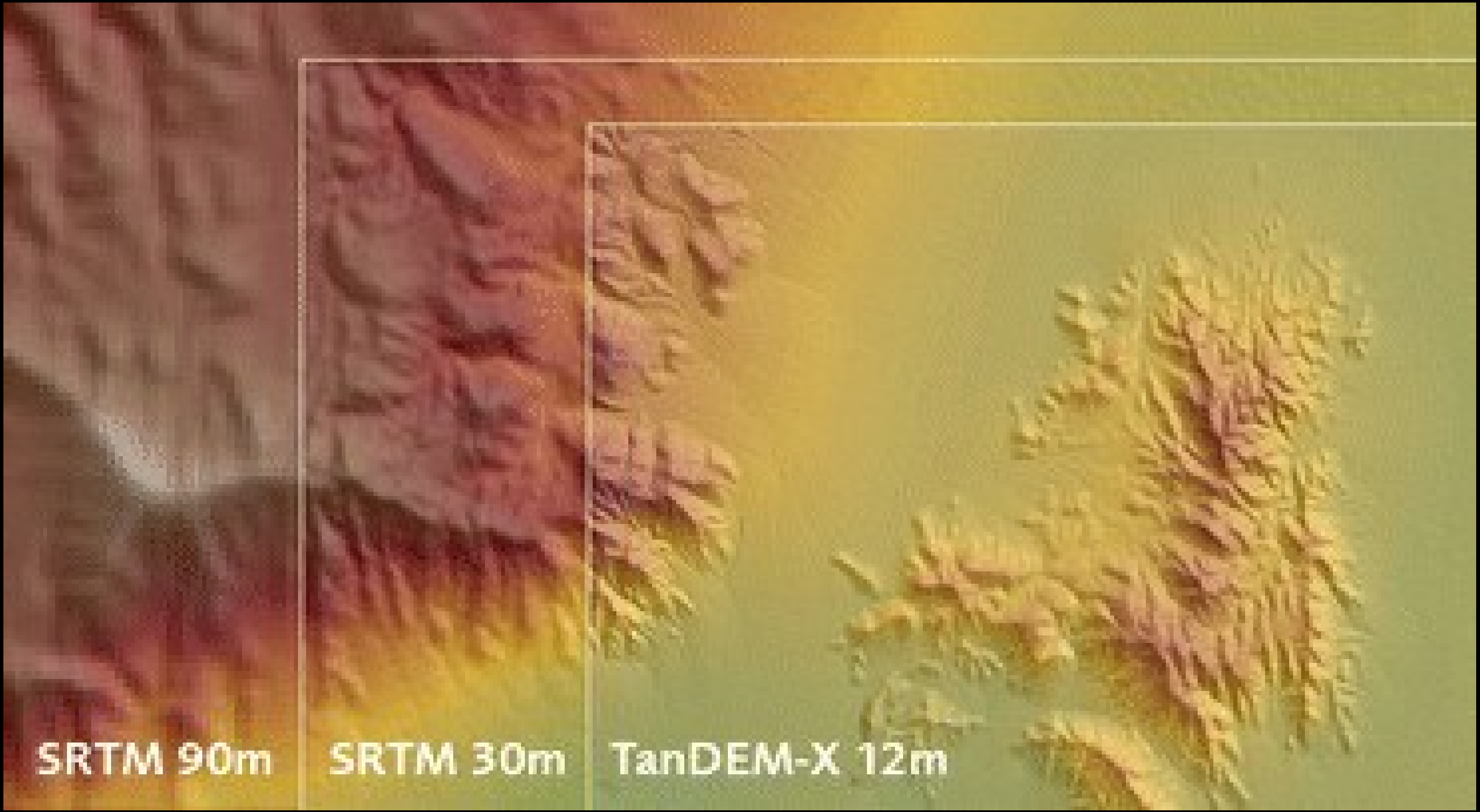
SRTM 90m
SRTM 30m
TanDEM-X 12m

Deformation measurement with small baseline and repeat pass

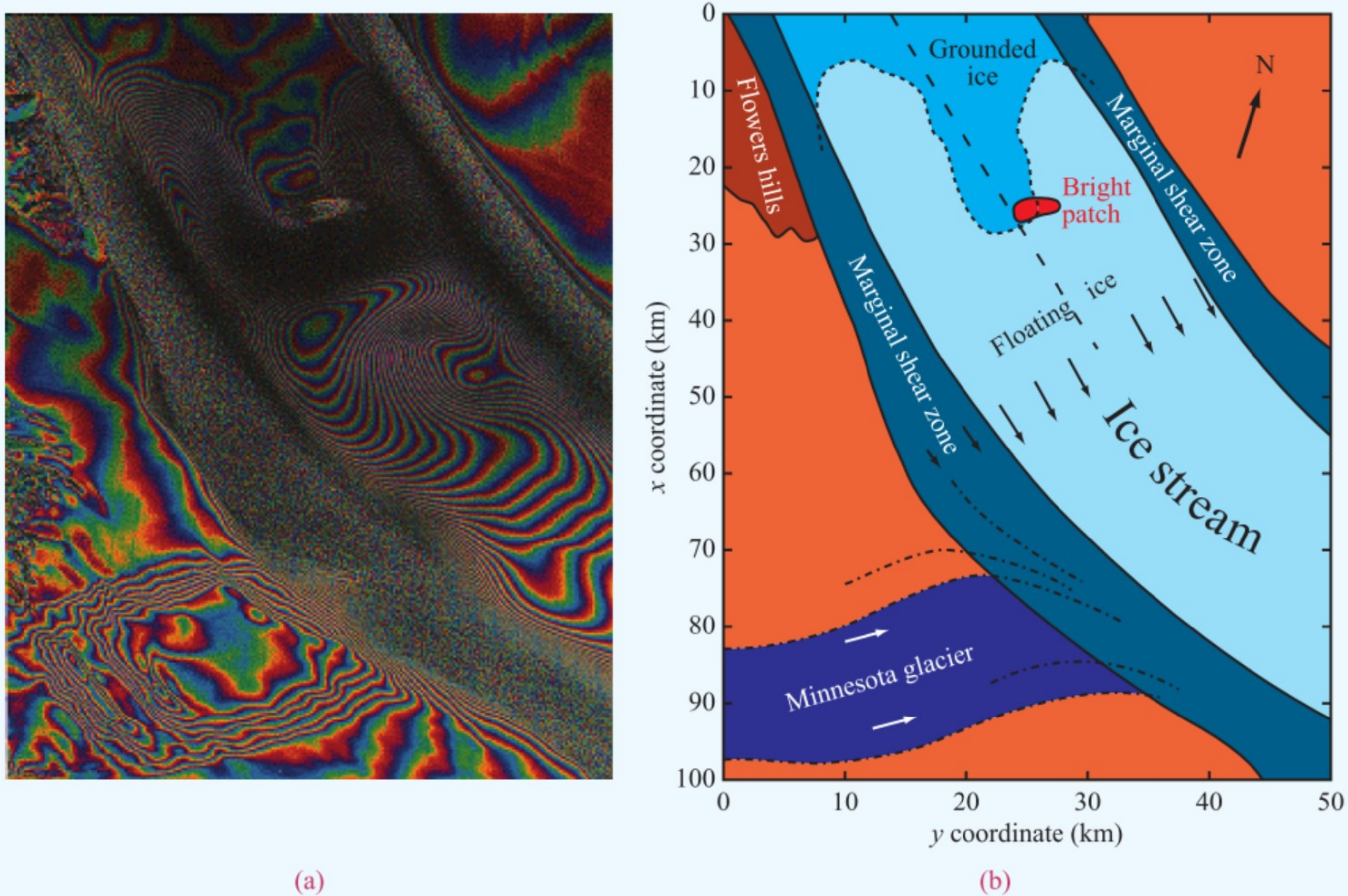

Figure 15-30: Radar interferogram of a portion of the Rutford ice stream in Antarctica, based on two ERS-1 images taken six days apart. The fringe pattern (color cycle) is essentially a map of ice-flow velocity, with one fringe representing 28 mm of range change along the radar line of site. [Image courtesy Jet Propulsion Laboratory, California Institute of Technology.]

From: Microwave Radar and Radiometric Remote Sensing, by Ulaby and Long, 2014, with permission.

Time series analysis

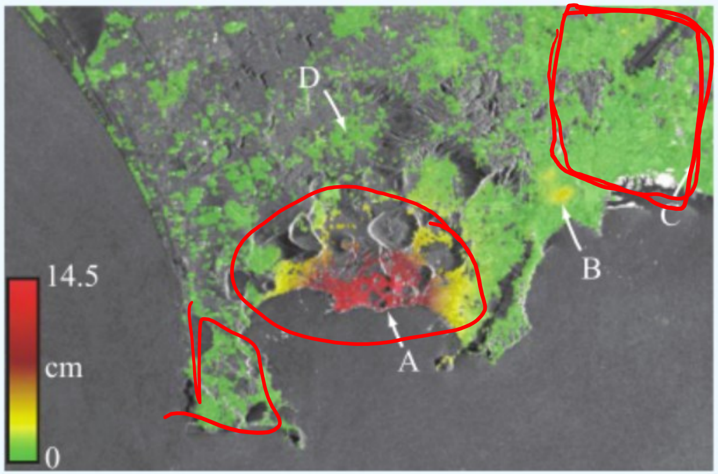

Figure 15-35: False-color map of the measured deformation rms superimposed on the SAR image amplitude of the investigated area. The temporal evolution of the deformations in the selected points identified by A, B, C are shown in Fig. 15-36(a)–(c), respectively [Berardino et al., 2002].

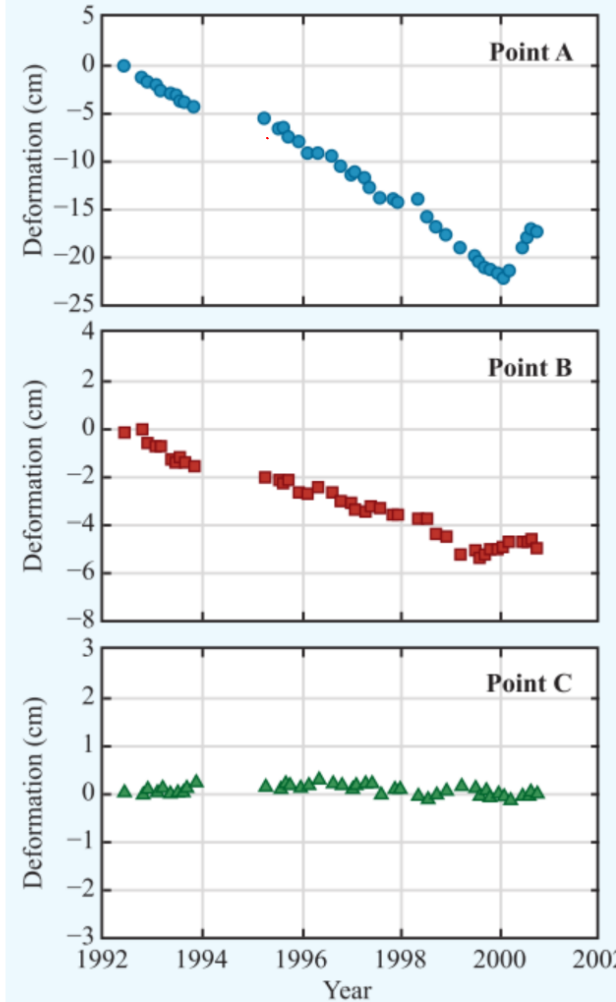

Figure 15-36: Time-series deformation measured at (a) point A, (b) point B, and (c) point C of Fig. 15-35 [Berardino et al., 2002].

Persistent scatterers

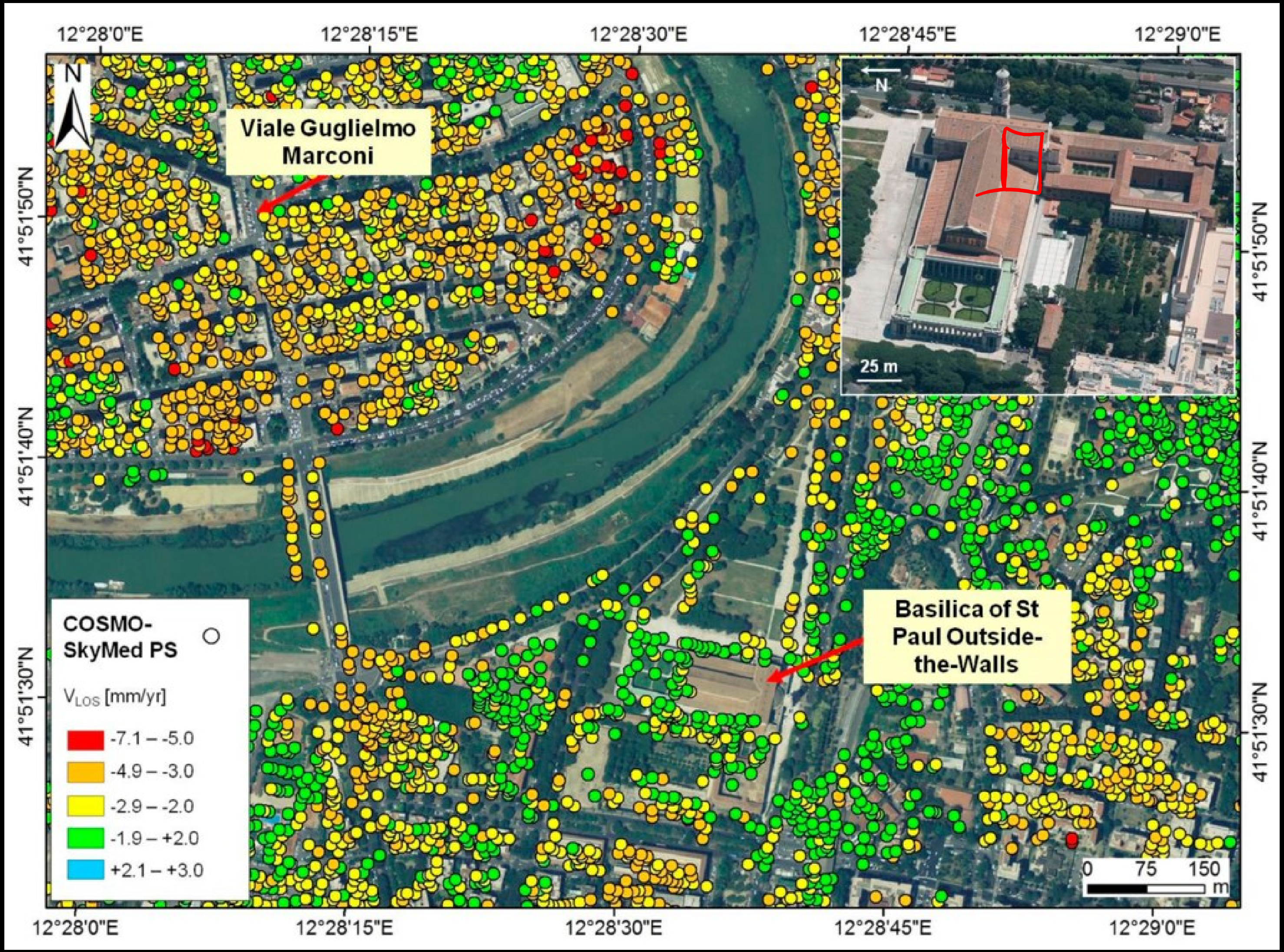

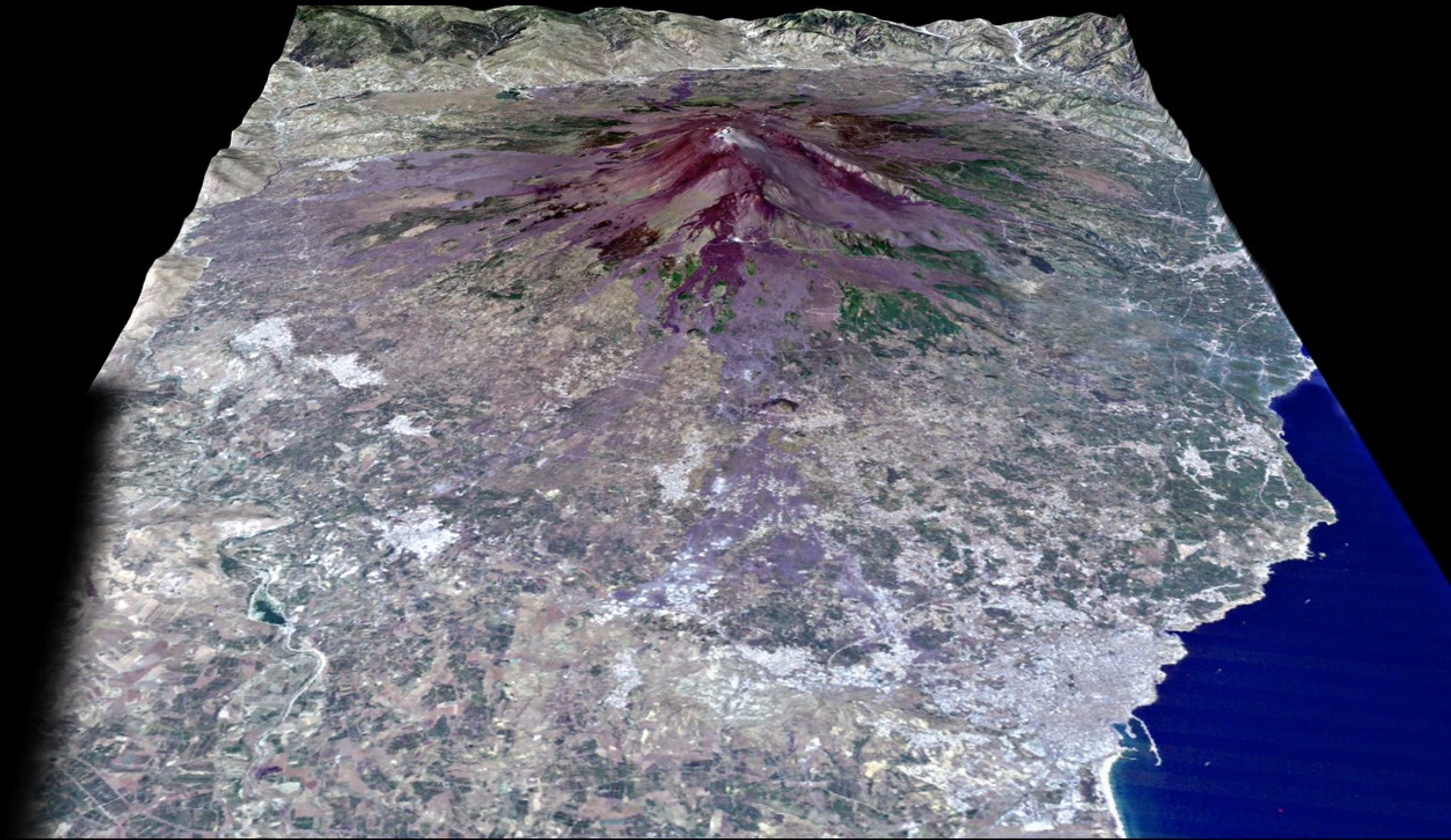

Coherent Change Detection

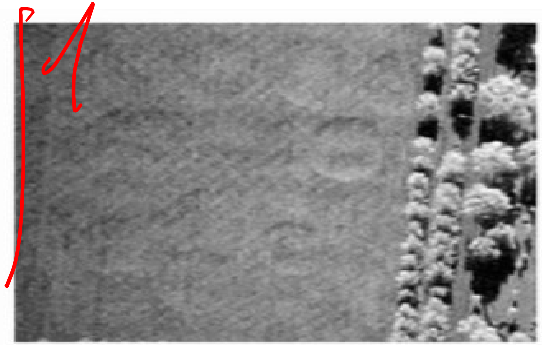

Reference SAR Image: Grassy Field

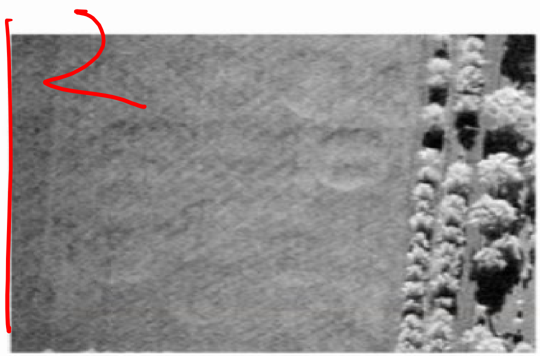

Current SAR Image: Grassy Field

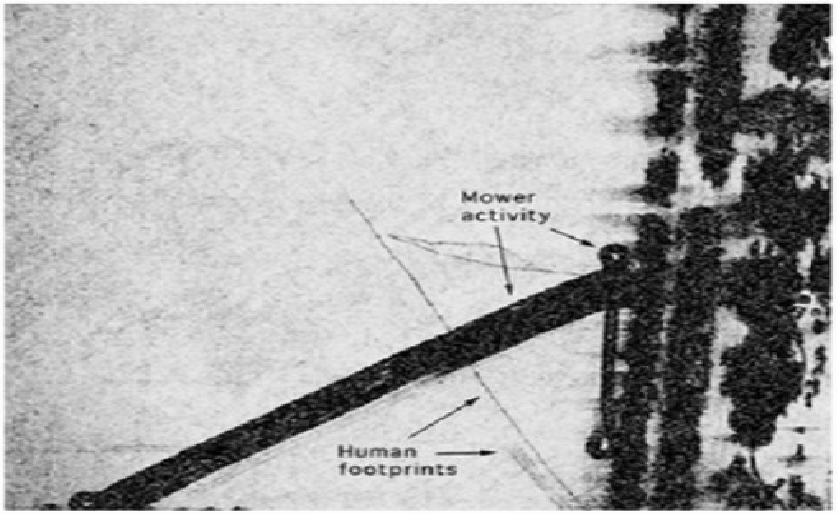

CCD Image – Changes denoted by dark areas

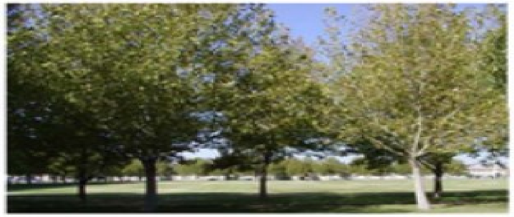

Applications: Multitemporal InSAR

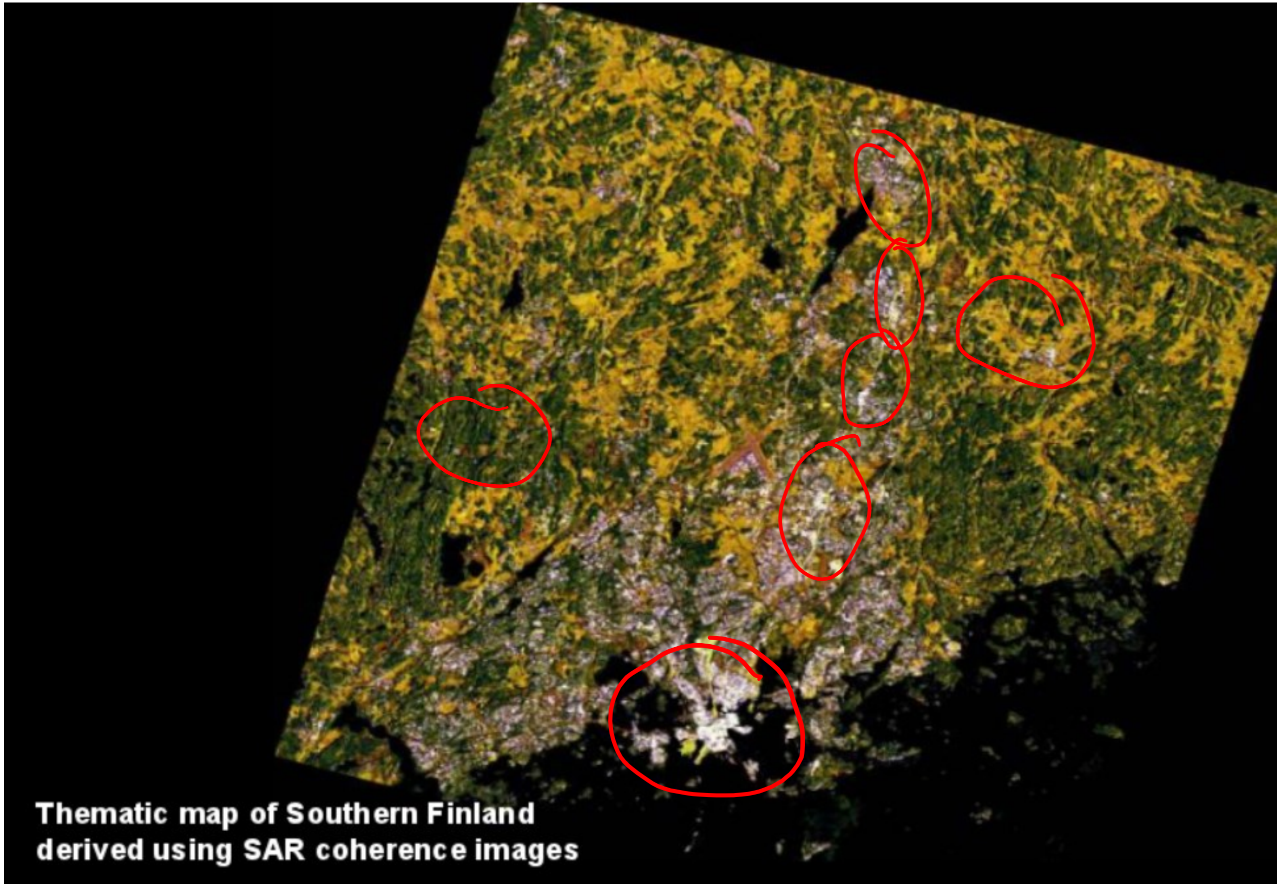

Applications: Forestry

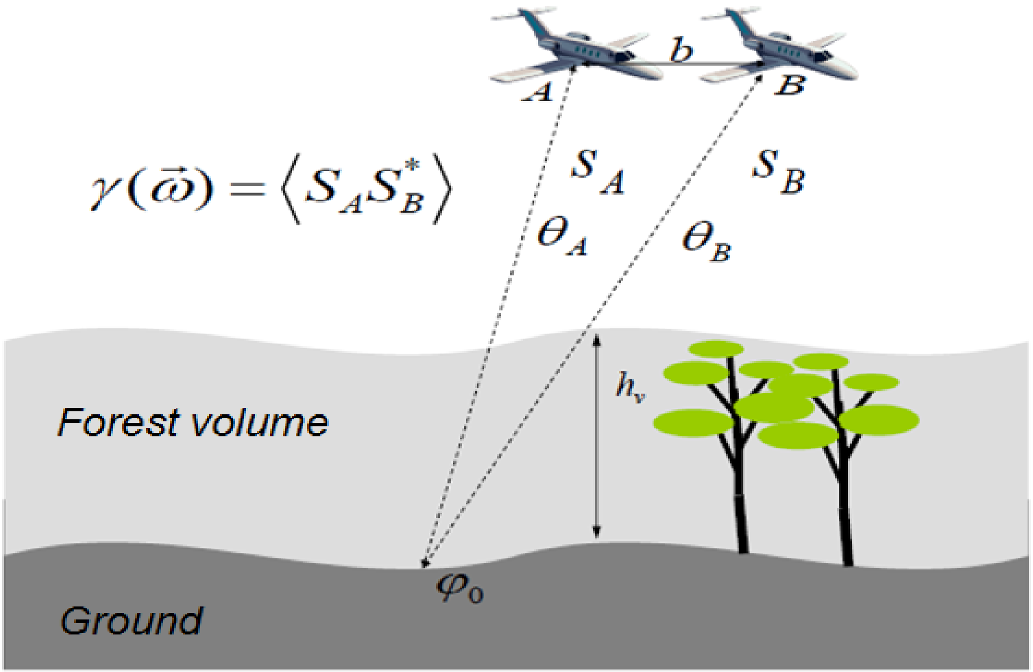

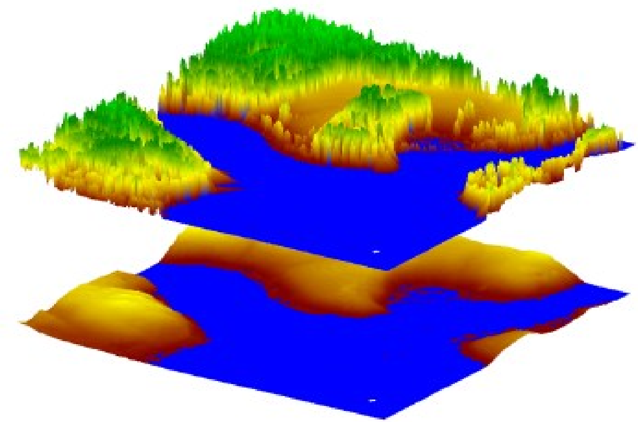

Applications: Forestry

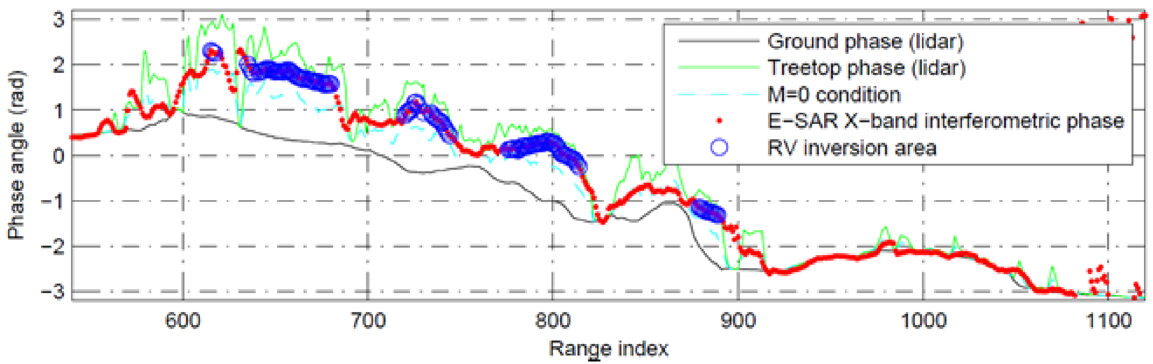

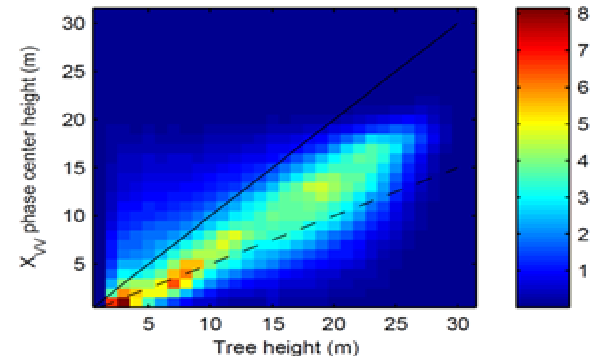

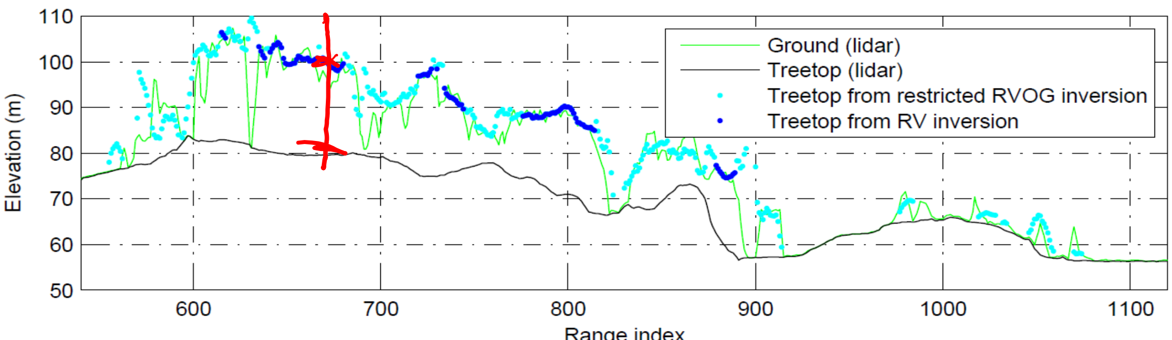

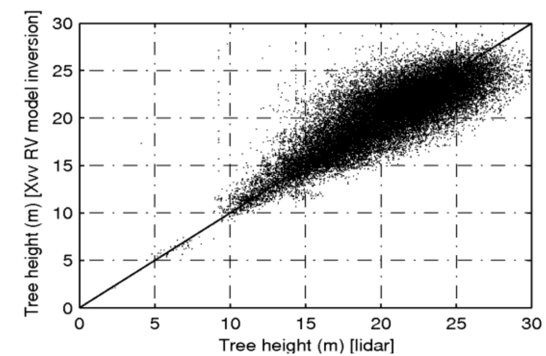

School of Electrical Engineering

Acknowlegment and further reading

- ERS-1/2 (ESA), TanDEM-X (DLR) scenes are used.
- Materials from DLR (K. Papathanassiou), University of Alicante (J.M. Lopes-Sanches), TU Delft (R. Hanssen), VTT, and Aalto University (J. Praks) are used.

- C. Oliver, S. Quegan, “Understanding Synthetic Aperture Radar Images”
- I. H. Woodhouse, “Introduction to Microwave Remote Sensing”
- F. T. Ulaby, R. T. Moore, A.K. Fung, “Microwave Remote Sensing: Active and Passive”
- J.A. Richards, “Remote Sensing with Imaging Radar”
- S. R. Cloude “Polarisation: Applications in Remote Sensing”
- R.F. Hanssen “Radar Interferometry: Data Interpretation and Error Analysis”

END

Aalto University
School of Electrical Engineering

Reminder about complex numbers

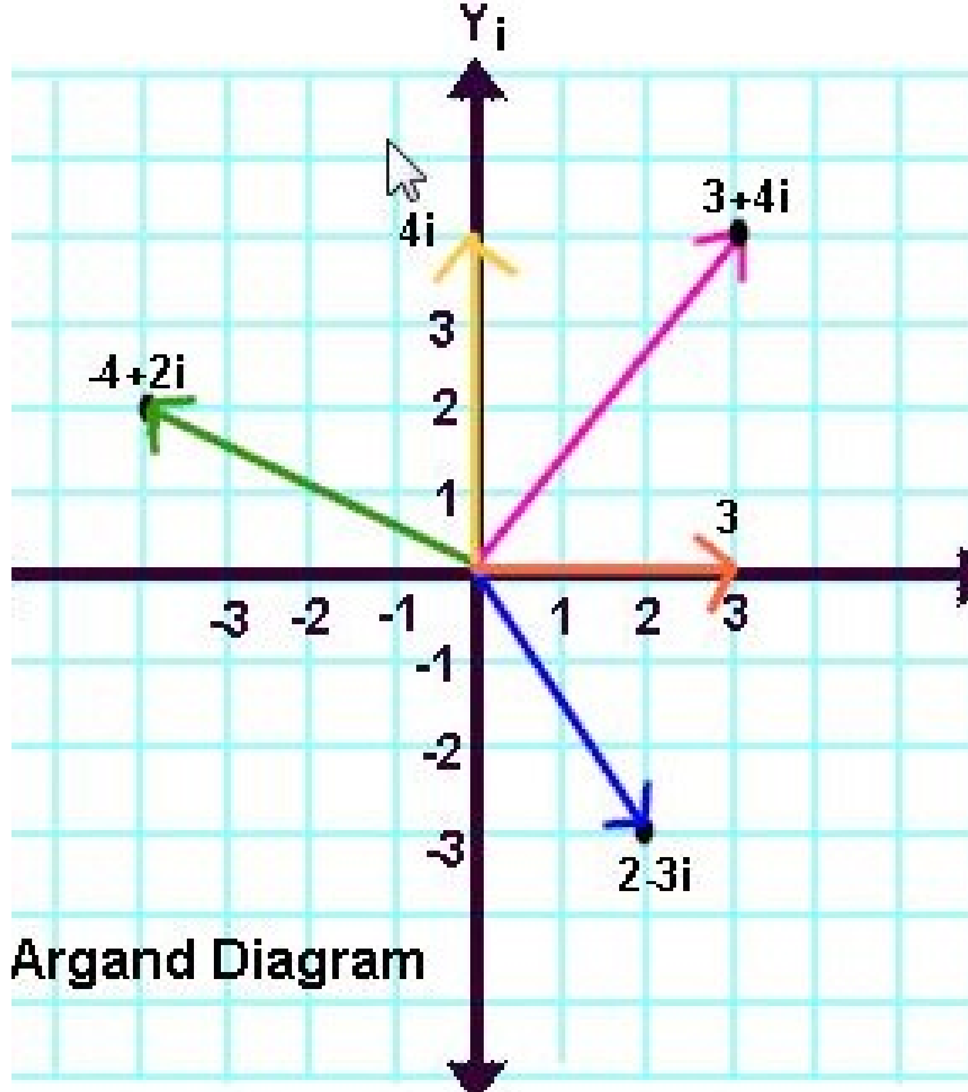

Complex conjugate

complex number	conjugate
$3+\frac{1}{2}i$	$3-\frac{1}{2}i$
$12-5i$	$12+5i$
$1-i$	$1+i$
$45i$	$-45i$
101	101

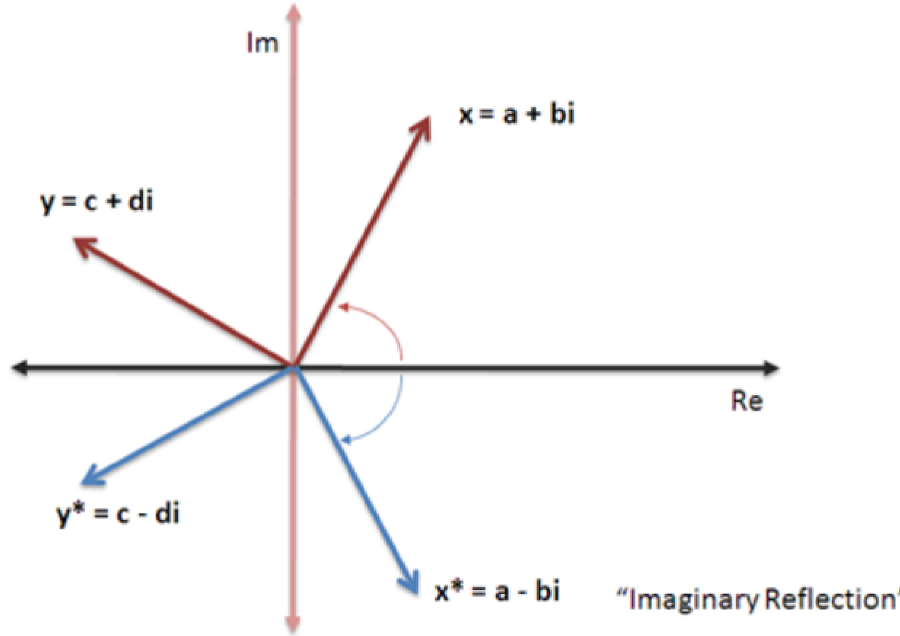

- Ulaby
- Long
- Blackwell
- Elachi
- Fung
- Ruf
- Sarabandi
- Zebker
- Van Zyl

Microwave Radar and Radiometric Remote Sensing

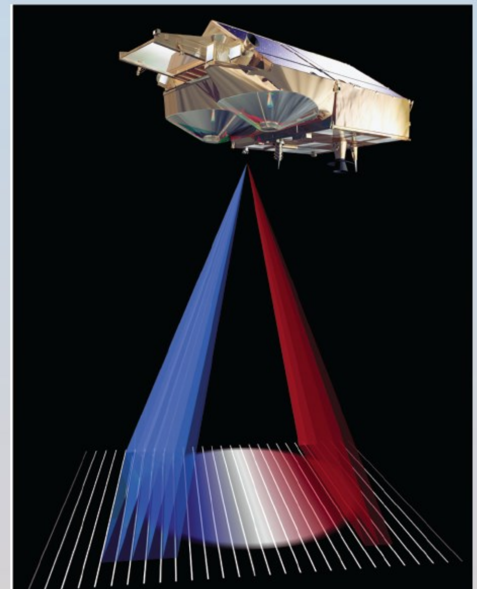

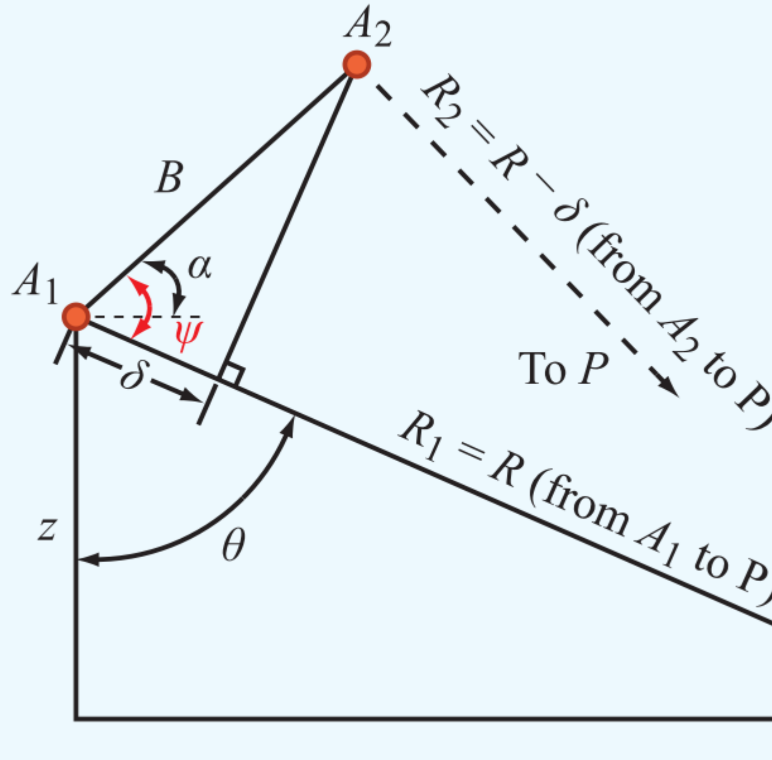

Figure 15-4: Parallel-ray approximation for InSAR geometry with $R_1 = R$ and $R_2 = R - \delta$. Note that R_1 is from A_1 to P.

Speckle

- Noisy appearance of an homogeneous area of the scene
- Difficult interpretation
- Erroneous quantitative estimation if based on one pixel
- Cause: SAR is a coherent system

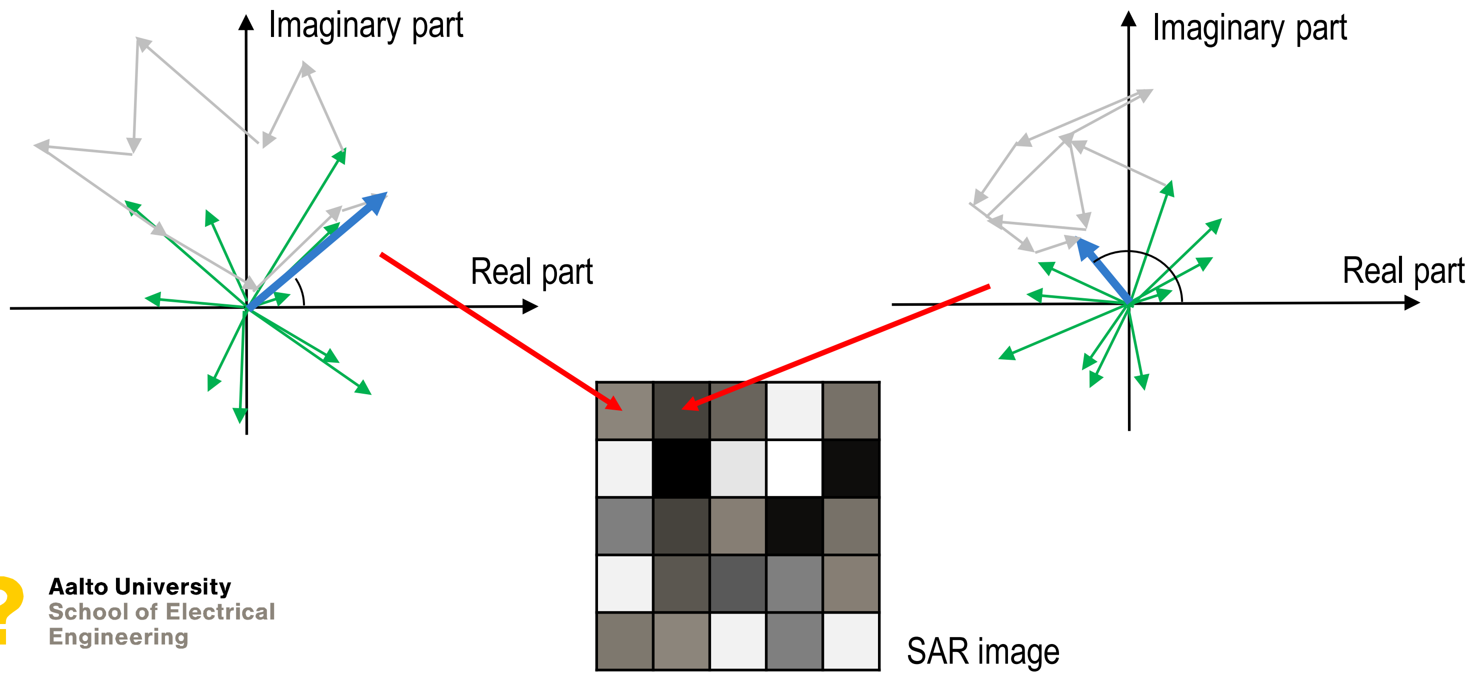

Aalto University
School of Electrical
Engineering

Classroom work

Watch the video:

https://www.youtube.com/watch?v=w6ilV74r2RQ&t=3287s

Link in the chat

We will resume here at Teams 11:20